Research and Development Office

Reclamation / R&D / Research Projects / Paleoflood Hydrology of the Colorado River System: Implication for Climate Changes

Paleoflood Hydrology of the Colorado River System: Implication for Climate Changes

Project ID: 1736
Principal Investigator: Jeanne Godaire
Research Topic: Managing Hydrologic Events

Funded Fiscal Years: 2017 and 2018
Keywords: *None*

Research Question

Although future climate simulations vary in the exact timing and magnitude of projected changes, considerable agreement exists amongst all models that hydrologic changes will be paramount in semi-arid regions of southwestern North America [Seager, 2007]. Hydrologic studies show differing results regarding the characteristics of extreme flood regimes and how they relate to climate change. In 2007, the Intergovernmental Panel on Climate Change (IPCC) stated that global warming would increase winter flooding in the western U.S. In 2013, the IPCC stated "There continues to be a lack of evidence and thus low confidence regarding the sign of trend in the magnitude and/or frequency of floods on a global scale over the instrumental record" (p. 112, Stocker et al., 2013) and that there is only medium confidence that modern floods have been larger than historical floods in central North America (Stocker et al., 2013).
Our understanding of flood hazard is based upon flood magnitude-frequency curves derived from a short observational period, limiting our knowledge of the potential for extreme flooding. In the southwestern U.S., the gaged and historical record rarely exceeds one hundred years; therefore, large floods are statistically under-represented (Thornycraft et al., 2003). Paleoflood studies produce flood chronologies that can be used to improve flood-frequency analysis (e.g. Benito and Thornycraft, 2005; Harden, et al., 2015) and maximum flood discharge-drainage area relationships (Enzel et al., 1993).
This research poses the following questions for the Upper Colorado River basin: (1) What is the magnitude and frequency of extreme paleofloods? (2) How does the addition of new paleoflood information alter flood frequency curves and confidence intervals at low annual exceedance probabilities (AEPs)? (3) How do paleoflood data alter the temporal context of modern and historical extreme floods with regard to their magnitude and frequency?

Need and Benefit

The proposed research addresses Priority Area 4.03 in the long term user needs document (Brekke et al., 2011). This was identified as a high priority research area within the Natural Systems Response step. With over 60 dams in the Upper Colorado River watershed and major infrastructure on the mainstem Colorado River, this work will help to inform flood risk for a broad range of infrastructure. Despite the powerful application of dendrochronology in the Colorado River basin as an excellent proxy for average annual streamflow, it provides little or no information for reconstructing extreme flood events because floodwaters are conveyed too rapidly across the landscape to allow for significant increases in soil moisture (a primary driver for tree growth). The lack of understanding of flood potential can lead to ineffective management of reservoirs during flood events, which may result in costly flood damage downstream and the lost opportunity for water storage. By working cooperatively with local universities and other federal agencies, this project will reduce the cost of obtaining this information by greater than 50% when accounting for cost share and lower daily rates for university staff.

Contributing Partners

Contact the Principal Investigator for information about partners.

Research Products

Bureau of Reclamation Review

The following documents were reviewed by experts in fields relating to this project's study and findings. The results were determined to be achieved using valid means.

Paleoflood Hydrology of the Colorado River System (final, PDF, 5.6MB)
By Jeanne Godaire
Research Product completed on September 30, 2019

This research product summarizes the research results and potential application to Reclamation's mission.

Paleoflood Hydrology of the Colorado River System (final, PDF, 1.3MB)
By Jeanne Godaire
R&D Bulletin completed on September 30, 2019

This research product summarizes the research results and potential application to Reclamation's mission.

Return to Research Projects

Last Updated: 4/4/17

STAY
IN
TOUCH

RECLAMATION
Managing Water in the West

U.S. Department of the Interior
Bureau of Reclamation

Paleoflood Hydrology of the Colorado River System

Deciphering the history of extreme floods from the geologic record

Research Bulletin
Science and Technology Program

S&T Project 1736

This project develops a history of extreme floods in the Upper Colorado River basin using paleoflood information from the geologic record. Paleoflood data improve the estimation of extreme floods, reducing the uncertainty in their magnitude and frequency for flood hazard assessments and long-term planning at Reclamation dams and reservoirs.

Mission Issue

Improved understanding of flood potential leads to effective management of reservoirs during flood events and in long term water planning, which may result in reduced downstream flood damage and greater opportunity for water storage.

Principal Investigator

Jeanne Godaire
Supervisory Geologist
Geotechnical Services Division
Technical Services Center
jgodaire@usbr.gov

Research Office Contact

Kenneth Nowak
Water Availability Research Coordinator
Research and Development Office
knowak@usbr.gov

Problem

Our understanding of flood hazard is based upon flood magnitude-frequency curves derived from a short observational period, limiting our knowledge of the potential for extreme flooding. In the southwestern U.S., the gaged and historical record rarely exceeds one hundred years; therefore, large floods are statistically under-represented (Thornycraft et al., 2003).

Despite the powerful application of dendrochronology in the Colorado River basin as an excellent proxy for average annual streamflow, it provides little or no information for reconstructing extreme flood events because floodwaters are conveyed too rapidly across the landscape to allow for significant increases in soil moisture (a primary driver for tree growth).

Paleoflood studies produce flood chronologies that can be used to improve flood-frequency analysis (e.g. Benito and Thornycraft, 2005; Harden, et al., 2015), maximum flood discharge-drainage area relationships (Enzel et al., 1993), and flood-climate linkages (e.g. Macklin and Lewin, 2003; Harden et al., 2010).

Solution

The project focused on the Green River, a major tributary to the Colorado River, and the Colorado River downstream of Lees Ferry, Arizona in order to investigate the magnitude and frequency of floods in the Upper Colorado River Basin (UCRB).

The sequence and ages of flood deposits were described; stage and associated discharges for each flood deposit were modeled using two-dimensional hydraulic models. These data were input into flood frequency analyses along with the systematic gage records to provide updated flood frequency curves. Using the chronological ages from flood deposits and paleoclimate records from sites in the UCRB and elsewhere, linkages between extreme floods and climate patterns were also explored. This provides an understanding of the hydroclimatology that can drive extreme floods in the UCRB.

Location map of study sites in the Upper Colorado River Basin (UCRB). Purple rectangles indicate paleoflood data developed and/or utilized for this project.

"The very real information on the most extreme floods that can be discovered through paleoflood studies offers a preferable alternative to conventional flood-frequency analyses, both for estimating the risks posed by the most extreme flood phenomena and for communicating those risks both to river managers and to the general public."

Jeremiah Bradshaw, P.E.
Electrical Engineer
Technical Service Center

Collaborators

Victor R. Baker
Department of Hydrology and Atmospheric Sciences
University of Arizona

Tessa Harden
Oregon Water Science Center
U.S. Geological Survey

Mark Miller
Moab Field Office
U.S. Bureau of Land Management

Ronda Newton
Grand Canyon National Park
U.S. National Park Service

More Information

https://www.usbr.gov/research/projects/detail.cfm?id=1736

Application and Results

The detailed investigation into the paleoflood record revealed that extreme floods are much more frequent than the systematic gage record would suggest and highlights the problem with the short length of gaging records. On the Green River, results from paleoflood investigations indicate that extreme floods occur on a much more frequent basis and have greater magnitudes than floods in the systematic record, the largest of which are about two times greater in magnitude than historical floods.

A test using the systematic gage record without the paleoflood data shows that the flood frequency analysis overestimates the return period of extreme floods. In other words, when paleoflood data are incorporated into the flood frequency analysis, the return period of extreme floods, as well as the 100-year flood, is much more frequent. Previous investigations on the Colorado River and new preliminary investigations on the Colorado River in Grand Canyon, Arizona indicate that the peak discharge associated with the highest stage of the slackwater deposits is 1.5-2.5 times larger than the peaks of record in the systematic gage records. By using 77 chronological ages from seven stratigraphic sites of slackwater deposits in the UCRB, several clusters of extreme flood activity are identified: 8040-7790, 3600-3640, 2880-2740, 2330-700 and 620-0 years BP.

Comparison of paleoflood records of extreme floods to paleoclimate records reveal that extreme floods occur in both wet and dry periods. The authors attribute the periods of extreme floods in the UCRB to an increased intensity of storms from the North Pacific that are associated with enhanced ENSO variability. The extreme floods appear to happen less frequently in more stable wet periods or stable dry periods. This research can be applied to water operations and flood hazard assessments in the Upper Colorado River Basin to model the actual frequency of extreme floods and in long term planning in the watershed.

Future Plans

The analyses and conclusions of this study are limited by the relatively small number of paleoflood sites and geochronological ages in the Upper Colorado River Basin. Most of Reclamation's data on tributaries to the Upper Colorado River are in the form of non-exceedance bounds, which only provide upper limits to flood magnitude.

More locations of paleoflood estimates would further refine the paleoflood history of the Upper Colorado River Basin and our understanding of flood-climate linkages. It is critical to continue the work on the Colorado River downstream of Lees Ferry, Arizona. This specific reach is important because it includes all the drainage area for the major dams and water supply from the Upper Colorado River Basin.

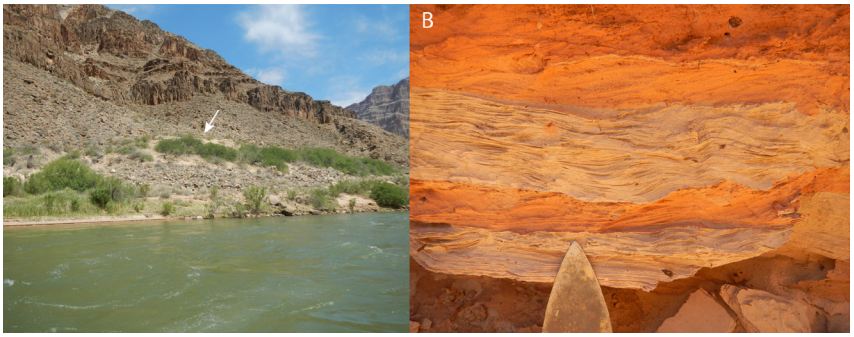

Slackwater deposits along the Colorado River, Grand Canyon. A. Example of a slackwater deposit, top of deposit is shown by white arrow; B. Example of the stratigraphy of flood deposits showing mainstem Colorado River flood deposits (light tan units) interbedded with tributary deposits (reddish-orange units). Photos courtesy of Tess Harden, USGS.

RECLAMATION

Managing Water in the West

Paleoflood Hydrology of the Colorado River System

Research and Development Office
Science and Technology Program
(Final Report) ST-2019-1736-01

U.S. Department of the Interior
Bureau of Reclamation
Research and Development Office

9/30/2019

Mission Statements

Protecting America's Great Outdoors and Powering Our Future

The Department of the Interior protects and manages the Nation's natural resources and cultural heritage; provides scientific and other information about those resources; and honors its trust responsibilities or special commitments to American Indians, Alaska Natives, and affiliated island communities.

REPORT DOCUMENTATION PAGE		*Form Approved* *OMB No. 0704-0188*
T1. REPORT DATE: 2019	**T2. REPORT TYPE:** RESEARCH	**T3. DATES COVERED** 8/24/2019-9/30/2019
T4. TITLE AND SUBTITLE Paleoflood Hydrology of the Colorado River System		**5a. CONTRACT NUMBER** XXXR4524KS-RR4888FARD1805701 (8)
		5b. GRANT NUMBER
		5c. PROGRAM ELEMENT NUMBER 1541 (S&T)
6. AUTHOR(S) Jeanne Godaire Seismology and Geomorphology Group Technical Services Center Bureau of Reclamation P.O. Box 25007 86-68330 Denver, CO 80225		**5d. PROJECT NUMBER** ST-2019-1736-01
		5e. TASK NUMBER
		5f. WORK UNIT NUMBER 86-6833000
7. PERFORMING ORGANIZATION NAME(S) AND ADDRESS(ES) Victor R. Baker Department of Hydrology and Atmospheric Sciences University of Arizona Tucson, AZ 85721		**8. PERFORMING ORGANIZATION REPORT NUMBER** ST-2019-1736-01
9. SPONSORING / MONITORING AGENCY NAME(S) AND ADDRESS(ES) Research and Development Office U.S. Department of the Interior, Bureau of Reclamation, PO Box 25007, Denver CO 80225-0007		**10. SPONSOR/MONITOR'S ACRONYM(S)** **R&D:** Research and Development Office **BOR/USBR:** Bureau of Reclamation DOI: Department of the Interior
		11. SPONSOR/MONITOR'S REPORT NUMBER(S) ST-2019-1736-01

12. DISTRIBUTION / AVAILABILITY STATEMENT
Final report can be downloaded from Reclamation's website: https://www.usbr.gov/research/

13. SUPPLEMENTARY NOTES

14. ABSTRACT *(Maximum 200 words)*

The project focused on the Green River, a major tributary to the Colorado River, and the Colorado River downstream of Lees Ferry, Arizona in order to investigate the magnitude and frequency of floods in the Upper Colorado River Basin (UCRB). The detailed investigation into the paleoflood record revealed that extreme floods are much more frequent than the systematic gage record would suggest and highlights the problem with the short length of gaging records.

15. SUBJECT TERMS paleoflood hydrology, Colorado River, climate, hydrology, floods

16. SECURITY CLASSIFICATION OF:			**17. LIMITATION OF ABSTRACT**	**18. NUMBER OF PAGES**	**19a. NAME OF RESPONSIBLE PERSON**
			U	122	Jeanne Godaire
a. REPORT	**b. ABSTRACT**	**c. THIS PAGE**			**19b. TELEPHONE NUMBER**
U	U	U			303-445-3164

S Standard Form 298 (Rev. 8/98)
P Prescribed by ANSI Std. 239-18

BUREAU OF RECLAMATION

Research and Development Office
Science and Technology Program

Seismology and Geomorphology Group, Technical Services Center, 86-68330

(Final Report) ST-2019-1736-01

Paleoflood Hydrology of the Colorado River System

Prepared by: Jeanne E. Godaire, M.S.
Supervisory Geologist, Seismology and Geomorphology Group, Technical Services Center, 86-68330

Peer Review: Giorgia Fulcheri, PhD
Geologist, Seismology and Geomorphology Group, Technical Services Center, 86-68330

This document has been reviewed under the Research and Development Office Discretionary peer review process https://www.usbr.gov/research/peer_review.pdf consistent with Reclamation's Peer Review Policy CMP P14. It does not represent and should not be construed to represent Reclamation's determination, concurrence, or policy.

Acknowledgements

This project was funded by the Science and Technology Program Research and Development Office, and Dam Safety Technology Development Program. Most of the work for this project was performed by the University of Arizona under Bureau of Reclamation Cooperative Agreement no. R16AC00021. Cost share partners include BLM Canyonlands and U.S. Geological Survey. Giorgia Fulcheri (Bureau of Reclamation) provided peer review for this report. Joanna Redwine (Bureau of Reclamation) participated in the field reconnaissance of the Grand Canyon, Arizona.

Acronyms and Abbreviations

UCRB: Upper Colorado River Basin

LCRB: Lower Colorado River Basin

OSL: Optically Stimulated Luminescence

Executive Summary

The Colorado River basin supplies southwestern U.S. states and Mexico with water for domestic and agricultural purposes, making it a critical water supply in the western U.S. Runoff is derived mainly from the Upper Colorado River Basin (UCRB), where flood flows from snowmelt or rain-on-snow events produce large volumes of water to be stored at Reclamation reservoirs. The record of extreme floods is limited by the short systematic gage record, which in turn limits the understanding of the real frequency of extreme floods. This study utilizes methods in paleoflood hydrology to document floods prior to the systematic gage record, effectively extending the record length of extreme floods by thousands of years in the UCRB. The research poses the following questions for the Upper Colorado River basin: (1) What is the magnitude and frequency of extreme paleofloods? (2) How does the addition of new paleoflood information alter flood frequency curves and confidence intervals at low annual exceedance probabilities (AEPs)? (3) How do paleoflood data alter the temporal context of modern and historical extreme floods with regard to their magnitude and frequency?

The project focused on the Green River, a major tributary to the Colorado River, and the Colorado River downstream of Lees Ferry, Arizona in order to investigate the magnitude and frequency of floods in the UCRB. The sequence and ages of flood deposits were described; stage and associated discharges for each flood deposit were modeled using 2-dimensional hydraulic models (SRH-2D); (Lai 2009). These data were input into flood frequency analyses along with the systematic gage records to provide updated flood frequency curves. Using the chronological ages from flood deposits and paleoclimate records from sites in the UCRB and elsewhere, linkages between extreme floods and climate patterns were also explored. This provides an understanding of the hydroclimatology that can drive extreme floods in the UCRB.

The detailed investigation into the paleoflood record revealed that extreme floods are much more frequent than the systematic gage record would suggest and highlights the problem with short gaging records. For example, when paleoflood data are incorporated into the flood frequency analysis for the Green River, the return period of extreme floods, as well as the 100-year flood, is much shorter. Preliminary investigations on the Colorado River in Grand Canyon, Arizona indicates that the peak discharge associated with the highest stage of the slackwater deposits is larger than peak discharges calculated for sites documented in previous investigations and larger than the peak of record in the systematic gage records. By using 77 chronological ages from seven stratigraphic sites of slackwater deposits in the UCRB, the authors identify several clusters of extreme flood activity: 8040-7790, 3600-3640, 2880-2740, 2330-700 and 620-0 years BP. Comparison of paleoflood records of extreme floods to paleoclimate records reveal that extreme floods occur in both wet and dry periods. The authors attribute the periods of extreme floods in the UCRB to an increased intensity of storms from the North Pacific that are associated with enhanced ENSO variability. The extreme floods appear to happen less frequently in more stable wet periods or stable dry periods.

The analyses and conclusions of this study are limited by the small number of paleoflood sites in major tributaries of the Upper Colorado River Basin and the corresponding small sample number of geochronological ages used to support the conclusions. More locations of paleoflood estimates would further refine the paleoflood history of the UCRB and our understanding of flood

generating mechanisms and climate patterns in a long-term context. A critical piece in developing the paleoflood hydrology of the Upper Colorado River system is to complete the work on the Colorado River in the Grand Canyon that was initiated during this study. This particular reach is important because it includes all the drainage area for the major dams and water supply for the Upper Colorado River Basin.

Contents

Executive Summary v
1.0 Introduction 1
1.1 Background 1
1.2 Project Goals 1
1.3 General Plan and Major Tasks 2
2.0 Methods 3
3.0 Previous Work 3
3.1 Reclamation studies 3
3.2 Published Literature and Theses 4
4.0 Results 6
5.0 Conclusions 9
6.0 Recommendations for Further Work 10
7.0 References 11
Appendix A – Paleoflood Hydrology on the lower Green River, Upper Colorado River Basin, USA: An Example of a Naturalist Approach to Flood-Risk Analysis A–001
Appendix B – Holocene Paleoflood and their Climatological Context, Upper Colorado River Basin, USA B–001
Appendix C – Final Program Performance Report: Paleoflood Hydrology of the Colorado River System C–1

Tables

Table 1. Radiocarbon ages of flood deposits from Reclamation studies. 9

Figures

Figure 1. Location map of study sites in the Upper Colorado River Basin (UCRB). Purple rectangles indicate paleoflood data developed and/or utilized for this project. 6
Figure 2. Location map of paleoflood sites in the Upper Colorado River Basin (UCRB). Purple rectangles indicate paleoflood data developed and/or utilized for this project. 8

1.0 Introduction

Extreme flooding and climate variability and continue to be topics of concern in watersheds managed by Reclamation. This study demonstrates that a lack of data can impact our understanding of the frequency and magnitude of extreme floods. This lack of understanding in turn can impact our ability to effectively manage water resources in the western U.S. Water operations are driven by the quality of data that informs Reclamation's decisions as a water management agency. The improved understanding of flood potential can lead to more effective management of reservoirs during flood events, which may result in reduced flood damage downstream and greater opportunity for water storage. With increasing demand for water storage in the western U.S., higher pool elevations during flood seasons could increase the likelihood of flood operations; improving the understanding of extreme floods and planning for these events is therefore critical to management of Reclamation's infrastructure.

1.1 Background

The Upper Colorado River Basin (UCRB) drains approximately 111,800 mi^2 (289,562 km^2) of Colorado, Utah, New Mexico, Wyoming and Arizona and is one of the major basins for domestic and agricultural water supply in the western U.S. Major tributaries to the Upper Colorado River include the Green River, the Gunnison River, the San Juan River, the Dolores River, the Escalante River and the Paria River. While snowmelt provides the main source of water supply in the basin headwaters, extreme floods can be derived from rain-on-snow or rainfall driven regional events. Tributaries that originate at lower elevations in the basin produce extreme floods primarily by heavy regional rainfall events or by local convective storms.

Over 60 dams and reservoirs impound water in the UCRB and on the mainstem Colorado River. The type of infrastructure is diverse, ranging from diversion dams to some of the largest dams and reservoirs in Reclamation's inventory. Their importance in the delivery of water to the American west is undeniable, with close to 40 million people in Arizona, Nevada, California, New Mexico and Colorado depending on its water for their livelihood. Recent droughts and increasing water demands heighten the challenges of water operations at Reclamation facilities in the Colorado River Basin.

1.2 Project Goals

Although future climate simulations vary in the exact timing and magnitude of projected changes, considerable agreement exists amongst all models that hydrologic changes will be paramount in semi-arid regions of western North America (IPCC 2007) . Hydrologic studies show differing results regarding the characteristics of extreme flood regimes and how they relate to climate change. In 2007, the Intergovernmental Panel on Climate Change (IPCC) stated that global warming would increase winter flooding in the western U.S. In 2013, the IPCC stated "There continues to be a lack of evidence and thus low confidence regarding the sign of trend in the magnitude and/or frequency of floods on a global scale over the instrumental record" (p. 112, Stocker, et al. 2013) and that there is only medium confidence that modern floods have been larger than historical floods in central North America (Stocker, et al. 2013).

Our understanding of flood hazard is based upon flood magnitude-frequency curves derived from a short observational period, limiting our knowledge of the potential for extreme flooding. In the southwestern U.S., the gaged and historical record rarely exceeds one hundred years; therefore, large floods are statistically under-represented. Despite its powerful application in the Colorado River basin as an excellent proxy for average annual streamflow, dendrochronology provides little or no information for reconstructing extreme flood events because floodwaters are conveyed too rapidly across the landscape to allow for significant increases in soil moisture (a primary driver for tree growth).Paleoflood studies produce flood chronologies that can be used to improve flood-frequency analysis (e.g. (Harden, O'Connor and Driscoll 2015); and maximum flood discharge-drainage area relationships (Enzel, et al. 1993).

This research poses the following questions for the Upper Colorado River basin: (1) What is the magnitude and frequency of extreme paleofloods? (2) How does the addition of new paleoflood information alter flood frequency curves and confidence intervals at low annual exceedance probabilities (AEPs)? (3) How do paleoflood data alter the temporal context of modern and historical extreme floods with regard to their magnitude and frequency?

To answer the study questions, there are three major objectives:

1. Determine the magnitude and age range of extreme floods prior to the observational record and temporal distribution of floods in subbasins of the Upper Colorado River basin and on the mainstem Colorado River. Paleoflood field studies, geochronology lab analysis and hydraulic modeling will be used to complete this objective.

2. Combine the paleoflood record and historical hydrologic record into flood frequency analyses using flood frequency tools that combine historical and paleoflood data.

3. Compare new flood frequency curves with paleoflood data to existing flood frequency analyses to determine the effect of the new paleoflood data on confidence intervals and on the annual exceedance probability (AEP) of modern and historical floods.

1.3 General Plan and Major Tasks

The study is focused on collecting paleoflood data on the major tributaries to the Upper Colorado River and on the mainstem Upper Colorado River. The data collected will be compiled and analyzed to provide an overall picture of the paleoflood history of the Upper Colorado River basin. For example, the record of extreme paleofloods from major tributaries will be compared to the record of extreme paleofloods on the mainstem Colorado River to determine whether the source of extreme flooding can be determined. For the major tributaries, this study focuses on paleoflood data collection on the lower Green River given that this tributary does not have any available paleoflood data while other major tributaries such as the Dolores River, San Juan River, Paria River and Escalante River have been studied previously. Study areas include:

- Lower Green River, near confluence with Colorado River
- Mainstem Upper Colorado River, Arizona

This project is a collaborative effort between the University of Arizona and Bureau of Reclamation and includes cost share from other federal agencies including BLM and USGS.

2.0 Methods

Paleoflood hydrology is defined as “the reconstruction of the magnitude and frequency of recent, past, or ancient floods using geological evidence” (Kochel, Patton and Baker 1982). Paleoflood hydrology uses procedures to reconstruct the magnitude and frequency of past floods, including the determination of paleoflood peak discharges and their time of occurrence (V. R. Baker 2008).

The paleoflood reconstruction uses fine-grained slackwater flood deposits (SWD) and other paleostage indicators (PSI), with the former deposited rapidly from suspension in sites where flow velocities are significantly reduced (Baker, Kochel and Patton, Long-term flood-frequency analysis using geologic data 1979); (Baker and Costa 1987). These indicators represent the high stage of the flood and provide the best natural record of large flood magnitudes. Ideal paleoflood sites preserve multiple flood stratigraphic records that can be separated into individual flow events using sedimentological criteria (V. Baker 1987). Age constraints from individual floods can usually be derived from slackwater deposits by locating charcoal and other organic materials for radiocarbon (^{14}C) dating (Arnold and Libby 1949); (Bowman 1990). If the sediment is composed of quarts grains, optically stimulated luminescence (OSL) dating can be used to directly date the sediments age of deposition (Wallinga 2008). Paleo-discharge estimates are obtained using one-dimensional (1D) or two-dimensional (2D) hydraulic models that generate water surface profiles for various discharge values ((Hydraulic Engineering Center 2015); (Lai 2009).

Flood frequency tools that incorporate gage records and paleofloods have been developed by various federal agencies, and have included PeakfqSA (Cohn, Lane and Baier 1997); (Griffis, Stedinger and Cohn 2004), FLDFRQ3 (O'Connell, et al. 2002) and most recently, Bulletin 17C (England, et al. 2018). These programs can be utilized to examine the frequency and magnitude of extreme floods. Flood frequency output can be evaluated for its validity by comparing to regional envelope curves, which provide regional discharge-drainage area relationships for extreme gaged floods, and for evaluating the statistics of the flood frequency distribution (Enzel, et al. 1993); (Blainey, et al. 2002).

3.0 Previous Work

3.1 Reclamation studies

Previous paleoflood investigations prior to this work have been performed by Reclamation in the UCRB, although many have been limited in scope (Figure 1). Reclamation has conducted paleoflood investigations on tributaries to the Colorado River near Reclamation facilities. These include Big Sandy River (Big Sandy Dam; (Godaire and Hilldale, Paleoflood Study, Big Sandy River near Big Sandy Dam, Wyoming 2016), Gunnison River (Blue Mesa Dam; (Klinger and Bauer 2007), Cimarron River (Silver Jack Dam; (Klinger and Bauer 2007), Duschesne River basin (Klawon, Bauer and Klinger 2006), Price River Basin (Klawon, Bauer and Klinger 2006), Taylor River (Taylor Park Dam; (Godaire, et al. 2016), Uncompaghre River (Ridgway Dam;

(Klinger and Bauer 2005), and Blue River (Green Mountain Dam; (Godaire and Bauer 2010). In addition, reconnaissance level investigations have been performed at several facilities as part of the Comprehensive Review process. These include Rifle Creek (Rifle Gap Dam), Fryingpan River (Ruedi Dam), Upper Green River (Flaming Gorge Dam and Fontenelle Dam), Strawberry River (Soldier Creek Dam and Starvation Dam), Los Pinos River (Vallecito Dam), Dolores River (McPhee Dam), Cottonwood Creek (Joes Valley Dam), unnamed drainage upstream from Steinaker Dam, and Brush Creek (Red Fleet Dam).

3.2 Published Literature and Theses

While some paleoflood hydrology studies have been completed in the Colorado River system, these studies have been site specific and have not attempted to develop a basin wide history of extreme paleofloods in the upper Colorado River basin (Figure 1). Results from paleoflood investigations on the Colorado River near Lees Ferry, AZ were published in the 1990s (O'Connor, et al. 1994). The Axehandle Alcove site is a small rock shelter that records a history of extreme floods greater than or equal to floods in the systematic gage record. The authors found at least one flood deposit of laminated silts and sands in a rock crevice 4 meters above the larger slackwater deposit that exceed the magnitude of the 1884 flood (~8500 m^3/s; ~300,000 ft^3/s) by 1.65 times. Based on radiocarbon dating, this flood occurred between 1600 and 1200 years ago. The record of the 1884 flood appears to be preserved at the top of the sequence of slackwater deposits. Preserved in the sequence below the 1884 flood deposit are 15 flood deposits, representing 15 separate floods, that equal or exceed the magnitude of the largest historical flood of 1921, which was measured at 6250 m^3/s (220,720 ft^3/s).

Through a previous Financial Assistance Agreement with the University of Arizona (no. 09-FC-81-1503), Reclamation partially supported paleoflood investigations in the Colorado River watershed. Outcomes from previous work include paleoflood investigations along the Colorado River near Moab, Utah, which indicate that at least 2 paleofloods within the last 2,000 years are more than 2.5 times larger than floods in the historical record (Greenbaum, et al. 2014). Flood frequency analysis incorporating paleoflood data indicates that the largest historical flood of 1884 has a recurrence interval of less than 100 years. The largest two paleofloods documented in this reach exceed the PMF calculated by the USGS (~8500 m^3/s; 300,000 ft^3/s) for the Colorado River near Moab, Utah. With the incorporation of paleoflood data in the flood frequency analysis, the PMF has a return period of about 1,000 years. In the Dolores River basin, paleoflood magnitude and frequency information were developed as part of a PhD dissertation (Cline 2010). Paleoflood field investigations along the lower Green River and in Cataract Canyon on the Colorado River were conducted in 2012 and included stratigraphic descriptions, sample collection, Optically Stimulated Luminescence (OSL) and radiocarbon analyses. The remaining hydraulic modeling for these sites were completed for lower Green River and Cataract Canyon during this project.

Other relevant investigations on tributaries to the Colorado River include paleoflood hydrology studies on the San Juan River (Orchard 2001), Paria River (Webb, Blainey and Hyndman 2002) and the Escalante River (Webb, O'Connor and Baker 1988); (Webb 1985). On the San Juan River, Orchard (2001) found that the 1911 flood was the largest flood recorded in slackwater deposits. Peak discharges for this flood were reconstructed using driftwood lines in the study

reach that were nearly continuous and that contained historical evidence such as sawn wood and wood with nails. The peak discharge estimate for this flood from step-backwater analysis was 4,200 m^3/s (148,300 ft^3/s) for a drainage area of 23,000 mi^2 and is the largest flood within the last 100 years or more. In the study reach, radiocarbon dating was not performed because all slackwater deposits were historical in age based on seeds of Russian thistle (a historically introduced plant) present in the deposits and burial of historical features by the slackwater sediment.

On the Escalante River, Webb et al. (1988) found evidence for paleofloods that were 5 to 7 times larger than the largest historical flood, which was measured at ~500 m^3/s (17,655 ft^3/s). Two separate sites were investigated and are located 3.2 and 7.8 km downstream from the USGS gaging station no. 09337500, Escalante River near Escalante, Utah. Paleofloods were documented at the two sites within the last 2100 years, with extreme floods recorded between 1100 and 980 yr BP and between 600 and 400 yr BP. The largest food in the paleoflood record had a modeled peak discharge of 720 m^3/s (~25,420 ft^3/s), which is within the range of the largest floods for similar sized basins on the Colorado Plateau and plots near the regional envelope curve developed in the study. Flood deposits younger than 300 years were also identified in the slackwater deposits and matched to anecdotal accounts and gage measurements of historic floods in 1909, 1916, 1927, and 1932. Incorporation of the peak discharge calculations for the historic floods into the flood frequency analysis increase the magnitude of the 100-year flood from 193 m^3/s (6,815 ft^3/s) to 480-630 m^3/s (16,949-22,245 ft^3/s).

The Paria River was investigated by Webb et al. (2002) at Bonza Alcove, located in a bedrock canyon that is about 15-30 km downstream from the Arizona-Utah border. Extreme paleofloods are documented in the slackwater deposits preserved at Bonza Alcove and range in age from10,400 BC to prehistoric. Peak discharges calculated by step-backwater modeling range from 1,200-2,400 m^3/s (~42,400-84,750 ft^3/s), which are much greater than peak discharges recorded in the systematic record, the largest of which was 456 m^3/s (16,103 ft^3/s) (USGS gaging station no. 09382000, Paria River at Lees Ferry, Arizona). Flood frequency analyses were also performed for this study; results indicate that the addition of paleofloods does not change the estimates for extreme floods on the Paria River but does reduce the uncertainty for those estimates by narrowing the confidence intervals at the longer recurrence intervals.

Figure 1. Location map of study sites in the Upper Colorado River Basin (UCRB). Purple rectangles indicate paleoflood data developed and/or utilized for this project.

4.0 Results

Results from this project focus on report results from paleoflood studies on the lower Green River and compiling paleoflood chronologies from tributaries to the Colorado River and the main stem Colorado River to investigate linkages between extreme floods and climate variability in the paleoflood and paleoclimate record.

On the Green River in Stillwater Canyon, Liu et al. (in press) described 9 stratigraphic sequences of slackwater deposits at six sites along a 35 km long reach from Deadhorse Canyon to the confluence with the Colorado River (Appendix A). Using the stage of the slackwater deposits and 2-dimensional hydraulic modeling (SHR-2D); (Lai 2009), they documented at least 14 paleofloods in the last 700 years with magnitudes greater than 2 times the largest historical gaged flow of 1,929 m^3/s (68,113 ft^3/s). The largest paleoflood has a minimum discharge of 7500 m^3/s (264,825 ft^3/s). This indicates that extreme floods occur on a much more frequent basis than the systematic record would suggest. Multiple methods were used to generate flood frequency curves, including Bulletin 17C (England, et al. 2018), Bulletin 17B (IACWD 1982), the log normal distribution (Chow, Maidment and Mays 1988), the self-similar model (Kidson and Richards 2005); (Malamud and Turcotte 2006) and the regional regression equation (Kenney, Wilkowske and Wright 2007). A test using the systematic gage record without the paleoflood data shows that the flood frequency analysis severely overestimates the return period of extreme floods. In other words, when paleoflood data are incorporated into the flood frequency analysis, the return period of extreme floods is much shorter.

The Upper Colorado River Basin was also investigated during this study to understand how extreme floods are associated with climate patterns in the paleorecord (Appendix B). Liu et al. (in press) compared the occurrence of extreme floods in the paleoflood record to paleoclimate records of climate variability in the Upper Colorado River Basin (UCRB) and from previous studies, the Lower Colorado River Basin (LCRB; (Ely, et al. 1993); (Ely 1997); (Harden, Macklin and Baker 2010) to highlight linkages between climate patterns and extreme floods in the paleoflood record and postulate the hydroclimatology of the extreme flood events. For the paleoflood records, they utilized 77 geochronological ages (39 radiocarbon, ^{14}C and 38 OSL) and the cumulative probability density functions of the calibrated ages to derive a flood chronology. Five flood episodes were identified within the last 8,000 years BP and are as follows: 8040-7790, 3600-3640, 2880-2740, 2330-700, and 620-0 years BP. The distribution of ages is skewed? toward the younger flood periods because of the greater likelihood of preservation of younger flood deposits. Paleoclimate records of precipitation variations were utilized to provide information on wet/dry periods during the Holocene (<10ka). They include: (1) δ^{18} records from alpine lakes (Yellow, Bison and San Luis Lakes) in the Colorado Rocky Mountains (Anderson, 2011; Anderson, 2012; Yuan et al., 2013); (2) high resolution δ^{18} records from Pink Panther Cave in the Guadalupe Mountains, New Mexico (Asmerom et al., 2007) and (3) Holocene ENSO variability derived from El Nino frequency from Ecuador and the Galapagos Islands (Moy et al., 2002; Conroy et al., 2008). The following patterns were identified:

- 10500-6700 years BP: prevailing dry period with arid conditions, punctuated by a brief wet period of increased probability of extreme flood episodes around 8000 years BP.
- 6700-~2800 years BP: stable wet period with a low probability of extreme flood episodes, except for two weak flood episodes defined (3600-3460 years BP, 2880-2740 years BP) in the UCRB, and several high probability extreme flood episodes in the Lower Colorado River Basin (LCRB).
- ~2800-~2300 years BP: dry conditions in the southern part of the UCRB and wet conditions in the northern part of the UCRB with a low probability of extreme flood episodes in the entire Colorado River Basin

- ~2300-620 years BP: overall dry conditions with megadrought conditions during the Medieval Climate Anomaly (MCA, 1150-700 years BP). Increasing ENSO dominance and negative excursions in the δ^{18} values suggest that some locations in the UCRB may have returned to wetter conditions. This period has a high probability of extreme flood episodes in both the UCRB from 2330-700 years BP and in the LCRB.
- Post-620 years BP: dry conditions with a slight increase in winter precipitation during the Little Ice Age (LIA, ~350-200 years BP). This period coincides with a high probability of extreme flood episodes in both the LCRB and UCRB (620-0 years BP).

The authors attribute the periods of extreme floods in the UCRB to an increased intensity of storms from the North Pacific that are associated with enhanced ENSO variability. The extreme floods appear to happen less frequently in more stable wet periods or stable dry periods. This may happen because the precipitation in the wet periods occurs in the winter and does not experience rapid melting or rain-on-snow events that would produce large floods in the basin and because in the dry periods the Pacific airstream may be located further to the north in the UCRB.

In April 2018, a field reconnaissance trip was completed to further identify slackwater deposits on the mainstem Colorado River between Glen Canyon Dam and Lake Mead that could be utilized to develop a paleoflood chronology to complement the work performed in the 1990s at Axehandle Alcove (Appendix C) (O'Connor, et al. 1994) (Figure 2). An abundance of slackwater deposits was found during the reconnaissance trip, some of which were located at a higher elevation than those investigated at Axehandle Alcove. Preliminary modeling of the slackwater sites indicates that the peak discharge associated with the highest stage of the slackwater deposits is larger than peak discharges calculated for the Axehandle Alcove site and comparable to the PMF peak discharge calculated for Glen Canyon Dam (~700,000 ft^3/s (~20,000 m^3/s); (U.S. Bureau of Reclamation 1990).

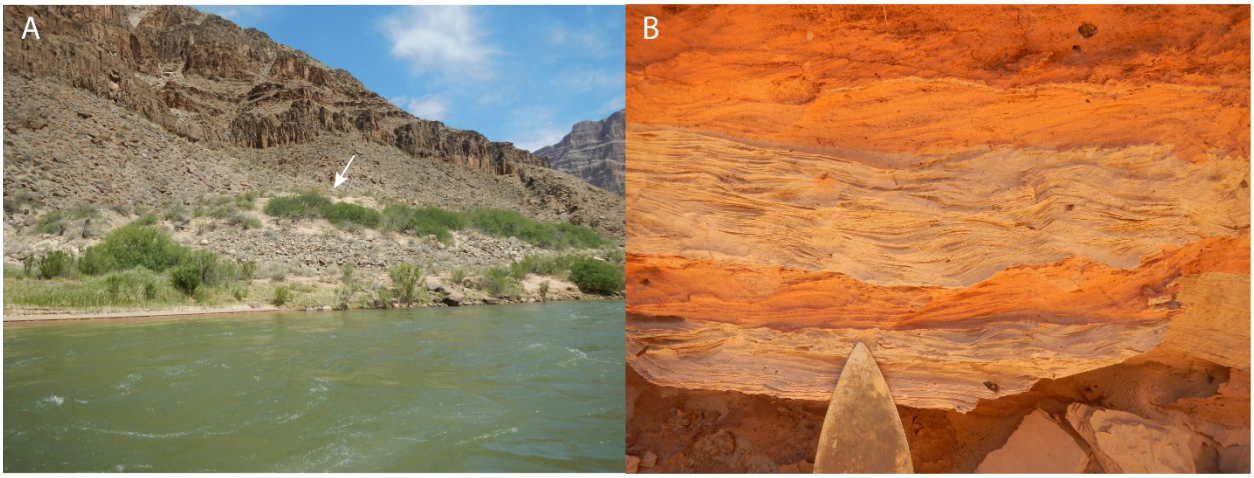

Figure 2. Location map of paleoflood sites in the Upper Colorado River Basin (UCRB). Purple rectangles indicate paleoflood data developed and/or utilized for this project.

Although Reclamation has completed investigations on many tributaries to the Upper Colorado River, much of the data developed in these investigations are in the form of non-exceedance bounds. The non-exceedance methodology utilizes stream terraces to estimate an upper limit to

the magnitude of floods over specific time intervals (Levish 2002). The ages and discharges are defined in a similar manner to paleoflood estimates; however, the non-exceedance bounds do not represent a record of extreme floods but only an upper limit based on the presence of stable soils. A few paleofloods are estimated that could be applied to the analysis in this project. These include estimates on the Big Sandy River, Blue River, Currant Creek, Red Creek and Taylor River (Table 1). Radiocarbon ages from flood deposits along these rivers are from charcoal that dates within the last ~2,000 years. Except for sample no. TRCR5-1, the ages plot within the periods of high probability for extreme flood episodes based on the work from this study. It is important to consider that the locations selected for Reclamation studies are based on proximity to the dam; the main priority is to accurately depict the flood hazard from the contributing drainage area at the dam. The reaches for these studies are not always ideal for the preservation of slackwater deposits; reaches in different parts of the watersheds could potentially be used to locate and describe slackwater deposits, and to develop an extreme flood history for tributaries in the UCRB.

Table 1. Radiocarbon ages of flood deposits from Reclamation studies.

Sample no.	River name	Radiocarbon age (BP)	Calibrated age (Cal yr BP)	Material
BSC5-1ROS	Big Sandy River[1]	150 ± 30	285-0	*Rosaceae*
BSC5-5ROS	Big Sandy River[1]	140 ± 30	285-0	*Rosaceae*
BR4-1	Blue River[2]	160 ± 20	290-0	*Salicaceae*
CC3-1QU	Currant Creek[3]	430 ± 30	530-330	*Quercus*
RC3-4JUN	Red Creek[3]	400 ± 40	520-320	*Juniper*
TRCR2-4CO	Taylor River[4]	2230 ± 30	2335-2150	Conifer
TRCR5-1	Taylor River[4]	826 ± 22	840-745	*Pinus*
TRCR5-7	Taylor River[4]	1708 ± 22	1760-1600	*Populus*

Notes: [1]Godaire and Hilldale 2016; [2]Godaire and Bauer 2011; [3]Klawon et al. 2006; [4]Godaire et al. 2017

5.0 Conclusions

This project utilizes methods in paleoflood hydrology to extend the record of extreme floods several thousand years beyond the systematic gage record. Paleoflood reconstructions on the lower Green River and mainstem Colorado River demonstrate that extreme floods in the UCRB are more frequent and of greater magnitude than is predicted by the systematic gage record alone. The use of paleoflood data in flood frequency analysis assists in refining estimates for the

100-year flood and for floods of longer return periods, in addition to reducing the uncertainty at longer return periods. As more paleoflood data are developed in the UCRB, linkages between climate variability and timing of extreme floods can be further explored. Data compilation and comparison of existing paleoflood age estimates and paleoclimate data indicates that extreme floods have happened in both wet and dry periods and are mainly associated with increased intensity of North Pacific storm tracks that bring moisture into the UCRB during phases of enhanced ENSO variability.

6.0 Recommendations for Further Work

The analyses and conclusions of this study are limited by the small number of paleoflood sites in major tributaries of the Upper Colorado River Basin and the corresponding small sample number of geochronological ages used to support the conclusions. Locations that specifically focus on reaches that preserve slackwater deposits in the upper basin would further refine the paleoflood history of the Upper Colorado River Basin and our understanding of flood generating mechanisms and climate patterns in a long-term context. Factors to consider in identifying future river reaches for research include the preservation potential and existence of slackwater deposits, basin areas and locations, stream gage data availability, channel constraints for modeling and assumptions of vertical and lateral stability, as well as the availability of existing information. The most useful locations to gather additional data, given that there are suitable reaches, include the Gunnison River, Dirty Devil River, mainstem Colorado River above the Green River (additional reach would help to corroborate data on Colorado River near Moab), and the San Juan River (locate slackwater stratigraphy with longer records).

A critical piece in the paleoflood hydrology of the Upper Colorado River system is to complete the work on the Colorado River in the Grand Canyon that was initiated during this study. This reach is important because it includes all the drainage area for the major dams and water supply for the Colorado River for the states of Arizona and California. These sites record the natural variability in flooding for the entire UCRB. Based on previous research by O'Connor et al. (1994), several thousand years of flood records are preserved in this reach. In addition, the gage record at Lees Ferry is one of the longest in the western U.S. and thus is a great data source for the flood frequency analysis. Previous work was limited in extent and could benefit greatly from a more detailed investigation of the flood deposits.

7.0 References

Arnold, J.R., and W. F. Libby. 1949. "Age determinations by Radiocarbon content: checks with samples of known age." *Science* 110 (2869): 678-680.

Baker, V. R. 2008. "Paleoflood hydrology: Origin, progress, prospects." *Geomorphology* 101 (1-2): 1-13.

Baker, V.R. 1987. "Paleoflood hydrology and extreme flood events." *Journal of Hydrology* 96: 79-99.

Baker, V.R., R. C. Kochel, and P. C. Patton. 1979. "Long-term flood-frequency analysis using geologic data." *International Association of Hydrological Science Publication* 128: 3-9.

Baker, Victor R., and John E. Costa. 1987. "Flood Power." In *Catastrophic Flooding*, by L. Mayer and D. Nash, 1-21. New York: John Wiley and Sons.

Blainey, J.B., R. H. Webb, M. E. Moss, and V. R. Baker. 2002. "Bias and information content of paleoflood data in flood-frequency analysis." In *Ancient Floods, Modern Hazards*, by P.K. House, R. H. Webb, V. R. Baker and D. R. Levish, 161-174. Washington, D.C.: American Geophysical Union.

Bowman, S. 1990. *Radiocarbon Dating.* Los Angeles: University of California Press.

Chow, V.T., D. R. Maidment, and L. W. Mays. 1988. *Applied Hydrology.* New York: McGraw-Hill.

Cline, M.L. 2010. *Extreme Flooding in the Dolores River Basin, Colorado and Utah: Insights from Paleofloods, Geochronology and Hydroclimate Analysis.* PhD Thesis, Tucson: University of Arizona.

Cohn, T.A., W. L. Lane, and W. G. Baier. 1997. "An algorithm for computing moments-based flood quantile estimates when historical flood information is available." *Water Resources Research* 33: 2089-2096.

Ely, L. L. 1997. "Response of extreme floods in the southwestern United States to climatic variations in the late Holocene." *Geomorphology* 19 (3-4): 175-201.

Ely, L.L., Y. Enzel, V. R. Baker, and D. R. Cayan. 1993. "A 5000-year record of extreme floods and climate change in the Southwestern United States." *Science* 262: 410-412.

England, J.F., Jr., T. A. Cohn, B. A. Faber, J. R. Stedinger, J. O. Thomas, A. G. Vielleux, J. E. Kiang, and R. R. Mason. 2018. *Guidelines for determining flood flow frequency--Bulletin 17C.* Techniques and Methods, book 4, chap. B5, Reston: U.S. Geological Survey, 148.

Enzel, Yehouda, Lisa L. Ely, P. Kyle House, Victor R. Baker, and Robert H. Webb. 1993. "Paleoflood evidence for a natural upper bound to flood magnitudes in the Upper Colorado River Basin." *Water Resources Research* 2287-2297.

Godaire, J.E., and R. H. Hilldale. 2016. *Paleoflood Study, Big Sandy River near Big Sandy Dam, Wyoming.* Technical Memorandum No. 85-833000-2016-04, Denver: U.S. Bureau of Reclamation.

Godaire, J.E., and T. R. Bauer. 2010. *Paleoflood Study of Blue River near Green Mountain Dam, Colorado.* Technical Memorandum No. 86-68330-2010-17, Denver: Bureau of Reclamation.

Godaire, Jeanne E., Tessa Harden, T. R. Bauer, E. Gordon, and R. E. Klinger. 2016. *Paleoflood Study, Taylor River near Taylor Park Dam, Colorado.* Technical Memoradum No. 85-833000-2016-08, Denver: Bureau of Reclamation.

Greenbaum, N., T. M. Harden, V. R. Baker, J. Weisheit, M. L. Cline, N. Porat, R. Halevi, and J. Dohrenwend. 2014. "A 2000-year natural record of magnitudes and frequencies for the largest Upper Colorado River floods near Moab, Utah." *Water Resources Research* 50 (6): 5249-5269.

Griffis, V.W., J. R. Stedinger, and T. A. Cohn. 2004. "Log Pearson type 3 quantile estimators with regional skew information and low outlier adjustments." *Water Resources Research* 40 (7).

Harden, T.M., M. G. Macklin, and V. R. Baker. 2010. "Holocene flood histories in southwestern USA." *Earth Surface Processes and Landforms* 35: 707-716.

Harden, Tessa M., Jim E. O'Connor, and Daniel G. Driscoll. 2015. "Late Holocene flood probabilities in the Black Hills, South Dakota with emphasis on the Medieval Climate Anomaly." *Catena* 130: 62-68.

Hydraulic Engineering Center. 2015. *HEC-RAS River Analysis System 2D Modeling User's Manual Version 5.0.* Davis: U.S. Army Corps of Engineers.

IACWD. 1982. *Guidelines for Determining Flood Flow Frequency, Bulletin 17B.* Technical report, Interagency Committee on Water Data, Hydrology Subcommittee.

IPCC. 2007. *Climate Change 2007: Synthesis Report. Contribution of Working Groups I, II, and III to the Fourth Assessment Report of the Intergovernmental Panel on Climate Change.* Synthesis Report, Geneva: IPCC, 104.

Kenney, T.A., C. D. Wilkowske, and S. J. Wright. 2007. *Methods for Estimating Magnitude and Frequency of Peak Flows for Natural Streams in Utah.* Scientific Investigations Report 2007-5158, U.S. Geological Survey, 28.

Kidson, R., and K. S. Richards. 2005. "Flood frequency analysis: assumptions and alternatives." *Progress in Physical Geography* 29: 392-410.

Klawon, J.E., T. R. Bauer, and R. E. Klinger. 2006. *Development of a Regional Paleoflood Approach.* Technical Memorandum, Denver: U.S. Bureau of Reclamation.

Klinger, R.E., and T. R. Bauer. 2005. *Paleoflood Study on the Uncompahgre River near Ridgway Dam, Colorado.* Technical Memorandum, Denver: Bureau of Reclamation.

Klinger, R.K., and T. R. Bauer. 2007. *Paleoflood study on the Cimarron River near Silver Jack Dam.* Technical Memorandum, Denver: Bureau of Reclamation.

Klinger, R.K., and T. R. Bauer. 2007. *Paleoflood study on the Gunnison River, Colorado.* Technical Memorandum, Denver: Bureau of Reclamation.

Kochel, R.C., P. C. Patton, and V. R. Baker. 1982. "Paleohydrology of southwestern Texas." *Water Resources Research* 18: 1165-1183.

Lai, Yong. 2009. "Two-Dimensional Depth-Averaged Flow Modeling with an Unstructured Hybrid Mesh." *Journal of Hydraulic Engineering* 12-23.

Levish, D.R. 2002. "Paleohydrologic Bounds--Non-Exceedance Information for Flood Hazard Assessments." In *Ancient Floods, Modern Hazards*, by P.K. House, R. H. Webb, V. R. Baker and D. R. Levish, 175-190. Washington, D.C.: American Geophysical Union.

Malamud, B.D., and D. L. Turcotte. 2006. "The applicability of power-law frequency statistics to floods." *Journal of Hydrology* 322: 168-180.

O'Connell, D.R.H., D. A. Ostenaa, D. R. Levish, and R. E. Klinger. 2002. "Bayesian flood frequency analysis with paleohydrologic bound data." *Water Resources Research* 38 (5): 16-1-16-13.

O'Connor, J.E., L. L. Ely, E. E. Wohl, L. E. Stevens, T. S. Melis, V. S. Kale, and V. R. Baker. 1994. "A 4500-year record of large floods on the Colorado River in the Grand Canyon, Arizona." *Journal of Geology* 102: 1-9.

Orchard, K.L. 2001. *Paleoflood hydrology of the San Juan River, southeastern Utah.* MS Thesis, Tucson: University of Arizona.

Stocker, T. F., D. Qin, G. K. Plattner, M. Tignor, S. K. Allen, J. Boschung, A. Nauels, Y. Xia, V. Bex, and P. M. Midgley. 2013. *Climate Change 2013: The Physical Science Basis. Contribution of Working Group I to the Fifth Assessment Report of the Intergovernmental Panel on Climate Change.* New York: Cambridge University Press.

U.S. Bureau of Reclamation. 1990. *Colorado River Basin, Probable Maximum Floods, Hoover and Glen Canyon Dams.* Denver: Bureau of Reclamation.

Wallinga, J. 2008. "Optically stimulated luminescence dating of fluvial deposits: a review." *BOREAS* 31 (4): 303-322.

Webb, R.H. 1985. *Late Holocene Flooding on the Escalante River, south-central Utah.* PhD Thesis, Tucson: University of Arizona.

Webb, R.H., J. B. Blainey, and D. W. Hyndman. 2002. "Paleoflood Hydrology of the Paria River, Southern Utah and Northern Arizona." In *Ancient Floods, Modern Hazards*, by P.K. House, R. H. Webb, V. R. Baker and D. R. Levish, 295-310. Washington, D.C.: American Geophysical Union.

Webb, R.H., J. E. O'Connor, and V. R. Baker. 1988. "Paleohydrologic Reconstruction of Flood Frequency on the Escalante River, south-central Utah." In *Flood Geomorphology*, by V. R. Baker, R. C. Kochel and P. C. Patton, 403-418. New York: John Wiley and Sons.

Appendix A – Paleoflood Hydrology on the lower Green River, Upper Colorado River Basin, USA: An Example of a Naturalist Approach to Flood-Risk Analysis

Elsevier Editorial System(tm) for Journal of Hydrology + OA Mirror

Manuscript Draft

Manuscript Number: HYDROL31884

Title: Paleoflood Hydrology on the lower Green River, upper Colorado River Basin, USA: An Example of a Naturalist Approach to Flood-Risk Analysis

Article Type: Research paper

Keywords: Paleoflood hydrology; Flood-Risk Analysis; Naturalist Approach; Green River; upper Colorado River Basin

Corresponding Author: Dr. Tao Liu, Dr.

Corresponding Author's Institution: The University of Arizona

First Author: Tao Liu, Dr.

Order of Authors: Tao Liu, Dr.; Noam Greenbaum; Victor R Baker; Lin ji; Jill Onken; John Weisheit; Naomi Porat; Tammy Rittenour

Abstract: Through a comprehensive paleoflood hydrological investigation we document natural evidence for at least 27 high-magnitude paleofloods at six sites on the Lower Green River, Utah. Hydraulic analysis, using the Sedimentation and River Hydraulic-2D model (SRH-2D), shows that the responsible peak paleoflood discharges ranged between 500 and 7500 m3/s. At least 14 of these paleoflood discharge peaks exceed a level twice that of the maximum systematic record of gauged flows: 1929 m3/s. Geochronological analyses, employing optically stimulated luminescence (OSL) and radiocarbon dating techniques, demonstrate that these 14 largest paleoflood peaks occurred during the past 700 years. Integration of the paleoflood data into flood frequency analyses (FFA) reveals considerably higher values for the upper tails of the flood distribution than does a FFA based solely on the systematic gauged record, indicating that extreme floods are larger and more frequent than implied by the relatively short gauged record. Through examination of three approaches to extreme flood estimation - conventional FFA, probable maximum flood estimation (PMF), and paleoflood hydrology (PFH) - we show the significance of the natural evidence for advancing scientific understanding of extreme floods that naturally occur in the Colorado River system. We argue that this kind of scientific understanding is absolutely essential for achieving a credible evaluation of extreme flood risk in a watershed of immense importance to economic prosperity of the southwestern U.S.

Suggested Reviewers: Gerardo Benito
benito@mncn.csic.es

Daryl Lam
r.lam@uq.edu.au

Jim E O'Connor
oconnor@usgs.gov

Willem Toonen
willem.toonen@kuleuven.be

Scott St. George
stgeorge@umn.edu

Tessa Harden
tharden@usgs.gov

Abstract
Click here to download Abstract: Abstract.docx

Abstract

Through a comprehensive paleoflood hydrological investigation we document natural evidence for at least 27 high-magnitude paleofloods at six sites on the Lower Green River, Utah. Hydraulic analysis, using the Sedimentation and River Hydraulic-2D model (SRH-2D), shows that the responsible peak paleoflood discharges ranged between 500 and 7500 m^3/s. At least 14 of these paleoflood discharge peaks exceed a level twice that of the maximum systematic record of gauged flows: 1929 m^3/s. Geochronological analyses, employing optically stimulated luminescence (OSL) and radiocarbon dating techniques, demonstrate that these 14 largest paleoflood peaks occurred during the past 700 years. Integration of the paleoflood data into flood frequency analyses (FFA) reveals considerably higher values for the upper tails of the flood distribution than does a FFA based solely on the systematic gauged record, indicating that extreme floods are larger and more frequent than implied by the relatively short gauged record. Through examination of three approaches to extreme flood estimation – conventional FFA, probable maximum flood estimation (PMF), and paleoflood hydrology (PFH) – we show the significance of the natural evidence for advancing scientific understanding of extreme floods that naturally occur in the Colorado River system. We argue that this kind of scientific understanding is absolutely essential for achieving a credible evaluation of extreme flood risk in a watershed of immense importance to economic prosperity of the southwestern U.S.

***Highlights (3 to 5 bullet points (maximum 85 characters including spaces per bullet point)**

High Lights:

- A comprehensive paleoflood investigation on the lower Green River, Utah.
- At least 27 extreme floods in the past 700 years were retrieved.
- Extreme floods are larger and more frequent than implied by gauged records.
- A truly scientific understanding of extreme floods can only emerge from nature.

Paleoflood Hydrology on the lower Green River, upper Colorado River Basin, USA: An Example of a Naturalist Approach to Flood-Risk Analysis

Tao Liu[1*], Noam Greenbaum[2], Victor R. Baker[1*], Lin Ji[1], Jill Onken[3], John Weisheit[4], Naomi Porat[5], Tammy Rittenour[6]

[1] Department of Hydrology and Atmospheric Sciences, University of Arizona, Tucson, Arizona, USA, 85721-0011.

[2] Department of Geography and Environmental Studies, University of Haifa, Haifa, Israel.

[3] Department of Geosciences, University of Arizona, Tucson, Arizona, USA.

[4] Living Rivers, Moab, Utah.

[5] Laboratory of Luminescence Dating, Geological Survey of Israel, Jerusalem, Israel.

[6] Department of Geology, Utah State University, Logan, Utah, USA.

Corresponding author: Tao Liu (liutao@email.arizona.edu) and Victor R. Baker (baker@email.arizona.edu)

Abstract

Through a comprehensive paleoflood hydrological investigation we document natural evidence for at least 27 high-magnitude paleofloods at six sites on the Lower Green River, Utah. Hydraulic analysis, using the Sedimentation and River Hydraulic-2D model (SRH-2D), shows that the responsible peak paleoflood discharges ranged between 500 and 7500 m^3/s. At least 14 of these paleoflood discharge peaks exceed a level twice that of the maximum systematic record of gauged flows: 1929 m^3/s. Geochronological analyses, employing optically stimulated luminescence (OSL) and radiocarbon dating techniques, demonstrate that these 14 largest paleoflood peaks occurred during the past 700 years. Integration of the paleoflood data into flood frequency analyses (FFA) reveals considerably higher values for the upper tails of the flood distribution than does a FFA based solely on the systematic gauged record, indicating that extreme floods are larger and more frequent than implied by the relatively short gauged record. Through examination of three approaches to extreme flood estimation – conventional FFA, probable maximum flood estimation (PMF), and paleoflood hydrology (PFH) – we show the significance of the natural evidence for advancing scientific understanding of extreme floods that naturally occur in the Colorado River system. We argue that this kind of scientific understanding is absolutely essential for achieving a credible evaluation of extreme flood risk in a watershed of immense importance to economic prosperity of the southwestern U.S.

Keywords:

Paleoflood hydrology; Flood-Risk Analysis; Naturalist Approach; Green River; upper Colorado River Basin

1 Introduction

1.1 Background/Problem:

Floods result in many of the most frequent and costly water-related natural disasters worldwide. Their global impacts include losses of life and billions of dollars in financial damages. Over the past century, national stream gauging networks were established in many countries to provide systematic and quantitative data on streamflow, including flooding. To make effective use of the resulting accumulation of hydrological and meteorological observations two primary methodologies were developed, mainly in the engineering community: flood-frequency analysis (FFA) and probable maximum flood (PMF) estimation, (National Environment Research Council, 1999; SL44-2006).

Conventional FFA combines systematical records with statistical/mathematical theories to provide actionable information for flood risk assessment. This is conducted by fitting functions to peak annual discharges obtained from gauged records for a drainage basin. Extrapolations are made from what is usually a very short instrumental flood record of relatively small flood peaks in order to estimate flood extremes that may have very long return periods. In other words, extreme flood estimates are based on the statistical properties of the relatively frequent, small-scale flooding that is most commonly represented in gauge records. It therefore is a matter of assumption that this record can be reliably extrapolated upscale to predict the magnitudes of unknown rare, extremes. A key FFA assumption is that the flood peaks are independently, identically distributed (iid), because this "iid" criterion is a necessity for achieving valid statistical inferences (Kesiel, 1969). However, in areas of high flood variability, such as the southwestern U.S., peak flood series are commonly mixed distributions, such that the most extreme flood peaks are generated by very different meteorological phenomena than are the

less extreme peaks (Hirschboeck, 1998). Though these and other shortcomings have been obvious for decades (Klemes, 1996), conventional FFA continues to be utilized as a matter of standard practice, often in ignorance that opportunities may be available to overcome shortcomings in regard to making credible extrapolations to flood extremes.

PMF procedures, like FFA, can be lacking in credibility. These procedures employ hydrological models that may embody highly problematic presumptions, particularly in regard to conditions representing the most extreme flood-generating parameters. By definition, PMF modeling predicts the most extreme flood peak that could conceivably occur at a particular location, i.e., a prediction of something at the absolute limit of what theoretically is supposed to occur. Were an exceedance of such flooding actually to occur, of course, the model would thereby, be falsified by an act of nature.

As a matter of logical inference, PMF procedures are largely deductive; they can indeed yield true conclusions, but only if the assumptions made are indeed true to reality. In contrast, FFA procedures are largely an inductive, in that various statistical methods are employed to generalize from data and address associated uncertainties. While these approaches have long applied engineering traditions in both empirical and theoretical hydrology, they also have limitations in regard to hydrology viewed as a complete scientific discipline (Baker, 2017). This paper employs a third mode of reasoning, abduction, which works in concert with both deduction and induction to generate enhanced understanding of the nature of extreme floods (Baker, 1996, 1998).

1.2 Paleoflood hydrology

Paleoflood hydrology (PFH) relies on the identification of physical evidence of past flood phenomena, including flood slackwater deposits and related paleostage indicators (SWD-PSIs)

that serve as high-water marks (HWMs) (Baker, 1987). SWD-PSIs are used to determine the associated flood magnitudes through the application of hydraulic principles (Baker, 2008; Benito and O'Connor, 2013). PFH results can provide both (1) a sound foundation for flood-frequency analysis (Costa, 1978; Baker et al., 1979, 2002; Stedinger and Baker, 1987) and (2) hydrological model improvements (England et al., 2014). PFH also provides real-world flood data with which to inform the search for flood-climate linkages in a broad context, as global and regional atmospheric circulation patterns and processes drive changing flood-generating meteorological elements over long time scales (Ely et al., 1993; Knox, 2000; Benito et al., 2003, 2015; Macklin, 2006; Huang et al., 2007; Harden et al., 2010; Merz et al., 2014; Toonen et al., 2017).

PFH was embraced for both scientific and engineering applications worldwide after early programs of paleoflood investigation were initiated in central Texas during the 1970s (Baker, 1975; Patton and Baker, 1977) and subsequent paleoflood studies were accomplished in the broader Southwestern U.S. (Patton and Dibble, 1982; Kochel et al., 1982; Ely and Baker, 1985; Webb et al., 1988; Jarrett, 1990; O'Connor et al., 1994; Ostenaa et al., 1996), and then in other parts of the North America (Knox, 1985, 1993, 2000; Springer and Kite, 1997; Brown et al., 2000; Saint-Laurent et al., 2001; O'Connor et al., 2003). Applications outside of the U.S. include Australia (Pickup et al., 1988), Spain (Benito et al., 2003), France (Sheffer et al. 2008), China (Huang et al., 2010; Liu et al., 2014), Japan (Jones et al., 2001), India (Kale et al., 1997), Thailand (Kidson et al., 2005), and Israel (Wohl et al., 1994; Greenbaum et al., 2000; 2006).

The Colorado River is the most important river in the southwestern U.S., providing water for municipal drinking water, agriculture irrigation systems, and hydropower needs for more than 35 million people in seven states. Extreme flooding along this river would also cause massive disasters along floodplains and bring about severe damage to infrastructure and high economic

costs, including the potential loss of major dams that are critical to the economy of the entire region. A large number of paleoflood investigations have been conducted in the lower Colorado River and its tributaries (e.g., Ely and Baker, 1985; Partridge and Baker, 1987; Fuller, 1987; Enzel et al., 1994; Webb et al., 1988; O'Connor et al., 1994). These studies and subsequent syntheses (Enzel et al., 1993; Harden et al., 2010) provide for robust knowledge of real-world floods that have actually occurred over the last several thousand years. In contrast, there have been relatively few paleoflood studies conducted in the upper Colorado River Basin, where more than 95% of the Colorado River's discharge originates (Blinn and Poff, 2005). An important exception is the study by Greenbaum et al., (2014) which found natural evidence for 44 extreme floods occurring during the last 2000 years on the upper Colorado River, near Moab, Utah. Two of these paleofloods exceeded the PMF of 8500 m3/s, and the whole assemblage of largest paleoflood peaks was found to be more frequent than could be estimated on the basis of the systematic gauge data alone. Given this example of combining long-term paleoflood records with high spatial-temporal resolution systematic observations, and their linkages to climate change, we hope further to advance understanding extreme flood generation mechanism and improve upon estimates for the occurrences and magnitudes of future extreme flooding in the upper Colorado River Basin.

In this study, we present the results of investigations along the Stillwater Canyon section of the lower Green River. We document the paleoflood events of the last 700 years, using SWD-PSIs and 2D hydraulic modeling to estimate the associated peak discharges. We then apply these new paleoflood data in FFA using different methodologies. The results are then discussed in terms of their great potential for gaining understanding of nature of extreme flood events and their linkages with climatic changes in the upper Colorado River Basin.

2 Study area

The Green River is a chief tributary of the upper Colorado River. It is 1,170 km long and has a drainage area of 124,600 km^2 that includes parts of Wyoming, Utah, and Colorado (Figure 1). It contributes nearly half of the total annual flow to the Colorado River at the confluence. Heading in the Wind River Range of Wyoming, the Green River receives tributary flows from western Colorado, then flows south through the Uinta Mountains and the Uinta Basin of Utah, finally traversing a long series of canyons before joining the main stem of the Colorado River in south-central Utah. In its lower reaches from the town of Green River UT to the junction with the Colorado River, the Green River meanders through steep, stable sandstone bedrock canyons (Cashion, 1967), Labyrinth and Stillwater, where gradients approach 0.1 m/km. The Green River joins the Colorado River roughly 63 km downstream of Moab, UT.

Figure 1. Green River Basin including the large tributaries, USGS gauging station, and the study reach.

Precipitation in the upper Green River Basin can exceed 1000 mm water equivalent per year, with most of this generally occurring in the form of winter snow. In contrast, the lower Green River Basin has a semiarid climate characterized by cold winters and hot, dry summers. NOAA COOP station (No. 421163) in Canyonlands National Park (1965-2018, Western Regional Climate Center, 2013) indicates annual mean temperature is 5.78 ℃ with the maximum monthly mean temperature in July, varying between 18.8 and 32.6 ℃, and the minimum monthly mean temperature in January, varying between -6.3 and 2.7 ℃. Annual mean precipitation is 229 mm, ranging between 117 and 338 mm. This precipitation is attributed to 1) summer and fall convective storms coming from the Gulf of Mexico or the Gulf of California, 2) large-scale

151 cyclonic storms resulting from Pacific air masses in summer and fall, and 3) North Pacific frontal
152 storms in winter (Blinn and Poff, 2005).

153 The USGS gauging station on the Green River at Green River, Utah (No. 09315000) is
154 situated ca. 200 km upstream from the confluence of the Green and Colorado Rivers (Figure 1).
155 The drainage area of the Green River at this location is 116,160 km^2, accounting for 93% of the
156 basin. The gauge has recorded the daily discharge rate since 1894 and is continuous except for
157 the period 1900-1904. At this station, the average annual discharge is 170.0 m^3/s with a
158 maximum of 347.8 m^3/s and minimum of 51.1 m^3/s. The annual maximum gauged flood peaks
159 range from a low of 183.0 m^3/s in 1934, to a high of 1928.6 m^3/s in 1917 with an average of
160 789.5 m^3/s (Figure 2). Besides the gaged record, there is no humanly recorded historical flood
161 record that we could find for the Green River.

162 *Figure 2. Annual maximum peak discharges on the Green River at the USGS gauging station*
163 *Green River, Utah, 1894-2016.*

164 This study involves six paleoflood study sites along Stillwater Canyon of the Lower
165 Green River. As the name suggests, this is a canyon that is free of rapids (swift turbulent flow)
166 where the river loops in sinuous curves bedrock meanders. The study sites are distributed
167 unevenly along a 35-km long reach from the mouth of Dead Horse Canyon to the confluence
168 with the Colorado River (Figure 3). The river channel averages about 250–350 m in width and
169 flows within a ~120 m deep canyon with near vertical bedrock walls.

170 *Figure 3. A map showing six study sites (DHC, RF, LS, HD, HB, and PC) on the Lower Green*
171 *River (left), the stratigraphic illustrations showing the paleoflood slackwater deposit layers*
172 *(black lines) and the river channel and valley dimensions of each stratigraphic section (middle),*

and the cross-sections at each site (right), showing the range of extreme flood water surface elevation.

3 Methodologies

3.1 Paleoflood Record Analysis

There are many techniques available for making inferences concerning the hydrological parameters for past flood events, employing principles of geomorphology and related aspects of Quaternary stratigraphy and sedimentology (Baker, 2008; England, 2010). The most accurate method involves slackwater deposits and paleostage indicators (SWD-PSI) in stable-boundary fluvial reaches (Baker, 1987). Slackwater deposits are fine grained sediments, mainly sand, conveyed in suspension during highly energetic flood flows and deposited in areas of flow separation that result in long-term preservation after the flood recession (Baker, 2008). During our detailed field paleo-hydrological investigations layered sequences of slackwater deposits were found at the six study sites along Stillwater Canyon of the lower Green River (Figure 3). The paleoflood SWDs include between 7-11 flood deposits at most of the sections with one section containing only two SWDs while another contained 30 SWDs. Sites are located up to 13.5 m above water level (a.w.l.). We exposed stratigraphic sections at each site, made detailed descriptions of the flood SWDs, and sampled for OSL and radiocarbon dating. The sedimentary units associated with paleoflood events, were identified using the well-established sedimentological criteria (Baker, 1987; Kochel and Baker, 1988; House et al., 2002; Benito and O'Connor, 2013).

3.2 Paleoflood Age Determination

We employed two geochronology techniques, accelerator mass spectrometry (AMS) radiocarbon (^{14}C) dating of charcoal and plant material and optically stimulated luminescence (OSL) dating of quartz sand, to develop a robust paleoflood chronology. Radiocarbon dating is the most widely used geochronology method in fluvial studies, and the analytical techniques have been highly refined over the past several decades. Three ^{14}C samples were collected at two of six sites to estimate ages of the SWDs. The samples were prepared and analyzed at the Arizona AMS Lab at The University of Arizona, with calibration to calendar years (OXCAL 4.3), using the IntCal13 calibration curve (Reimer et al. 2013) and reported as two-sigma calibrated age ranges (Table 2). Because of insufficient amounts of the organic matter needed for radiocarbon dating, most of this study employed OSL dating. Twelve OSL samples were submitted to the Dating Laboratory of the Israel Geological Survey in Jerusalem, and three were analyzed at the Luminescence Lab at the Utah State University. We employed the latest single-aliquot regenerative-dose (SAR) procedures for OSL dating of quartz sand (Murray and Wintle, 2000, 2003; Wintle and Murray, 2006). Dose-rate calculations were determined by chemical analysis of the U, Th, K and Rb content using ICP-MS and ICP-AES techniques and conversion factors from Guérin et al. (2011). The contribution of cosmic radiation to the dose rate was calculated using sample depth, elevation, and latitude/longitude following Prescott and Hutton (1994). Dose rates are calculated based on water content, sediment chemistry, and cosmic contribution (Aitken and Xie, 1990; Aitken, 1998).

3.3 Paleoflood hydraulic analysis

Paleoflood discharge estimation can be accomplished by methods ranging from simple hydraulic formulae applied at a single cross-section to a variety of one-, two- or even three-dimensional hydraulic modeling codes applied to high-resolution channel geometry data. For this

218 study, we used the two-dimensional hydraulic model SHR-2D (Sedimentation and River
219 Hydraulics-2D, Lai, 2009) to estimate peak discharges for the paleofloods. Roughness values
220 were identified and delineated within zones for the modeled study reach. The Manning's n
221 values chosen for the hydraulic model are 0.028 for the channel and 0.045 for the banks, based
222 on observations made in the field and comparison to values previously published for a similar
223 reach of the upper Colorado River (Greenbaum et al., 2014). A sensitivity analysis was
224 performed to examine changes in hydraulic calculations response to the uncertainty of roughness
225 coefficient. Mesh cells chosen for the model in the river channel had an approximate size of 2-6
226 meters, but, where the canyon walls were more widely spaced, we increased the dimensions to
227 between 6 and 8 meters. For areas of interest, especially those near the SWD sites, we employed
228 finer mesh cells to provide more detail. The 2D model results also displayed the water depth and
229 velocity distribution in the study reach, information of importance to understanding the
230 depositional environment of SWDs.

231 The downstream boundary for each flow estimate was the normal depth. The location of
232 the downstream boundary was established far enough downstream so that any uncertainty in this
233 value would not affect model results in areas of interest. The model run was initiated from a dry
234 condition and continued with a two second time step. The simulation time for each modeled flow
235 varied from 10-16 hours, in which time the incoming and outgoing flows and water surface
236 elevation at monitoring points stabilized. LiDAR data were used to develop the geometry of the
237 channel for the hydraulic model, and this provided a high-resolution Digital Elevation Model
238 (DEM) with a 0.5-meter grid spacing and ≤19.6 cm vertical accuracy.

239 We input successive discharges for the upstream boundary and obtained discharge-stage
240 (Q-S) relationships for each site. The paleoflood discharges were acquired from the resulting

241 rating curves, which were fitted based on the relevant Q-S relationships. Because the elevation of
242 a SWD is somewhat lower than the actual water surface during the flooding, the reconstructed
243 discharge is treated as the minimum value with an underestimation of 10–20% (Kochel et al.,
244 1982, Baker, 1987, Enzel et al., 1993).

245 The two main assumptions for discharge calculation are 1) that significant aggradation
246 and/or degradation of the channel has not occurred during the time-span of the flooding
247 represented by the SWDs; and 2) that significant scour and/or fill in the river channel has not
248 occurred during large flood events (Baker et al., 1983). For the study reach, both assumptions are
249 acceptable because the river loops in sinuous curves of sandstone bedrock over a stable rock bed,
250 which indicates very little bed change during the late Holocene (the last several thousand years).

251 3.4 Flood Frequency Analysis (FFA)

252 The annual maximum flood series and a partial duration flood series (PDS) were
253 extracted from USGS gage 09315000 on the Green River at Green River, Utah. There are 117
254 annual peak flows (1895-1899, 1905-2016, Fig. 2). However, only the unregulated annual
255 maximum series (1895-1899, 1905-1961) is used, which closely represents the natural flow on
256 the Green River. These 62 peaks were adjusted to the drainage area at the study site using the
257 method of Cudworth (1989). It is assumed that the ratio of the peak discharges at the two
258 locations is equal to the square root of their respective drainage areas, therefore the peak flows at
259 the study sites are larger than the USGS gage values by 4.9%. The largest seven paleoflood peak
260 flows were incorporated into the FFA.

261 The FFA was conducted under the newly updated Guidelines for Determining Flood
262 Flow Frequency Bulletin 17C (England, et al., 2018), which continues to fit the Log Pearson
263 Type III (LP-III) distribution using the Expected Moments Algorithm (EMA) (Cohn et al., 1997,

2001; England et al., 2003, 2018) with the Multiple Grubbs-Beck test (MGBT) (Cohn et al., 2013; Lamontagne et al., 2013, 2015). EMA provides a direct fit of the LP-III distribution utilizing multiple types of at-site flood information including the systematic record, historical floods as well as paleofloods, while adjusting for any potentially influential low floods (PILF), missing values due to an incomplete record, or zero flood years.

We also employed the Bulletin 17B method (IACWD, 1982), the log normal distribution (Chow et al., 1988), the regional-regression equation (Kenney et al., 2007) and the self-similar model (Kidson and Richards, 2005; Malamud and Turcotte, 2006) with the systematic gauged peaks and the paleoflood data.

4 Results

4.1 Paleoflood slackwater deposits and chronology of the paleoflood events

Nine stratigraphic sequences of fine-grained flood deposits were found at the six study sites located along a 35-km long reach of Stillwater Canyon of the lower Green River (Figure 3). Different slackwater depositional areas occurred in low-velocity flow environments during flooding, accumulating on stable rock platforms and alluvial terraces during flood recession. Suspended flood sediments were deposited and accumulated, and eventually experienced long-term preservation in these regions. Characteristics of the slackwater depositional environments of the lower Green River paleoflood SWDs are summarized in Table 1.

Figure 4. Particle tracings and water depths associated with sites of DHC, PC, HB, and HD on the Lower Green River. Areas of slack-water deposition develop through combinations of flow direction, speed, and depth. For sites location see figure 3.

285 The 2D hydraulic model generated the paleoflood flow and velocity distributions in two
286 dimensions, indicating the slackwater depositional zones (Figure 4). The SWDs at the Dead
287 Horse Canyon site (DHC-1 and 2) are located in a low-velocity backwater area at the tributary
288 mouth, while SWDs at the High Driftwood (HD) site is located on a high-velocity site at a >90
289 degrees curve where the sediments are probably super-elevated. The entire paleoflood record for
290 the six sites consists of 68 paleoflood SWDs and two driftwood lines at the HD site. These two
291 driftwood lines are located 5 m and 12 m a.w.l. They are composed of coarse driftwood and logs.
292 Since this is a multi-site record, it may well be that floods are presented at more than one sites.
293 The results of the AMS and OSL dating at the various sections indicate that all 70 units at six
294 sites fall in 680-140 a (or 940-110 a bracketing the error), which can be represented by the RF-1
295 and DHC-1 sections. The OSL ages (550 -190 a) of 26 SWD layers at the RF-1 site cover all
296 units at the other five sites except for the DHC-1. The oldest unit at the DHC-1 section is 680 ±
297 250 a. At least 27 paleoflood events are therefore considered to have occurred in the past 680
298 years (Table 2 and 3).

299 4.2 Paleoflood hydrodynamics

300 The 2D hydraulic model was run for approximately 12 different discharge levels at each
301 SWD site. These levels ranged upward from 50 m^3/s, which is a flow just large enough to begin
302 submerging the lowest SWDs at the six sites. Rating curves were then fitted based on the
303 stimulated discharge-stage (Q-S) points following the equation:

304 $$\boldsymbol{Q = C(h - e)^{\beta}},$$

305 where Q is the stimulated flow discharge for a certain height of the water surface, m^3/s; h
306 is the height of the water surface, m; e is the height of the lowest point of a particular cross-
307 section, m; (h – e) is head or water depth, m; and β is the slope of the rating curve.

Water dynamic conditions are represented in the model output by particle tracings and water depth near each SWD site on the study reach (Figure 4). The paleoflood peak discharges were estimated using the rating curve equations combined with the relevant water stages (Figure 5 and Table 4). All the paleoflood peaks ranged between -20.4% and 7.2% when the Manning's n value was adjusted by ±25% (Figure 5 and Table 4). The largest magnitude of paleoflood was about 7499 m^3/s (-9.2-3.0%) with a water stage of 13.50 meters above the river water level. There are at least 14 paleofloods with magnitudes larger than twice the maximum systematic gauged record of 1929 m^3/s.

Figure 5. Rating curves (solid lines) and corresponding results (dashed lines) for the 25% of Manning's n variation for six cross sections at the paleoflood sites on the Lower Green River. The sensitivity test shows an error of 3.0-20.4% can be introduced by the uncertainty of Manning's n.

4.3 Flood Frequency Analysis (FFA)

The results of FFA based on various methods and flood series are shown in Figures 6-8 and Table 5-7. For the Bulletin 17C method, the annual peak flows including the systematic record and paleofloods are all described by flow interval (QY,lower, QY,upper) and perception thresholds (TY,lower, TY,upper) in Figure 6 and Table 5-6. The station skew was used in this study. Expected quantiles for the interval floods are shown with 95% confidence limit in Figure 7a and b. Combining both the paleoflood data and systematic peaks, the FFA shows the largest paleoflood (7499 m^3/s) has an AEP (annual exceedance probability) of 0.057% or a return period of 1750 years, while the AEP and return period for the largest gaged flood (2023 m^3/s) are 3.770% and 26.5 years (Fig. 7a). In contrast, the FFA using only the systematic peaks shows that the return period for the largest paleoflood is longer than 1,000,000 years, for the largest gaged

flood 68.5 years (Fig. 7b). The ratio of 95% confidence interval to the expected quantile (CI/EQ) is used to illustrate the effects of change with the integration of paleoflood data (Fig. 7c). Paleofloods increased both the expected quantiles and confidence intervals of the 25-year-flood and the longer recurrence interval floods to various extents, while the CI/EQ was reduced by 20% for 25-year-flood, 27% for 50-year-flood, 24% for 100-year-flood, and 17% for 200-year-flood.

Figure 6. Graph showing approximate systematic peak discharge and paleoflood estimates, with paleoflood exceedance thresholds, on the Lower Green River in the Stillwater Canyon reach. A scale break is used to separate the gaging station data from the much longer paleoflood record. Flood intervals for large floods in the paleoflood period are shown as red squares and black vertical bars with caps that represent minimum peaks and an additional 20% of the minimum. Mean values of paleofloods threshold age data are plotted for simplicity. Perception threshold ranges are shown as orange lines for the paleoflood period, blue lines for the systematic period, and green lines for the discontinued period. The gray shaded areas represents: (1) floods of unknown magnitude less than the perception thresholds for the paleoflood periods Tp,lower ; (2) the discontinued period Td,lower; (3) post-regulation floods after 1961.

Figure 7. Results of flood frequency analysis (FFA) using Expected Moments Algorithm (EMA) with Multiple Grubbs-Beck Test (MGBT) on the Lower Green River in the Stillwater Canyon reach, using (a) both systematic and paleoflood data; (b) systematic peaks only. The solid line is the fitted log-Pearson Type III frequency curve and the dash lines are the 95% confidence limits. Peak discharge estimates from the gage are shown as open circles; vertical bars represent estimated data uncertainty for paleofloods; the solid black circle is the potentially influential low

flood (PILF) threshold as identified by the MGBT. Y-axis of the subplot (c), CI/EQ, is the ratio of confidence limits to expected quantiles.

Figure 8. Comparison of different techniques for flood frequency analysis (FFA) on the Lower Green River in the Stillwater Canyon reach, including systematic and paleoflood data. Subplots a-e include nine FFA curves using five techniques and all of them were synthesized in the subplot f. Annual exceedance probability (AEP), return period (T), and discharge (Q) for these curves are summarized in Table 7. The numbers refer to the discussion of each curve in the text and table.

Other flood probability models also showed a good fit with most data points (Fig. 8). Curves 1, 3, 5, 7 were calculated using the Bulletin 17C, Bulletin 17B methods, a log-normal distribution, and the self-similar model, combining paleoflood data with the systematic annual maximum flood series (except that the partial duration flood series was used for the self-similar model). Curves 2, 4, 6, 8 were calculated using the same approaches, but with only the systematic peaks. Curve 9 employed the regional-regression equation. Relatively good agreement is observed among the different FFA techniques for recurrence intervals of less than ten years. Two clusters appeared with increasing recurrence intervals. Curves 1, 3, 5, 7, and 8 occupied the first cluster, showing high upper tails. The low values were estimated by curves 2, 4, 6, and 9, which are limited to analysis of only the systematic peaks. Clearly, the paleoflood data swing up the upper tails for the log P-III and lognormal distributions (Fig. 7a, b, and c). However, curves 7 and 8 demonstrated that the expected quantiles correspond very closely with a power-law distribution for recurrence interval larger than 25 years; they both were in good agreement with paleoflood involved Bulletin 17C results (curve 1).

5 Discussion and Conclusions

The protection against extreme floods for large, high-hazard, water-related projects and engineered systems, including high-level dams and nuclear power plants, is a long-standing hydrological issue. Hydrologists developed two primary procedures for flood-protection decision-making: (1) FFA, based on the statistical analysis of peak flood distributions, and (2) probable maximum flood (PMF) calculations. Despite inherent difficulties and controversies involving both methods, emerging since the 1960s (e.g., Yevjevich, 1968) or earlier, both procedures have, nevertheless, been applied extensively and established either as engineering standards or official guidance in the United States and many other countries (U.S. Water Resources Council, 1977; National Environment Research Council, 1999; SL44-2006).

It has now been more than a century, since 1914, when the concept of a return period of a flood event of a given magnitude or average recurrence interval was proposed by Fuller (1914), and statistical techniques were introduced for the hydrological analysis of flood extremes. Early on this procedure was known to require a sufficiently large number of flood events for statistical validity such that the parameters met the requirement of being, independent, identically-distributed random variables (Kisiel, 1969). These requirements reflect fundamental assumptions necessary for FFA that a specific magnitude of flood corresponds to a specific probability or return period. The objective of FFA is to find this relationship, especially to predict the upper tails for the relevant distributions (Klemeš, 2000). However, it is almost always, not possible to collect statistically large enough samples to validly estimate the greatest extremes, even in the U.S. where the hydrological gauging network has been established since late 19th century (U.S. Water Resources Council, 1988). The gauged data are always restricted to samples overwhelming dominated by small and common floods, whereas data on extremely large, rare

floods are not captured in the instrumental data, making this assumption inadequate for making valid statistical inferences. This circumstance inevitably leads to extrapolation from the existing gauged data.

The incorporation of paleoflood data into FFA started in the late 1970s (Costa, 1978; Baker et al., 1979). In a seminal study Stedinger and Cohn (1986) examined three methods for utilizing paleoflood information in flood-frequency analysis (see also Stedinger and Baker, 1987). Cohn et al. (1997) developed a method of expected moments algorithm (EMA) for utilizing paleoflood information in FFA, and this procedure has become the basis for the newly published Bulletin 17C (England, et al., 2018). Frances (2001) showed how to include paleoflood data in FFA using the Maximum Likelihood Estimation (MLE) method. Lam et al. (2017) integrated paleoflood data into FFA using Bayesian Inference methods, thereby showing a significant reduction in uncertainty for 100-yr flood estimation in subtropical Australia. Multiple studies have focused on assessing the contribution of PFH to FFA improvement by promoting the incorporation of paleoflood data. In these many studies, the utilization of paleoflood information for FFA simply enriches the flood samples for the statistical manipulation. As Klemeš (1987, 1994) strongly asserted, "… much of FFA is just a part of small sample theory in disguise, the term 'flood' being used merely as a name for numbers employed."

PMF estimation employs both meteorological and hydrological approaches to calculate the theoretically maximum flood for a basin of interest (WMO, 2009). The PMF for a given basin is derived from the probable maximum precipitation (PMP), which is defined by American Meteorological Society as, "…the theoretically greatest depth of precipitation for a given duration, that is physically possible over a particular drainage at a certain time of the year." This means the PMF method must assume that there is a natural upper limit to precipitation for a

given duration and area. Based on this assumption, the PMF can then be estimated to an upper limit of flood magnitude by hydrological modeling that incorporates the most extreme combination of hydrological conditions. However, it is difficult, if not impossible for the reality of a changing world, to establish the validity of any assumed upper limit to either precipitation or flooding. The established methods for PMP/PMF estimation are, necessarily based on known, limited observations and the current state of knowledge, specific to the circumstances of time and place. However, in the real world both data and the intelligence with which to understand things, i.e., science, are increasing (Jakob et al., 2009; Song et al., 2015). PMP/PMF estimates are consequently observed to increase as more sophisticated meteorological phenomena observed and recognized (Kunkel, 2013). Moreover, the magnitude of PMP/PMF can also vary widely by using different methods (Douglas and Barros, 2003; Jakob et al., 2009; Rouhani and Leconte, 2016). The hydrological model transforming the PMP into PMF uses a science-as-knowledge approach, of which it underpins valid reasoning about what can be said to the world. The extreme floods generated by a hydrological model are therefore, considered as what we human created, rather than what really happened in nature. The most controversial observation is that PMP/PMF values have been exceeded by actual extreme events (Bewsher & Maddocks, 2003). A relevant example is the recent discovery of two naturally-evidenced extreme floods, i.e., paleofloods, occurring in the last 2000 years, and found to be larger than the PMF for the upper Colorado River (Greenbaum et al., 2014).

This review of problems and criticisms of both the FFA and PMF methodologies raises even more fundamental concerns about the epistemological underpinnings in regard to the scientific understanding of the nature of extreme floods. While these are not usually issues considered in the practical expediency necessary to achieve engineering solutions, they do

emerge when phenomena are at the limits of scientific understanding. Extreme flooding lies at those limits. Both the FFA and PMF methods employ theory-directed, science-as-knowledge approaches, which hold the world to be a system that permits the application of deductive logic through mathematics to provide the certainty associated with that kind of reasoning (Baker, 2017). But that certainty only applies if the assumptions made are absolutely true.

In this study, state-of-the-art paleoflood hydrology (PFH) was applied to provide information on extreme floods not captured in the short instrumental record. PFH derives from a science-as-seeking point of view and employs a world-directed, investigative approach (Baker, 2017) to discover the extreme floods that have actually happened over a geological span of time (commonly limited to the Holocene epoch, a period about the last 10,000 years, characterized by Earth's non-glacial climate regimes). PFH thereby provides reliable, fundamental knowledge concerning extreme flood behavior in nature. It thus makes previously unknown extreme floods known to appropriately experienced investigators, thereby revealing what would otherwise be hidden within hydrological assumptions. By directly compiling evidence from the world, in a sense listening to the nature what nature presents to us, and thinking based on realities, PFH investigators study the clues, signals, and signs of the most extreme floods found in nature. In following these signs, an explanatory working hypothesis emerges as to what is actually possible, and every inference to what is probable must also infer what is possible. This is abductive inference (Baker, 2017) and the associated natural historical approach yields real-world discoveries about extreme floods, which form the basis for advancing scientific understanding about such flooding.

By employing paleoflood hydrological investigation, this study identified at least 27 real extreme floods that occurred on the lower Green River during the last 700 years. Combining the

469 water stages inferred by the tops of paleoflood SWD layers, the 2D hydraulic modeling
470 retrodicted the minimum peak paleo-discharges at six study reaches. Among them at least 14
471 paleofloods were larger than twice of the maximum systematic gauged record of 1929 m^3/s. The
472 largest paleoflood has a minimum peak discharge of 7500 m^3/s.

473 These numbers more accurately reflect the actual history of extreme floods on the Green
474 River, rather than either (1) the extrapolated ones from small-scale flood samples, or (2) the
475 derived outputs from a hydrological (watershed) model. This is unlike both conventional FFA or
476 the hydrological rainfall-runoff models used for PMF estimation, which respectively, involve
477 either generating probabilistically extrapolated upper tails or the deterministically deduce
478 limiting upper values via models and assumptions, providing the established practical tools for
479 predicting extreme floods in flood mitigation projects or design flood estimations (U.S. Army
480 Corps of Engineers, 1991; U.S. Bureau of Reclamation, 2003). However, these practical tools
481 can only be claimed to be science-based if their predictions are compared to the information
482 nature provides to us about extreme flood events, i.e., there is agreement with empirical
483 evidence—not just empirical evidence that is convenient in the artificial repositories of our
484 existing data sets, but all possible empirical evidence, which includes that being held by nature
485 itself in its natural repositories. To ignore realities is to be "unscientific." PFH continues the
486 exploratory imperative of what is most essential in a doing science of extreme flooding by
487 making discoveries of viable and efficient data sources from real-world evidence, which can act
488 as a "spotlight" for improving both FFA (Schendel and Thongwichian, 2017; Lam et al., 2017)
489 and hydrological modeling (England et al., 2014) of extreme floods.

490 Finally, it can be observed that the clustering of paleoflood patterns offers an opportunity
491 to explore complex, spatially highly interrelated flood-climate links in a global perspective

(Baker, 1987; 2008; Ely et al., 1993; Hischboeck et al., 1988; Knox, 2000;; Macklin, 2006; Merz et al., 2014; Benito et al., 2015; Toonen et al., 2017), which, combined with other information on paleoclimates, can provide valuable insights into understanding the nature of extreme floods (Merz et al., 2014). Ely et al. (1993; 1997) displays the clustered extreme paleofloods in the last 4000 years in the southwestern U.S. and identified the hydroclimatic effect on the increased flood frequency. Harden et al. (2010) also suggests that hydroclimatic dynamics strongly affected the episodes of major flood events during the Holocene based on a broader paleoflood dataset for the southwestern U.S. The results of this study agree with previous research (Ely et al., 1993; Harden et al., 2010; Greenbaum et al., 2014) that frequent large floods happened during periods of cool and dry climate. Knox (1993, 2000) highlighted that significant changes in magnitudes and frequencies of extreme paleofloods are regional hydrological responses to global climatic change. Huang et al. (2007, 2010) and Liu et al. (2014) inferred that major Holocene flood episodes are associated with transitional periods of climatic change, forced by monsoonal shifts in northern and central China. Benito et al. (2015) examined the relationship between Holocene flood patterns and short-term climatic variability in Europe and North Africa, suggesting the importance of paleoflood information for understanding future spatial-temporal changes of flood frequency. Toonen et al. (2017) implied that individual flood events and multiyear episodes generally fall within extended flood-rich phases controlled by climate, demonstrating the value of paleoflood datasets as useful multiscale hydromorphic signals of climate change. Recent studies (Munoz et al., 2017 and 2018) suggest that El Niño increase the risk of Mississippi flooding and conventional flood prediction techniques-based engineering control measures might actually be making floods worse.

Much remains for research in the future, but the only resource and basis we can rely on is to find out what's naturally true of extreme floods is the history of past manifestations. It cannot be overemphasized that a truly scientific understanding of extreme floods can only emerge from our exploration in nature of flood signs in all their temporal contexts (paleo-, historical, and systematically gauged), to be followed by the explanation of the discovered (not presumed) phenomena through a mechanistic understanding of their causal drivers.

Acknowledgments

This research was supported by the U.S. Bureau of Reclamation under Assistance Agreement no. R16AC00021. V.R.B.'s 45-year program of developing paleoflood hydrological science received critical early support from the U.S. National Science Foundation. This paper is Contribution Number 105 of the Arizona Laboratory of Paleohydrological and Hydroclimatological Analysis (ALPHA).

References

Aitken, M.J. 1998: An Introduction to Optical Dating: The dating of Quaternary sediments by the use of photon-stimulated luminescence. New York, Oxford University Press, 267 p.

Aitken, M.J., Xie, J., 1990. Moisture correction for annual gamma dose. Ancient TL 8 (2), 6-9.

Baker, V.R., 1975. Flood hazards along the Balcones Escarpment in central Texas: alternative approaches to their recognition, mapping and management. University of Texas Bureau of Economic Geology Circular, vol. 75–5. 22 pp.

Baker, V.R.,1987. Paleoflood hydrology and extreme flood events. Journal of Hydrology 96, 79–99.

Baker, V.R., 1996, Discovering the future in the past: Palaeohydrology and geomorpho¬logical change, in Branson, J., Brown, A.G., and Gregory, K.T., editors, Global continental changes: The context of palaeohydrology: The Geological Society of London, Special Publication No. 115, p. 73-83.

Baker, V.R., 1998, Paleohydrology and the hydrological sciences, in Benito, G., Baker, V.R., and Gregory, K.J., editors, Palaeohydrology and environmental change: John Wiley and Sons, Chichester, p. 1-10.

Baker, V. R., 2017. Debates—Hypothesis testing in hydrology: Pursuing certainty versus pursuing uberty, Water Resour. Res., 53, doi:10.1002/2016WR020078.

Baker, V.R., Kochel, R.C., Patton, P.C., 1979. Long-term flood-frequency analysis using geological data. International Association of Hydrological. Science Publication, vol. 128, pp. 3–9.

Baker, V. R., Kochel, R. C., Patton, P. C., and Pickup, G.: 1983, Paleohydrologic analysis of Holocene flood slack-water sediments, Internat. Assoc. of Sedimentologists Special Publ. 6, 229–239.

Baker, V.R., Pickup, G., Polach, H.A., 1985. Radiocarbon dating of flood deposits, Katherine Gorge, Northern Territory, Australia. Geology 13, 344–347.

Baker, V.R., Webb, R.H., House, P.K., 2002. The scientific and societal value of paleoflood hydrology. In: House, P.K., Webb, R.H., Baker, V.R., Levish, D.R. (Eds.), Ancient Floods, Modern Hazards: Principles and Applications of Paleoflood Hydrology. Water Science and Application, vol. 5. American Geophysical Union,Washington, D.C., pp. 1–19.

Baker, V. R. 2008. Paleoflood hydrology: Origin, progress, prospects, Geomorphology, 101, 1–13, doi:10.1016/j.geomorph.2008.05.016.

Benito, G., Sopeña, A., Sánchez, Y., Machado, M.J., Pérez González, A. (2003). Palaeoflood Record of the Tagus River (Central Spain) during the Late Pleistocene and Holocene. Quaternary Science Reviews 22, 1737-1756.

Benito, G., and J. E. O'Connor (2013), Quantitative paleoflood hydrology, in Treatise on Geomorphology, edited by J. Shroder, vol. 9, Fluvial Geomorphology, edited by E. E. Wohl, pp. 459–474, Academic, San Diego, Calif.

Benito, G., Macklin, M.G., Panin, A., et al., (2015). Recurring flood distribution patterns related to short-term Holocene climatic variability. Scientific reports 5, 16398.

Blinn DW, Poff N.L. 2005. Colorado river basin. In Rivers of North America, Benke AC, Cushing CE (eds). Elsevier Academic Press: Burlington, Massachusetts; 483–526.

Brown, S.L., Bierman, P.R., Lini, A., Southon, J., 2000. 10,000 yr record of extreme hydrologic events. Geology 28, 69–82.

Cashion W. B. 1967. Geology and Fuel Resources of the Green River Formation Southeastern Uinta Basin, Utah and Colorado, USGS Professional Paper 548, 47 p.

Costa, J.E., 1978. Holocene stratigraphy in flood-frequency research. Water Resources Research 14, 626–632.

Cohn, T.A., Lane, W.L., Baier, W.G., 1997. An algorithm for computing moments-based flood quantile estimates when historical flood information is available. Water Resources Research 33, 2089–2096.

578 Chow, V. T., Maidment, D. R., and Mays, L. W. 1988. Applied Hydrology. McGraw-Hill, New
579 York. 572 pp.

580 Cudworth, A. G., 1989, Flood Hydrology Manual, 243 p., U.S. Dep. of Interior, Bur. of Reclam.,
581 Denver, Colo.

582 Douglas, E. M., & Barros, A. P., 2003. Probable maximum precipitation using multifractals:
583 Application in the Eastern United States. Journal of Hydrometeorology, 4, 1012–1024.

584 Ely, L.L., Baker, V.R., 1985. Reconstructing paleoflood hydrology with slackwater deposits:
585 Verde River, Arizona. Physical Geography 6, 103–126.

586 Ely, L.L., Webb, R.H., Enzel, Y., 1992. Accuracy of post-bomb 137 Cs and 14 C in dating
587 fluvial deposits. Quaternary Research 38, 196–204.

588 Ely, L. L., Y. Enzel, V. R. Baker, and D. R. Cayan (1993), A 5000-year record of extreme floods
589 and climate change in the Southwestern UnitedStates. Science, 262, 410–412.

590 Ely, L.L., 1997. Response of extreme floods in the southwestern United States to climatic
591 variations in the late Holocene. Geomorphology 19, 175–201.

592 England, J.F., Jr., Cohn,T.A., Faber,B.A., Stedinger, J.R., Thomas, W.O., Jr., Veilleux, A.G.,
593 Kiang, J.E., and Mason, R.R., Jr., 2018, Guidelines for determining flood flow
594 frequency—Bulletin 17C: U.S. Geological Survey Techniques and Methods, book4,
595 chap. B5, 148p., https://doi.org/10.3133/tm4B5.

596 England, J.F. Jr., Julien, P.Y., and Velleux, M.L., 2014. Physically-Based Extreme Flood
597 Frequency Analysis using Stochastic Storm Transposition and Paleoflood Data on Large
598 Watersheds, J. Hydrol., 510, doi:10.1016/j.jhydrol.2013.12.021, pp. 228-245.

England, Jr. J.F., Godaire, J.E., Klinger, R.E., Bauer, T.R., Julien, P.Y., 2010. Paleohydrologic bounds and extreme flood frequency of the Upper Arkansas River, Colorado, USA. Geomorphology 124, 1–16.

Enzel, Y., Ely, L.L., House, P.K., Baker, V.R. and Webb, R.H., 1993. Paleoflood evidence for a natural upper bound to flood magnitudes in the Colorado River Basin. Water Resources Research, 29(7): 2287-2297.

Enzel, Y., Ely, L.L., Martinez-Goytre, R., Vivian, R.G., 1994. Paleofloods and a dam-failure flood on the Virgin River, Utah and Arizona. Journal of Hydrology 153: 291–315.

Francés F. 2001. Incorporating Non-Systematic Information to Flood Frequency Analysis Using the Maximum Likelihood Estimation Method. In: Glade T., Albini P., Francés F. (eds) The Use of Historical Data in Natural Hazard Assessments. Advances in Natural and Technological Hazards Research, vol 17. Springer, Dordrecht

Fuller, W. E., 1914. Flood flows. Transactions of the American Society of Civil Engineers, 68, 564–618.

Fuller, J.E. 1987. Paleoflood hydrology of the alluvial Salt River, Tempe, Arizona. M.S. thesis, University of Arizona, Tucson.

Greenbaum, N., Schick, A.P., Baker, V.R., 2000. The paleoflood record a hyperarid catchment, Nahal Zin, Negev Desert, Israel. Earth Surface Processes and Landforms 25, 951–971.

Greenbaum, N., A. Ben-Zvi, I. Haviv, Y. Enzel, 2006. T hydrology and paleohydrology of the Dead Sea tributaries. In: Y. Enzel, A. Agnon, M. Stein (Eds.), New Frontiers in Dead Sea Paleoenvironmental Research, Geological Society of America, Special Paper 401, p. 63-94.

621 Greenbaum, N., T. M. Harden, V. R. Baker, J. Weisheit, M. L. Cline, N. Porat, R. Halevi, and J.
622 Dohrenwend (2014), A 2000 year natural record of magnitudes and frequencies for the
623 largest Upper Colorado River floods near Moab, Utah, Water Resour. Res., 50,
624 doi:10.1002/2013WR014835.

625 Guérin, G., Mercier, N., Adamiec, G., 2011. Dose-rate conversion factors: update: Ancient TL
626 29, 5-8.

627 Harden, T.M., Macklin, M. G. and Baker, V. R. 2010, Holocene flood histories in south-western
628 USA. Earth Surf. Process. Landforms, 35: 707–716. doi:10.1002/esp.1983.

629 Hirschboeck KK. 1988. Flood hydroclimatology. In Flood Geomorphology, Baker VR, Kochel
630 RC, Patton PC (eds). John Wiley and Sons: New York; 27–49.

631 House, P.K., Webb, R.H., Baker, V.R., Levish, D. (Eds.), 2002. Ancient Floods, Modern
632 Hazards: Principles and Applications of Paleoflood Hydrology. Water Science and
633 Application, vol. 5. American Geophysical Union. 385 pp.

634 Huang, C.C., Pang, J.L., Zha, X.C., Su, H.X., 2007. Impact of monsoonal climatic change on
635 Holocene overbank flooding along the Sushui River within the Middle Reaches of the
636 Yellow River, China. Quaternary Science Reviews 26, 2247-2264.

637 Huang, C.C., Pang, J.L., Zha, X.C. et al., 2010. Extraordinary floods of 4100-4000 a BP
638 recorded at the late Neolithic ruins in the Jinghe River gorges, middle reach of the
639 Yellow River, China. Palaeogeography Palaeoclimatology Palaeoecology 289, 1-9.

640 IACWD, 1982. Guidelines for determining flood flow frequency, Bulletin 17-B. Technical
641 report, Interagency Committee on Water Data, Hydrology Subcommittee.

642 Jakob, D., Smalley, R., Meighen, et al., 2009. Climate change and probable maximum
643 precipitation. Melbourne: Bureau of Meteorology, Australian Government,
644 Hydrometeorological Advisory Service, Water Division.

645 Jarrett, R.D., 1990. Paleohydrologic techniques used to define the spatial occurrence of floods.
646 Geomorphology 3, 181–195.

647 Jones, A.P., Shimazu, H., Oguchi, T., Okuno, M., Tokutake, M., 2001. Late Holocene slackwater
648 deposits on the Nakagawa River, Tochigi Prefecture, Japan. Geomorphology 39, 39–51.

649 Kale, V.S., Mishra, S., and Baker, V.R., 1997, A 2000-year palaeoflood record from Sakarghat
650 on Narmada, central India: Journal of the Geological Society of India, 50, 283-288.

651 Kidson, R., Richards, K.S., 2005. Flood frequency analysis: assumptions and alternatives.
652 Progress in Physical Geography 29, 392–410.

653 Kiseiel, C.C. 1969. Time series analysis of hydrologic data. Adv. Hydrosci. 5, 1-119.

654 Klemeš V., 1987. Hydrological and engineering relevance of flood frequency analysis. In Singh,
655 V. P., editor, Hydrologic Frequency Modeling, pages 1-18, Louisiana State University,
656 Baton Rouge. D. Reidel Publishing Company.

657 Klemeš, V., 1994, Statistics and probability: Wrong remedies for a confused hydrologic modeler,
658 in Statistics for the Environment 2: Water Related Issues, edited by V. Barnett and K.F.
659 Turkman, pp. 345-366, John Wiley and Sons, London.

660 Klemeš V., 2000. Tall Tales about Tails of Hydrological Distributions. I. Journal of Hydrologic
661 Engineering, 5(3):227–231.

662 Kenney, T.A., Wilkowske, C.D., and Wright, S.J., 2007, Methods for Estimating Magnitude and
663 Frequency of Peak Flows for Natural Streams in Utah: U.S. Geological Survey Scientific
664 Investigations Report 2007-5158, 28 p.

665 Knox, J.C., 1985. Responses of floods to Holocene climatic change in the Upper Mississippi
666 Valley. Quaternary Research 23, 287–300.

667 Knox, J.C., 1993. Large increases in flood magnitude in response to modest changes in climate.
668 Nature 361, 430–432.

669 Knox, J.C., 2000. Sensitivity of modern and Holocene floods to climatic change. Quaternary
670 Science Reviews 19, 439-457.

671 Kochel, R.C., Patton, P.C., Baker, V.R., 1982. Paleohydrology of southwestern Texas. Water
672 Resources Research 18, 1165–1183.

673 Kochel, R.C., Baker, V.R., 1988. Paleoflood analysis using slackwater deposits. In: Baker, V.R.,
674 Kochel, R.C., Patton, P.C. (Eds.), Flood Geomorphology. Wiley, NY, pp. 357–376.

675 Kunkel, K. E., T. R. Karl, D. R. Easterling, et al., (2013), Probable maximum precipitation and
676 climate change, Geophys. Res. Lett., 40, 1402–1408, doi:10.1002/grl.50334.

677 Lai, Y.G. 2009. Two-Dimensional Depth-Averaged Flow Modeling with an Unstructured Hybrid
678 Mesh. Journal of Hydraulic Engineering, ASCE, 136(1), pp 12-23.

679 Lam, D., C. Thompson, J. Croke, A. Sharma, and M. Macklin (2017), Reducing uncertainty with
680 flood frequency analysis: The contribution of paleoflood and historical flood information,
681 Water Resour. Res., 53, 2312–2327, doi: 10.1002/2016WR019959.

682 Liu, T., Huang, C.C., Pang, J.L., et al., 2014. Extraordinary hydro-climatic events during 1800–
683 1600 yr BP in the Jin–Shaan Gorges along the middle Yellow River, China.
684 Palaeogeogr., Palaeoclimatol., Palaeoecol., 410: 143–152.

685 Macklin, M. G. et al., 2006. Past hydrological events reflected in the Holocene fluvial record of
686 Europe. Catena 66, 145–154.

687 Merz, B., Aerts, J., Arnbjerg-Nielsen, K., et al. 2014. Floods and climate: emerging perspectives
688 for flood risk assessment and management. Nat. Hazards Earth Syst. Sci., 14, 1921–1942.

689 Munoz, S. E. and Dee, S. G., 2017. El Niño increases the risk of lower Mississippi River
690 flooding. Sci. Rep. 7, https://doi.org/10.1038/s41598-017-01919-6.

691 Munoz, S. E., Giosan, L., Therrell, M. D., etc., 2018. Climatic control of Mississippi River flood
692 hazard amplified by river engineering. Nature, 556 (7699): 95 DOI:
693 10.1038/nature26145.

694 SL44-2006, 2006. Regulation for calculating design flood of water resources and hydropower
695 projects, Ministry of Water Resources, P.R. China. China Water&Power Press, Beijing:
696 1-92.

697 Macklin MG, Benito G, Gregory KJ, et al., 2006. Past hydrological events refl ected in the
698 Holocene fl uvial record of Europe. Catena 66: 145–154.

699 Malamud, B.D., Turcotte, D.L., 2006. The applicability of power-law frequency statistics to
700 floods. Journal of Hydrology 322, 168–180.

701 Murray, A.S., Wintle, A.G., 2000. Luminescence dating of quartz using an improved single
702 aliquot regenerative-dose protocol. Radiation Measurements 32, 57-73.

703 Murray, A.S., Wintle, A.G., 2003. The single aliquot regenerative dose protocol: potential for
704 improvements in reliability. Radiation Measurements 37, 377-381.

705 U.S. Water Resource Council, Hydrology Committee, 1977. Guidences for Determining Flood
706 Frequency Information, Bulletin 17A, Washington, D.C.

707 U.S. Army Corps of Engineers, "Inflow Design Floods for Dams and Reservoirs," Engineer
708 Regulation No. 1110-8-2 (FR), 1991.

709 U. S. Bureau of Reclamation (2003), Flood Hazard Analysis: Seminoe and Glendo Dams
710 Kendrick Project and Pick Sloan Missouri Basin Program, Wyoming, Tech. Serv. Cent.,
711 Denver.

712 National Environment Research Council, 1999: Flood Studies Report, (in five volumes)
713 Wallingford: Institute of Hydrology.

714 National Research Council, 1988: Committee on techniques for estimating probabilities of
715 extreme floods: estimating probabilities of extreme floods –methods and recommended
716 research. Washington, DC: National Academy Press.

717 O'Connor, J.E., Ely, L.L., Wohl, E.E., Stevens, L.E., Melis, T.S., Kale, V.S., Baker, V.R., 1994.
718 A 4500-year record of large floods on the Colorado River in the Grand Canyon, Arizona.
719 Journal of Geology 102, 1–9.

720 O'Connor, J.E., Curran, J.H., Beebee, R.A., Grant, G.E., Sarna-Wojcicki, A., 2003. Quaternary
721 geology and geomorphology of the lower Deschutes River Canyon, Oregon. In: Grant,
722 G.E., O'Connor, J.E. (Eds.), A Peculiar River: Geology, Geomorphology, and Hydrology
723 of the Deschutes River, Oregon. Water Science and Applications, vol. 7. American
724 Geophysical Union, pp. 77–98.

725 Ostenaa, D.A., Levish, D.R., O'Connell, D.R.H., 1996. Paleoflood study for Bradbury Dam,
726 Cachuma Project, California. U.S. Bureau of Reclamation Seismotectonic Report 96-3,
727 Denver, CO.

728 Patton, P.C., Baker, V.R., 1977. Geomorphic response of central Texas stream channels to
729 catastrophic rainfall and runoff. In: Doehring, D. (Ed.), Geomorphology of Arid and
730 Semi-arid Regions. Allen and Unwin, London, pp. 189–217.

731 Patton, P.C., Dibble, D.S., 1982. Archeologic and geomorphic evidence for the paleohydrologic
732 record of the Pecos River in west Texas. American Journal of Science 82, 97–121.

733 Partridge, J. and Baker, V. R. (1987), Palaeoflood hydrology of the Salt River, Arizona. Earth
734 Surf. Process. Landforms, 12: 109–125. doi:10.1002/esp.3290120202

735 Pickup, G., Allan, G., Baker, V.R., 1988. History, palaeochannels, and palaeofloods of the Finke
736 River, central Australia. In: Warner, R.F. (Ed.), Fluvial Geomorphology of Australia.
737 Academic Press, Sydney, pp. 177–200.

738 Prescott, J. R., Hutton, J.T., 1994. Cosmic ray contributions to dose rates for luminescence and
739 ESR dating: Radiation Measurements 23, 497-500.

740 Rouhani, H., and R. Leconte, 2016. A novel method to estimate the maximization ratio of the
741 Probable Maximum Precipitation (PMP) using regional climate model output, Water
742 Resour. Res., 52, 7347–7365, doi:10.1002/2016WR018603.

743 Saint-Laurent, D., Couture, C., McNeil, E., 2001. Spatio-temporal analysis of floods of the Saint-
744 Francois drainage basin, Quebec, Canada. Environments 29, 74–90.

745 Sheffer, N., Enzel, Y., Benito, G. et al., 2003. Historical and paleofloods of the Ardech River,
746 France. Water Resources Research 39. doi: 10.1029/2003WR002468.

Song, X.Y., Song S.B., Sun W.Y., et al., 2015. Recent changes in extreme precipitation and drought over the Songhua River Basin, China, during 1960–2013. Atmospheric Research 157, 137-152.

Springer, G.S., Kite, J.S., 1997. River-derived slackwater sediments in caves along Cheat River, West Virginia. Geomorphology 18, 91–100.

Stedinger, J.R., and Baker, V.R., 1987, Surface water hydrology: historical and paleo-flood information: Reviews of Geophysics, v. 25, p. 119 124.

Stedinger, J.R., Cohn, T.A., 1986. Flood frequency analysis with historical and paleoflood information. Water Resources Research 22, 785–793.

Stedinger, J.R., Griffis, V.W., 2008. Flood Frequency Analysis in the United States: Time to Update. Journal of Hydrologic Engineering, 13(4): 199-204. https://doi.org/10.1061/(ASCE)1084-0699(2008)13:4(199)

Webb, R.H., O'Connor, J.E., Baker, V.R., 1988. Paleohydrologic reconstruction of flood frequency on the Escalante River. In: Baker, V.R., Kochel, R.C., Patton, P.C. (Eds.), Flood Geomorphology. John Wiley and Sons, N.Y., pp. 403–418.

Western Regional Climate Center. (2013). Cooperative Climatological Data Summaries. Retrieved from http://wrcc.dri.edu/climatedata/climsum/

Toonen, W.H.J., Foulds, S.A. Macklin, M.G. et al., 2017. Events, episodes, and phases: Signal from noise in flood-sediment. Geology, doi:10.1130/G38540.1.

Wintle, A.G. Murray, A.S., 2006. A review of quartz optically stimulated luminescence characteristics and their relevance in single-aliquot regenerative protocols: Radiation Measurements, v. 41, p. 369-391.

769 WMO, 2009. Manual on Estimation of Probable Maximum Precipitation (PMP). World
770 Meteorological Organization, Switzerland, pp 257.

771 Wohl, E.E., Greenbaum, N., Schick, A.P., Baker, V.R., 1994. Controls on bedrock channel
772 morphology alongNahal Paran, Israel. Earth Surface Processes and Landforms 19, 1–13.

773 Yevjevich, V., 1968. 'Misconceptions in Hydrology and their Consequences.' Water Resource
774 Research, 4(4), 225-232.

***Declaration of Interest Statement**

Declaration of interests

☒ The authors declare that they have no known competing financial interests or personal relationships that could have appeared to influence the work reported in this paper.

☐The authors declare the following financial interests/personal relationships which may be considered as potential competing interests:

Figure1
Click here to download high resolution image

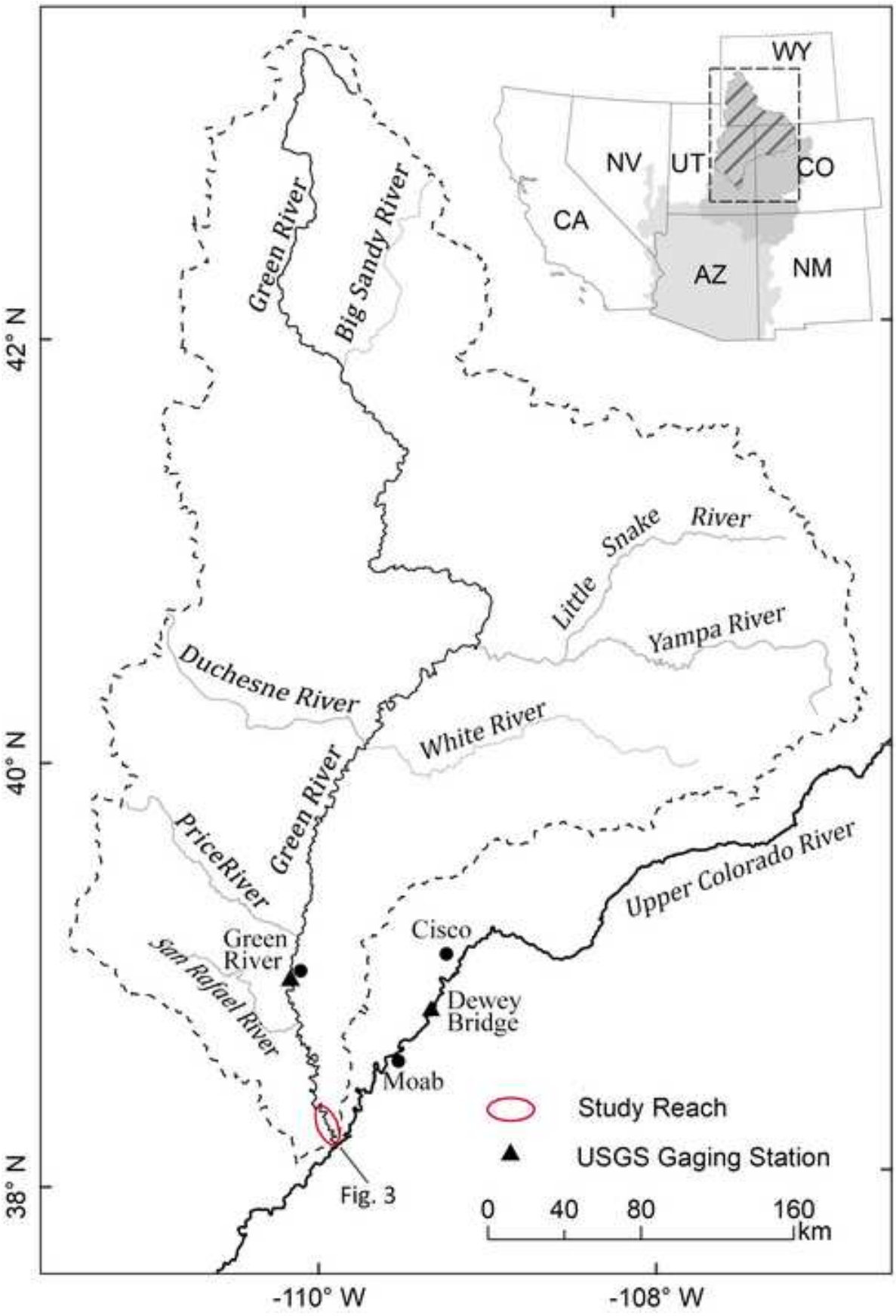

Figure 2
Click here to download high resolution image

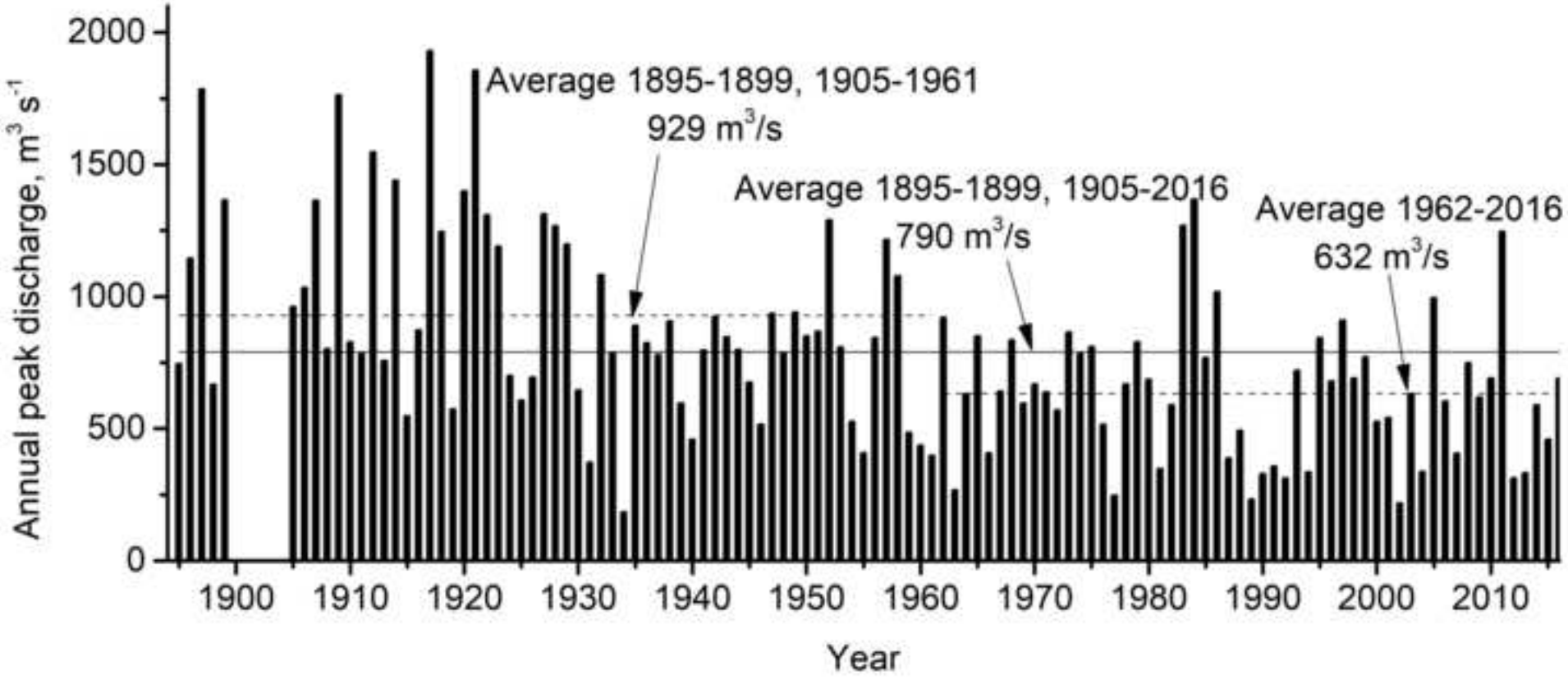

Figure 3
Click here to download high resolution image

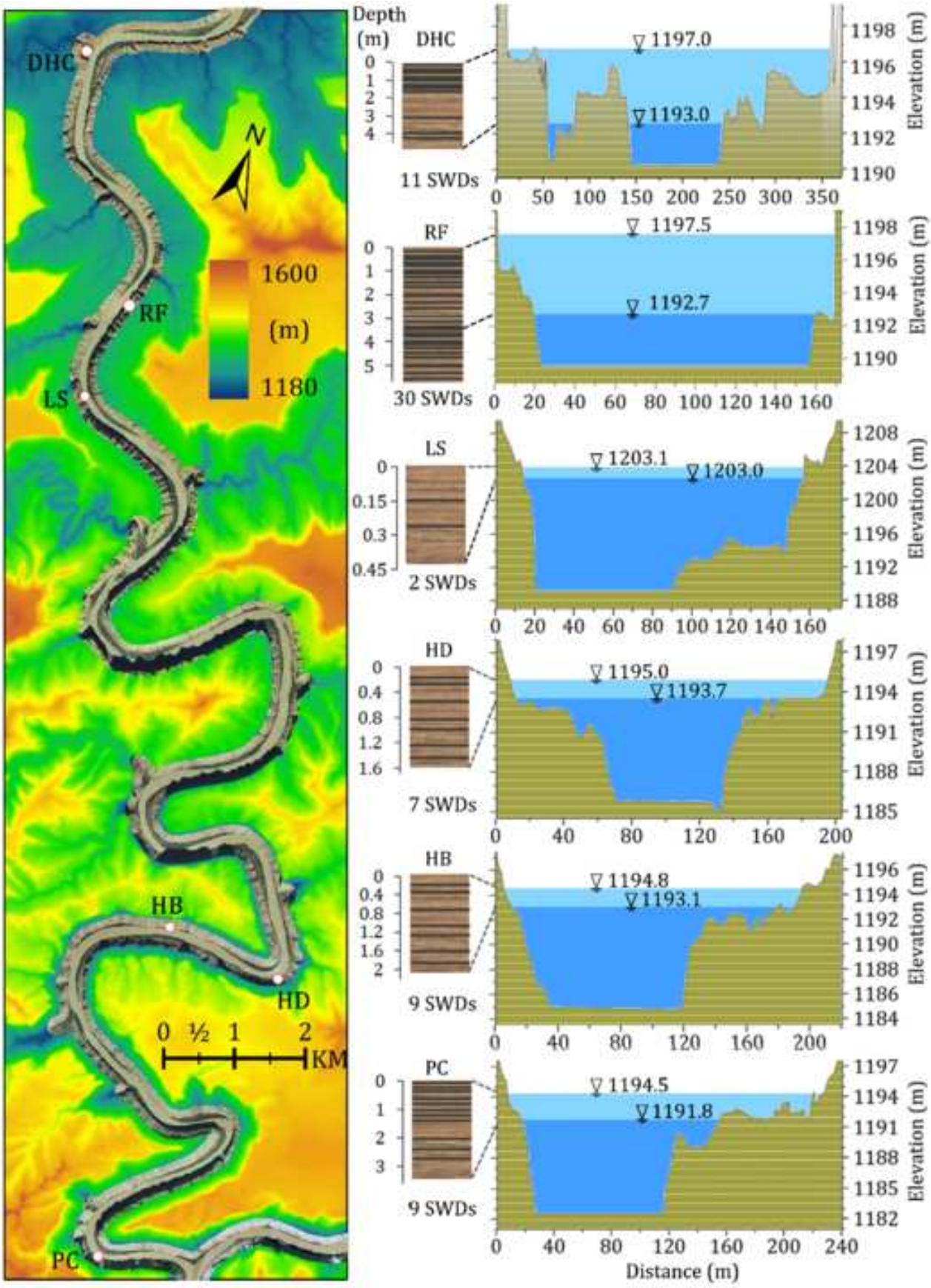

Figure4
Click here to download high resolution image

Figure5
Click here to download high resolution image

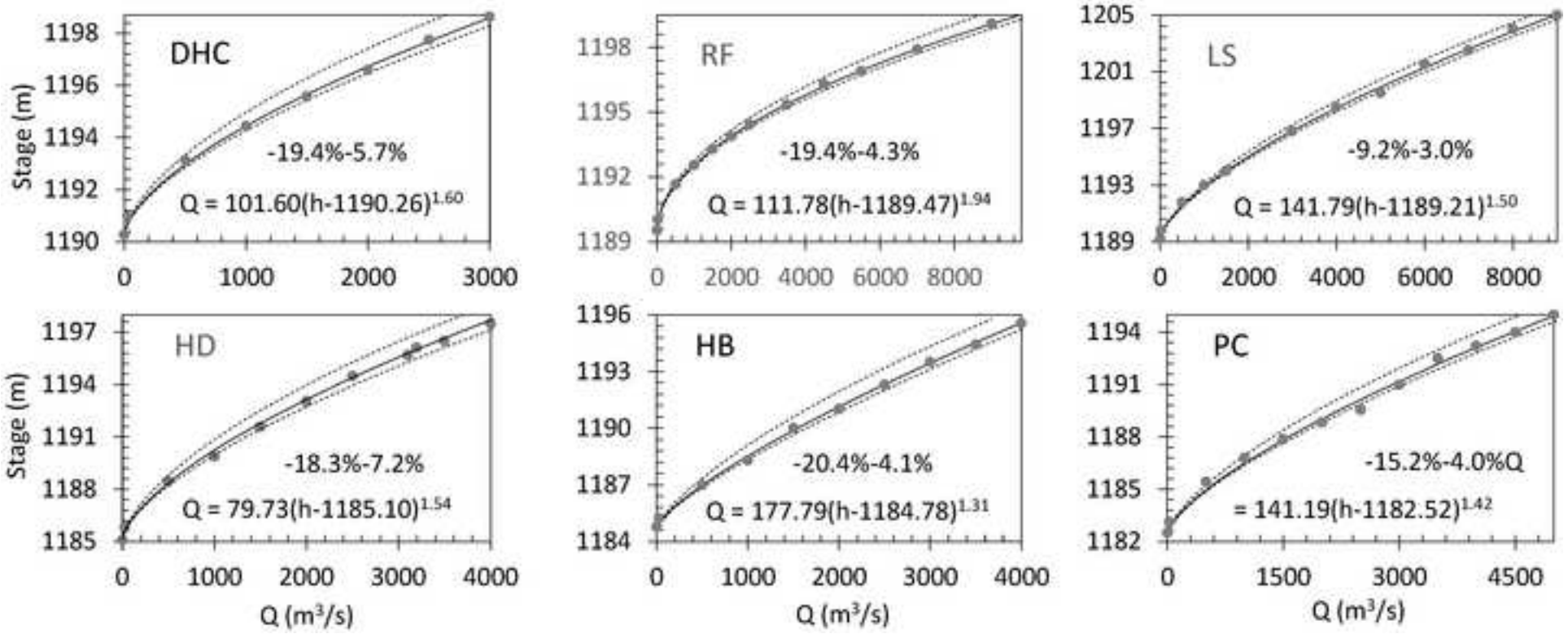

Figure6
Click here to download high resolution image

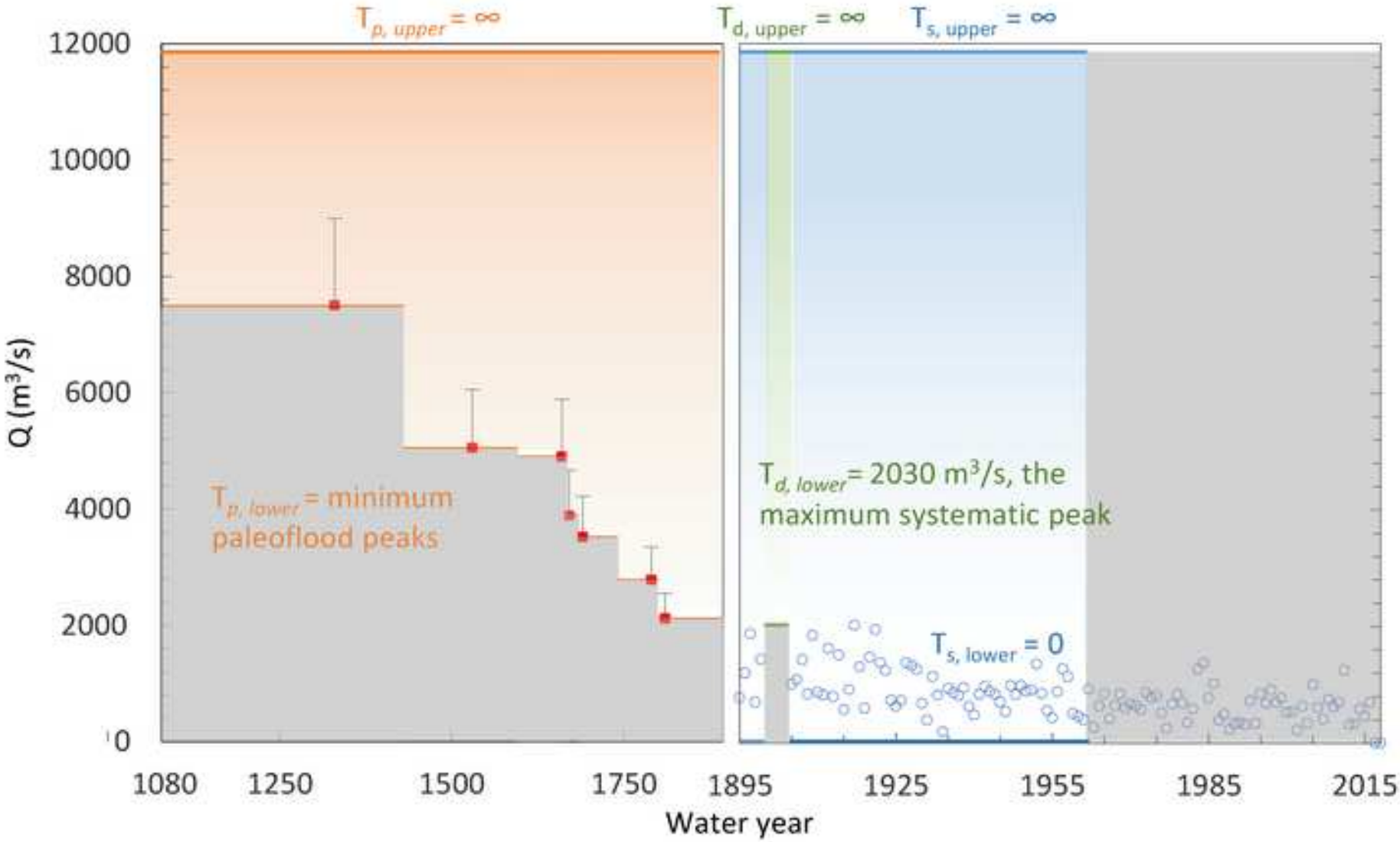

Figure7
Click here to download high resolution image

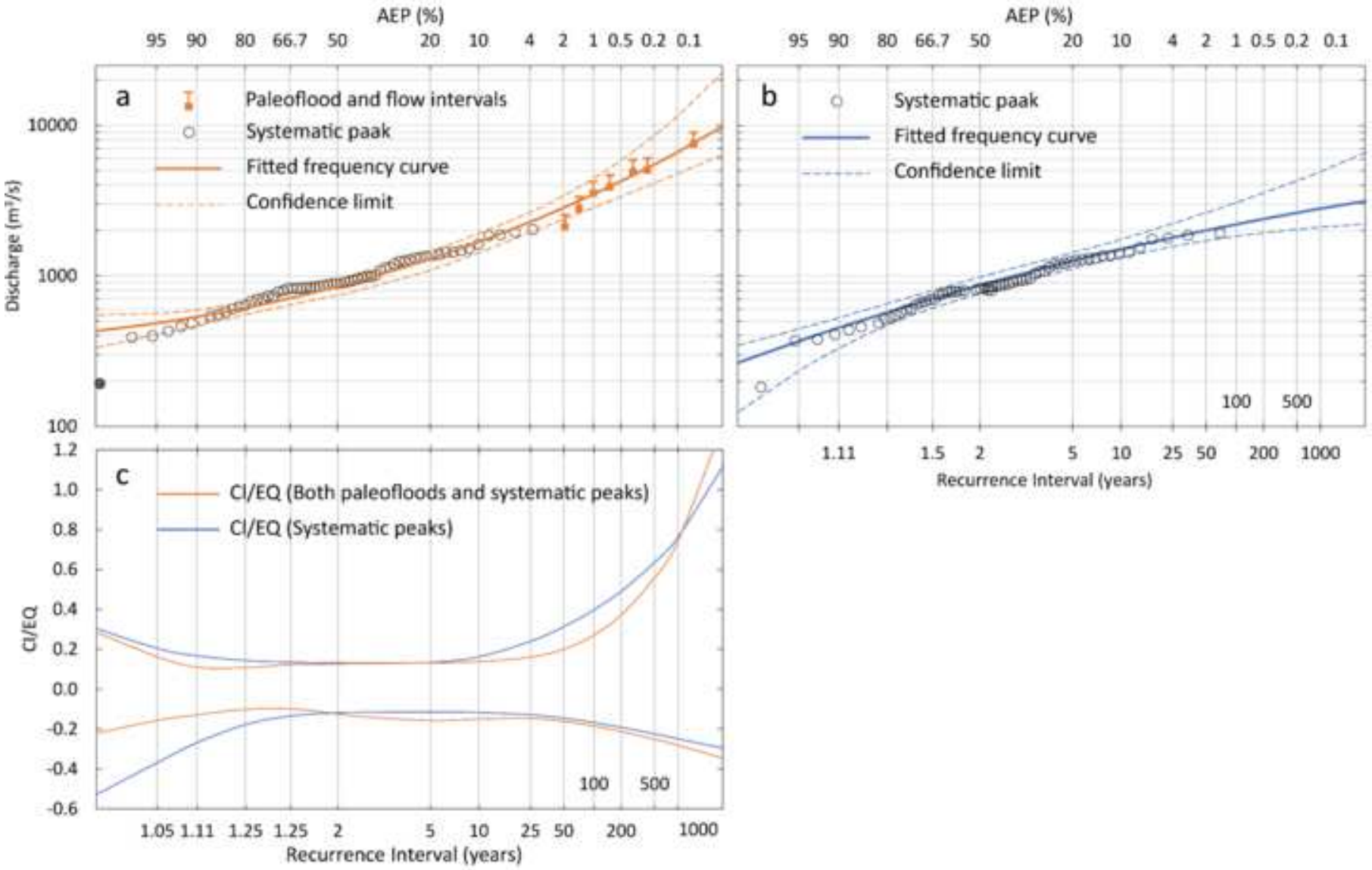

Figure8
Click here to download high resolution image

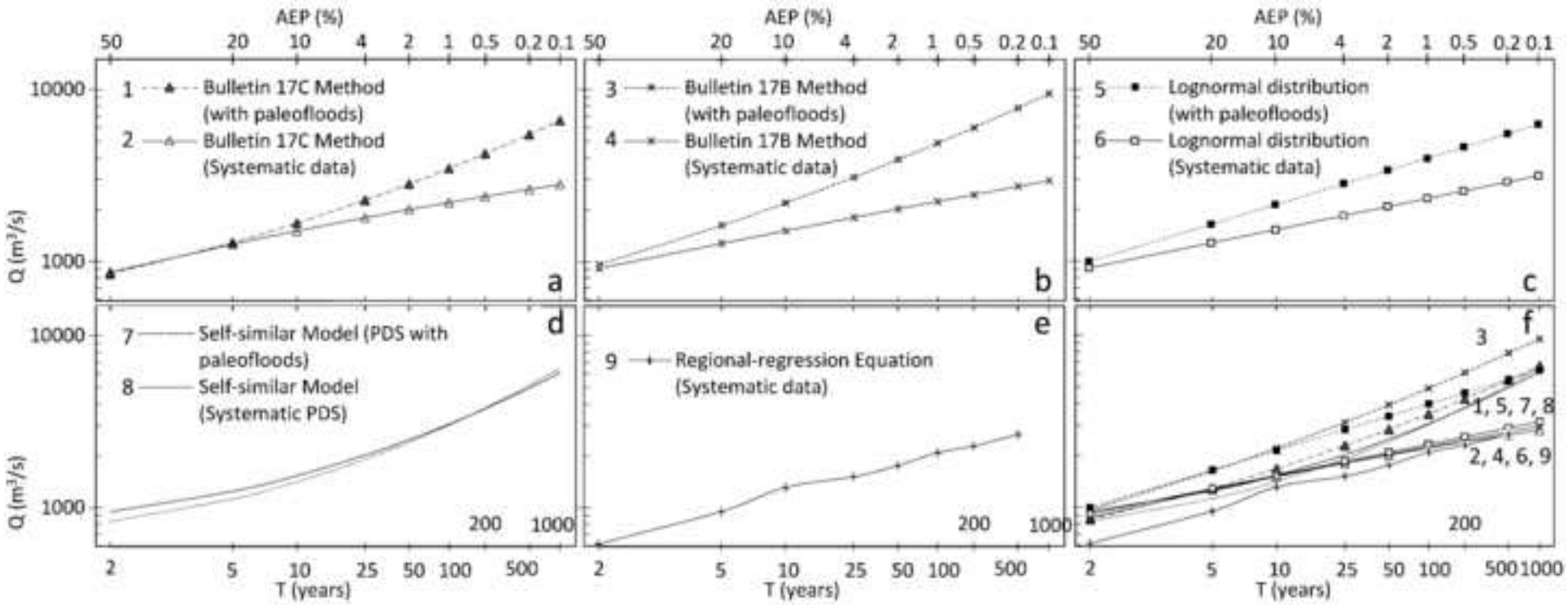

Tables

Click here to download Table: Tables.docx

Table 1. Characteristics of slackwater depositional environments for paleoflood SWDs in Stillwater Canyon of the lower Green River.

Stratigraphic section	Thickness (m)	SWD Layers	Texture	Top unit elevation (m a.w.l.)	Depositional environment
DHC-1	1.25	8	silt and fine sand	7.00	At a tributary mouth;
DHC-2	>4.00	4	clay, silt and fine sand	6.35	On a high rock ledge
RF-1-1	2.50	8	silt and fine sand	8.00	On the top of a rock-fall; Covered by stony colluvium
RF-1-2	4.20	18	clay, silt and fine sand	5.50	
RF-2	1.55	4	medium and fine sand	8.00	
LS	0.70	2	silt and fine sand	13.50	On a high rock ledge; Area of widening canyon
HD	1.50	7	silt and fine sand	10.00	Severe channel bend (>90°); Covered by stony colluvium
HB	2.00	9	clay, silt and fine sand	10.00	On the top of high alluvial terrace; Covered by stony colluvium
PC	>8.00	9	silt and fine sand	>12.00	Severe channel bend (>90°)

Table 2. Results of AMS 14C Dating of Paleoflood Deposits on lower Green River

Site, SWD Unit No.	Lab Sample no.	Type of dated material	Radiocarbon age (years BP)	Calibrated Age range (years AD)
DHC, #8	AA101614	Charred wood	90 ± 38	1681-1739 (26.6%) 1802-1938 (67.2%)
PC, #4	AA101615	Charred leaf	80 ± 39	1682-1736 (26.3%) 1805-1936 (69.1%)
PC, #5	AA101613	Charred bark	52 ± 38	1690-1730 (23.6%) 1810-1926 (71.8%)

Table 3. Results of OSL Dating of Paleoflood Deposits on lower Green River

Site, SWD Unit No.	Lab No.	Depth (m)	K (%)	U (ppm)	Th (ppm)	Cosmic (Gy/ka)	Dose rate (Gy/ka)	De (Gy)	Age ± 2σ (ka)
DHC-1, #1	GRV-2	1.00	1.66	1.9	6.0	0.19	2.58 ± 0.07	1.75 ± 0.64	0.68 ± 0.25
DHC-2, #2	GRV-3	4.00	1.74	2.5	8.0	0.13	2.68 ± 0.06	1. 25 ± 0.43	0.47 ± 0.16
DHC-2, #11	USU-2310	1.10	1.78	2.8	8.4	0.18	3.10 ± 0.14	0.61 ± 0.25	0.20 ± 0.08
RF-1, #2	GRV-11	4.00	1.66	3.0	10.7	0.13	2.63 ± 0.06	1.43 ± 0.44	0.55 ± 0.17
RF-1, #11	USU-2309	1.25	1.72	1.9	5.9	0.23	2.69 ± 0.12	0.85 ± 0.22	0.31 ± 0.09
RF-1, #14	GRV-9	0.30	1.66	2.8	7.8	0.23	3.00 ± 0.06	1.20 ± 0.30	0.40 ± 0.10
RF-2, #19	GRV-12	0.40	1.66	2.3	7.5	0.22	2.85 ± 0.07	0.83 ± 0.16	0.29 ± 0.06
RF-1, #20	USU-2307	2.60	1.74	2.6	9.0	0.19	3.08 ± 0.14	0.58 ± 0.24	0.19 ± 0.08
RF-1, #30	GRV-10	0.30	1.66	2.5	8.1	0.23	2.95 ± 0.06	0.64 ± 0.31	0.22 ± 0.11
LS, #2	GRV-6	0.30	1.58	1.4	4.6	0.23	2.36 ± 0.06	0.51 ± 0.10	0.22 ± 0.04
HB, #1	GRV-5	1.90	1.58	1.9	5.4	0.17	2.40 ± 0.06	1.07 ± 0.16	0.35 ± 0.07
HB, #8	GRV-4	0.30	1.66	2.2	7.0	0.23	2.80 ± 0.07	0.88 ± 0.07	0.32 ± 0.07
PC, #2	GRV-8	2.50	1.74	2.5	8.6	0.15	2.74 ± 0.08	0.94 ± 0.24	0.34 ± 0.09
PC, #7	USU-2306	0.55	1.56	2.0	6.7	0.24	2.65 ± 0.12	0.53 ± 0.26	0.20 ± 0.10
PC, #8	GRV-7	0.30	1.83	2.5	8.5	0.23	3.13 ± 0.08	1.51 ± 0.25	0.48 ± 0.17

Table 4. Results of the minimum paleoflood peak discharges using SHR-2D model with the percentage of variation resulting from a 25% change in the Manning's n values.

Site Name	Deposit unit	Water level during the LiDAR Flight (m)	Elevation above the water level (m)	Estimated peak stage (m)	Minimum peak discharge (m^3/s)	Variation
Dead Horse	DHC-9	1190.97	7.00	1197.97	2747	-14.3-6.2%
	DHC-8		6.65	1197.62	2558	-14.7-6.3%
	DHC-1		5.80	1196.77	2120	-15.5-6.5%
	DHC-2		3.00	1193.97	920	-17.7-6.9%
Rock fall	RF-19	1190.03	8.00	1198.03	7271	-13.1-4.8%
	RF-30		5.50	1195.53	3768	-16.1-5.5%
	RF-20		5.10	1195.13	3313	-16.5-5.5%
	RF-2		1.40	1191.43	507	-18.9-6.1%
Ledge Site	LS-top	1189.73	13.50	1203.23	7499	-6.4-4.9%
	LS-2		13.35	1203.08	7379	-6.5-4.9%
	LS-1		13.25	1202.98	7299	-6.5-4.9%
High Driftwood	HD-7	1185.82	10.00	1195.82	3207	-12.4-7.6%
	HD-1		8.40	1194.22	2520	-13.7-8.0%
High Bank	HB-9	1184.78	10.00	1194.78	3615	-11.6-4.4%
	HB-8		9.80	1194.58	3520	-11.8-4.5%
	HB-1		8.20	1192.98	2790	-13.6-5.1%
Powell Canyon	PC-9	1183.13	12.00	1195.13	5104	-9.3-4.1%
	PC-8		11.90	1195.03	5047	-9.4-4.1%
	PC-7		11.65	1194.78	4905	-9.6-4.2%
	PC-2		9.80	1192.93	3891	-10.7-4.3%

Table 5. EMA (Expected Moments Algorithm) flow intervals for the paleoflood and systematic records during 1080-2016 on the lower Green River, Utah.

Water Year	$Q_{Y,lower}$ (m^3/s)	$Q_{Y,upper}$ (m^3/s)	Comment
1330	7500	9000	
1530	5050	6060	
1660	4910	5890	For paleofloods, estimated peaks are minimal values; with an addition 20% as upper level for each estimation.
1670	3890	4670	
1690	3520	4220	
1790	2790	3350	
1810	2120	2540	
1895-1899	$Q_{Y,lower} = Q_{Y,lower} = Q_Y$		Gaged data are nearly exactly known equaling to measured value (Q_Y).
1905-1961			

Table 6. EMA (Expected Moments Algorithm) perception threshold for the paleoflood and historical period from 1080 to 1961 on the lower Green River, Utah.

Start Year	End Year	EMA perception threshold (m^3/s)		Comments
		$T_{Y,lower}$	$T_{Y,upper}$	
1080	1961	0	Infinity	Total Record
1080	1430	7500	Infinity	Top of paleoflood SWD
1431	1595	5050	Infinity	Top of paleoflood SWD
1596	1665	4910	Infinity	Top of paleoflood SWD
1666	1680	3890	Infinity	Top of paleoflood SWD
1681	1740	3520	Infinity	Top of paleoflood SWD
1741	1800	2790	Infinity	Top of paleoflood SWD
1801	1894	2120	Infinity	Top of paleoflood SWD
1895	1899	0	Infinity	Systematic data
1900	1904	2030	Infinity	Broken; Largest systematic data
1905	1961	0	Infinity	Systematic data

Table 7. A Comparison between flood frequency results using different methods on the lower Green River, Utah (in m^3/s)

No.	Method	T								
		2	5	10	25	50	100	200	500	1000
1	Bulletin 17C Method (with paleofloods)	847	1289	1671	2274	2825	3475	4245	5483	6616
2	Bulletin 17C Method (Systematic data)	867	1259	1504	1798	2004	2201	2389	2628	2801
3	Bulletin 17B Method (with paleofloods)	962	1623	2196	3101	3925	4894	6032	7845	9487
4	Bulletin 17B Method (Systematic data)	913	1275	1511	1806	2023	2238	2452	2736	2954
5	Lognormal distribution (with paleofloods)	995	1641	2132	2818	3374	3968	4602	5507	6247
6	Lognormal distribution (Systematic data)	914	1279	1526	1840	2078	2317	2560	2888	3144
7	Self-similar Model (PSD with paleofloods)	828	1121	1409	1907	2398	3015	3791	5131	6451
8	self-similar Model (Systematic PSD)	945	1243	1531	2014	2479	3052	3756	4944	6085
9	Regional-regression Equation (Systematic data)	615	949	1308	1509	1753	2082	2283	2654	

Figure captions

Figure 1. Green River Basin including the large tributaries, USGS gauging station, and the study reach.

Figure 2. Annual maximum peak discharges on the Green River at the USGS gauging station Green River, Utah, 1894-2016.

Figure 3. A map showing six study sites (DHC, RF, LS, HD, HB, and PC) on the Lower Green River (left), the stratigraphic illustrations showing the paleoflood slackwater deposit layers (black lines) and the river channel and valley dimensions of each stratigraphic section (middle), and the cross-sections at each site (right), showing the range of extreme flood water surface elevation.

Figure 4. Particle tracings and water depths associated with sites of DHC, PC, HB, and HD on the Lower Green River. Areas of slack-water deposition develop through combinations of flow direction, speed, and depth. For sites location see figure 3.

Figure 5. Rating curves (solid lines) and corresponding results (dashed lines) for the 25% of Manning's n variation for six cross sections at the paleoflood sites on the Lower Green River. The sensitivity test shows an error of 3.0-20.4% can be introduced by the uncertainty of Manning's *n*.

Figure 6. Graph showing approximate systematic peak discharge and paleoflood estimates, with paleoflood exceedance thresholds, on the Lower Green River in the Stillwater Canyon reach. A scale break is used to separate the gaging station data from the much longer paleoflood record. Flood intervals for large floods in the paleoflood period are shown as red squares and black vertical bars with caps that represent minimum peaks and an additional 20% of the minimum. Mean values of paleofloods threshold age data are plotted for simplicity. Perception threshold ranges are shown as orange lines for the paleoflood period, blue lines for the systematic period, and green lines for the discontinued period. The gray shaded areas represents: (1) floods of unknown magnitude less than the perception thresholds for the paleoflood periods Tp,lower ; (2) the discontinued period Td,lower; (3) post-regulation floods after 1961.

Figure 7. Results of flood frequency analysis (FFA) using Expected Moments Algorithm (EMA) with Multiple Grubbs-Beck Test (MGBT) on the Lower Green River in the Stillwater Canyon reach, using (a) both systematic and paleoflood data; (b) systematic peaks only. The solid line is the fitted log-Pearson Type III frequency curve and the dash lines are the 95% confidence limits. Peak discharge estimates from the gage are shown as open circles; vertical bars represent estimated data uncertainty for paleofloods; the solid black circle is the potentially influential low flood (PILF) threshold as identified by the MGBT. Y-axis of the subplot (c), CI/EQ, is the ratio of confidence limits to expected quantiles.

Figure 8. Comparison of different techniques for flood frequency analysis (FFA) on the Lower Green River in the Stillwater Canyon reach, including systematic and paleoflood data. Subplots a-e include nine FFA curves using five techniques and all of them were synthesized in the subplot f. Annual exceedance probability (AEP), return period (T), and discharge (Q) for these curves are summarized in Table 7. The numbers refer to the discussion of each curve in the text and table.

Appendix B – Holocene Paleoflood and their Climatological Context, Upper Colorado River Basin, USA

Progress in
Physical Geography

Holocene Paleofloods and Their Climatological Context, Upper Colorado River Basin, USA

Journal:	*Progress in Physical Geography*
Manuscript ID	PPG-19-061.R1
Manuscript Type:	Main Article
Keywords:	Palaeofloods, Meta-analysis, Extreme floods, Climate Change, Holocene, Upper Colorado River Basin

Abstract:	Given its singular importance for water resources in the southwestern U.S., the Upper Colorado River Basin (UCRB) is remarkable for the paucity of its conventional hydrological record of extreme flooding. This study uses paleoflood hydrology to examine a small portion of the underutilized, but the very extensive natural record of Holocene extreme floods in the UCRB. We perform a meta-analysis of 77 extreme paleofloods from seven slackwater deposit sites in the UCRB to show linkages between Holocene climate patterns and extreme floods. The analysis demonstrates several clusters of extreme flood activity: 8040-7790, 3600-3460, 2880-2740, 2330-700, and 620-0 years BP. The extreme paleofloods were found to occur during both dry and wet periods in the paleoclimate record. When compared with independent paleoclimatic records across the Rocky Mountains and the southwestern U.S., the observed temporal clustering pattern of UCRB extreme paleofloods shows associations with periods of abruptly intensified North Pacific-derived storms connected with enhanced El Niño variability.

Holocene Paleofloods and Their Climatological Context, Upper Colorado River Basin, USA

Abstract

Given its singular importance for water resources in the southwestern U.S., the Upper Colorado River Basin (UCRB) is remarkable for the paucity of its conventional hydrological record of extreme flooding. This study uses paleoflood hydrology to examine a small portion the underutilized, but very extensive natural record of Holocene extreme floods in the UCRB. We perform a meta-analysis of 77 extreme paleofloods from seven slackwater deposit sites in the UCRB to show linkages between Holocene climate patterns and extreme floods. The analysis demonstrates several clusters of extreme flood activity: 8040-7790, 3600-3460, 2880-2740, 2330-700, and 620-0 years BP. The extreme paleofloods were found to occur during both dry and wet periods in the paleoclimate record. When compared with independent paleoclimatic records across the Rocky Mountains and the southwestern U.S., the observed temporal clustering pattern of UCRB extreme paleofloods shows associations with periods of abruptly intensified North Pacific-derived storms connected with enhanced El Niño variability.

Key words

Palaeofloods; Meta-analysis; Extreme floods; Climate Change; Holocene; Upper Colorado River Basin

1. Introduction

Floods are among the most destructive natural hazards causing widespread loss of life, serious damage to infrastructure and economic deprivation. Stream gauge and meteorological station networks established in many countries during the past century provide extensive systematic information about floods, as well as their meteorological and climatological contexts. The classical extreme flood estimations made in hydrological engineering (e.g., flood frequency analysis or FFA) commonly utilize several decades of stream gauge observations to estimate flood magnitudes and their associated exceedance probabilities or return periods. However, because of their short record lengths, systematic hydrological records largely consist of frequent, small magnitude flood events. This leads to very great aleatory uncertainties about infrequent, extreme flood events and about their climate-driven causal associations. Moreover, FFA inherits, as a necessary assumption for statistically valid inferences, that they be restricted to stochastic hydrological processes with independent, identically-distributed random variables (Kisiel, 1969). The problem with this assumption is not merely that it is nearly always violated in a FFA; the bigger problem is that its imposition actually ensures that, beyond the actual flood events themselves, a FFA can add no new scientific information, as opposed to the abstract expediencies needed to achieve an engineering design decision (Klemeš, 1987, 1989).

Another defect with FFA, from a scientific point of view, is the common tendency of conventional statistical flood estimation to relegate the most extreme flood events to "outlier" status, thereby minimizing their consideration. This produces a lack of knowledge or ignorance of potentially known facts, i.e., an epistemic uncertainty. In extreme cases this epistemic uncertainty will lead to what Taleb (2010) has termed a "black swan" event, which is an extreme deemed to be sufficiently improbable that it tends to be unexpected, with the consequence that it will lead to immense disasters for society. Recent incidents of very high-profile "black swan" event have led Taleb (2010) to a blanket criticism of probabilistic risk assessment as a productive means for decision-making in high-risk situations, i.e. where there are real possibilities for extreme disasters. The irony here is that a methodology, FFA, used for expediency in coming to

design decisions, can, in rare cases, lead to consequences that totally invalidate the utility of those decisions.

Paleoflood hydrology (PFH), by combining stratigraphic geology, geomorphology, geochronology, hydraulic modeling, and flood hydrology, aims to discover and understand the very real extreme floods that have occurred on the planet (Baker, 1982; Kochel and Baker, 1982; Baker, 2008). PFH employs an investigative methodology to discover extreme flood events that occurred in the past, thereby demonstrating what flooding is possible for the future. This can provide a kind of epistemic certainty: that what has happened can indeed happen in the future.

Natural PFH evidence of past extreme hydrological events can also be linked to Earth's climate variability over long timescales (Baker, 1987; Ely, 1997; Wohl et al., 1994; Knox, 2000; Harden et al., 2010; Benito et al., 2015). The extensive global application of PFH is now making regional and global palaeohydrological reconstructions and syntheses available for many rivers worldwide (Baker, 2006, 2013). A major recent advance for relating these data to climate is the meta-analysis developed by Macklin and Lewin (2003). This involves systematic, probability-based analysis of geochronologically dated fluvial units (Jones et al., 2015), and it provides for a synthesis of the growing spatial coverage and increasing chronological precision of fluvial archives for reconstructing past river responses to environmental changes (Macklin et al., 2006; Benito et al., 2015). Meta-analysis has now been employed in regional analyses of extreme flood events for many different parts of the world including Northern Europe (Macklin and Lewin, 2003; Willem et al., 2017), the Mediterranean region (Macklin et al., 2006; Benito et al., 2015; Rossato et al., 2015), North Africa (Macklin et al., 2015), the southwestern and central U.S. (Harden et al., 2010; Harden et, al., 2015), and the north-eastern Tibet Plateau (Stauch G., 2016).

In this study we apply the meta-analysis method to retrieve the extreme flood history of the Upper Colorado River Basin (UCRB). We then compare the retrieved flood history with long-term climate variable proxies during the Holocene. The results advance the scientific understanding of extreme flood events and their linkages with climatic changes in the UCRB.

2. Study area

The Colorado River lies within the intermontane plateaus of the western U.S. and is the most important water resources of the seven states (parts of Colorado, New Mexico, Wyoming, Utah, Nevada, and California, and nearly all of Arizona) in southwestern U.S. (U.S. Bureau of Reclamation 2012). The upper Colorado River basin (UCRB), the portion of the Colorado River basin (CRB) upstream of the Lees Ferry USGS stream gauge, encompasses 289,600 km^2, accounting for 45% of the total CRB drainage area, while providing up to about 90% of the streamflow of the entire basin (USGS Fact Sheet 2004-3062). This is mainly due to about 70% of Colorado River streamflow coming from snowmelt in the highest 14% of the UCRB (Christensen and Lettenmaier, 2007; National Research Council. 2007).

Regional to local-scale hydroclimatic variability in the UCRB is controlled at multiple scales by physiographic, oceanic, and atmospheric factors, each operating at different spatial and temporal scales (Mock, 1996; Hirschboeck, et al., 2000). Large-scale atmospheric circulation governs the precipitation pattern of the UCRB. Concretely, cool-season Pacific airstream originated precipitation dominates in the northern portions of the basin and the warm-season monsoon derived rainfall in the southern portions (McCabe, 1996; McGinnis, 2000). North Pacific air masses bring most of the winter precipitation in the UCRB, entering as mid latitude cyclones or extratropical storms, and these account for the majority of precipitation in the region. Summer convective storms draw their moisture from the North American Monsoon (Adams and Comrie, 1997; Seastrand et al., 2015), but these storms tend to only produce floods in the smaller tributaries. A more recently recognized mechanism for generating anomalously high precipitation in the Western U.S. is the “atmospheric river.” During winter months this phenomenon can move streams of highly concentrated water vapor from North Pacific into the western U.S. through a variety of pathways (e.g., Ralph et al., 2006; Dettinger et al., 2011). Two main trajectories have been identified for the large precipitation event incursions into the UCRB: one involves flow from the southwest, drawing the Pacific moisture into the southern portion of the UCRB; the

other follows flow from the west, advecting Pacific moisture into the northern portion of the UCRB (Kirk and Schmidlin, 2018; Alexander et al., 2015).

Given its singular importance of the Upper Colorado River Basin (UCRB) as a critical water resource in the southwestern U.S. it is surprising to find that the conventionally characterized flood history of the UCRB is remarkably poor and short. Interestingly, the poor conventional record of flooding poses a particular problem because of the basin's complex hydroclimatology (Hirschboeck, 1987; Mock, 1996; Cline, 2010). Prevailing conditions of severe draught, alarmingly intense flood events, and rapidly growing water demand with climatic warming have been posing immense challenges for both water resource and flood risk management in the southwestern U.S. (National Research Council. 2007; IPCC, 2012).

Given the considerable climatic uncertainty for UCRB water resources, much attention is being focused on supply-side options to increase water availability, robustness, and resilience; however, the demand side has received considerably less attention. Increasing water storage in reservoirs is being considered a feasible strategy for practical dam operations (Eugene et al., 2016). However, this strategy, involving the filling of reservoirs during wet periods, will necessarily reduce the flood control function of those reservoirs and thereby increase flood risks for downstream areas. This problem will be especially acute for the most extreme floods, which pose risks to the safety of the dams themselves. Based on natural evidence extreme flood records, long-term flood frequency has been linked to climate variability, which can provide new insights into a comprehensive understanding of extreme hydrological events (Wilhelm, et al., 2018).

The USGS gauging station (No. 09380000) at Lees Ferry, Arizona, serves as the dividing point between the Upper and Lower basins of the Colorado River (Fig. 1). Established in 1921, this gage has accumulated one of the most extensive streamflow records in the U.S. The average annual discharges at the gage were 470.4 $m^3 s^{-1}$ during period 1922-1962 and 374.4 $m^3 s^{-1}$ after the 1963 closure of Glen Canyon Dam created Lake Powell. The annual maximum flood series ranges from a low peak of 716.4 $m^3 s^{-1}$

in 1934, to a high of 6230 $m^3 s^{-1}$ in 1921 with, an average annual maximum of 2342.6 $m^3 s^{-1}$ before 1962 (Fig. 2). The maximum pre-gage historical flood at Lees Ferry occurred on July 7, 1884, with an estimated peak discharge of 8500 $m^3 s^{-1}$. This number was estimated by extrapolating the Lees Ferry rating curve from its highest stage/discharge measurement of 3400 $m^3 s^{-1}$ to the presumed stage reached by the 1884 flood. That stage height was inferred 4 decades after the flood event, and it relied solely on the memory of a local resident, who recalled rescuing his cat from the branch of an apple tree at which level the cat had escaped the peak flow of the 1884 flood (LaRue, 1925). This 1884 "cat-in-the-tree" estimate is exemplary of the state of scientific understanding for the most extreme Colorado River flooding prior to the advent of PFH estimates that began in the 1990s (O'Connor et al, 1994).

3. Paleoflood chronology and meta-analysis

The importance of PFH investigations for understanding extreme floods in the UCRB is exemplified by a recent study conducted on the Upper Colorado River near Moab, UT (Greenbaum et al., 2014). In that study, paleoflood stratigraphy revealed 44 extreme floods that occurred during the last 2000 years, several of which lie near the maximum flood envelope curve for the Southwestern U.S. (Enzel et al., 1993), and two of which exceeded the probable maximum flood (PMF) for that portion of the river. The study revealed the natural occurrence of extreme floods that are significantly larger than those of the recent historical record, such that they posed a substantial risk to major infrastructure.

This study moves beyond the use of paleofloods in FFA in order to explore possible linkages between climate patterns and rare, extreme floods in the UCRB. This study relies on the currently available paleoflood data for the UCRB in a meta-analysis to be described below. Because there is an immense untapped wealth of potential paleoflood sites in the UCRB, the current study should be viewed as preliminary, limited to the current state of hydrologically analyzed paleoflood sites, but aimed more at

demonstrating the potential for this kind of analysis than providing a definitive, data-rich compendium.

A total of 77 geochronological ages (39 radiocarbon (^{14}C) and 38 optically stimulated luminescence (OSL) ages) provide quantitative age estimates of paleoflood SWD deposits (Table 1). These data come from three main-stem Colorado River reaches (near Moab and in Cataract Canyon, Utah, and near Lees Ferry, Arizona) and from two reaches in downstream portions of major upper Colorado River tributaries: the Green and Delores rivers (Fig. 1). The Green River is the primary tributary of the upper Colorado River. It is 1,170 km long with a drainage area of 124,600 km^2 and it contributes nearly half of the total annual flow to the Colorado River. The Delores River is 388 km long with a drainage area of 11, 860 km^2. This relatively small tributary empties nearly 10% of the Colorado's annul flow upstream of Moab, UT.

A previous fluvial paleohydrological dataset study for the entire southwestern U.S., (Harden et al., 2010) included only a small portion of the UCRB data from the present study and considered data from a broad range fluvial unit types from basins of various scales in the states of Arizona, Utah, New Mexico, Nevada and Texas. The paleoflood dataset presented here is an initial collection of extreme flood evidence for the last 10,000 years in the UCRB.

For the meta-analysis the dataset is inferred to consist of flood deposit ages (Macklin et al., 2010), in which each data point represents an individual extreme flood interpreted from sedimentological evidence and hydraulic analysis (O'Connor et al., 1994; Cline, 2010; Greenbaum et al., 2014). An age calibration was first performed on the dataset using the program OxCal (version 4.3, Bronk Ramsey, 2009). The individual probability distribution of each calibrated radiocarbon age was then summed, producing a cumulative probability distribution function (CPDF) plot. Next, this CPDF curve was normalized by dividing each date by the highest value in the curve. Finally, various flooding episodes were identified in the CPDF curve by noting intervals where the relative probability exceeds the mean probability (Macklin et al., 2010; Harden et al., 2010).

The resulting CPDF curve (Figure 3a) suggests the extreme floods cluster on certain

decades and centuries during the past 10,000 years. Five flood episodes are identified at 8040-7790, 3600-3460, 2880-2740, 2330-700, and 620-0 a BP. Several peaks occur around 7970, 3580, 2780, 1420, 1280, and 200 a BP. Below-average probabilities are evident in the early to middle Holocene except for a few short and weak flood episodes at around 9000, 8000, 4500, 3500 and 2800 a BP. Most flood units clustered in the late Holocene (after ~2300 a BP) indicating that it was a period of more frequent, extreme flooding.

4. Paleoflood episodes and their implications for extreme flood-climate links

Unlike the Lower Colorado River Basin, where the compilation of extreme paleofloods is well developed (Ely et al., 1993; Ely, 1997) and updated (Harden et al., 2010), and despite an abundance of sites containing detailed paleoflood evidence, very few paleoflood hydrological analysis has been done for vast portions of the UCRB—a critical water resource region because of its extensive winter snowpack. This study is an early step in developing the UCRB chronology and probability record of extreme paleoflood incidences. Nevertheless, the existing record draws needed attention to evidence of naturally occurring floods that are much larger than those previously measured and documented for the basin. The result is a truer understanding of the naturally occurring range of possibilities for flood magnitudes. The result is an expansion of understanding the actual flood hazard in terms of what can be expected in the current period of rapidly changing climate, i.e., that what has happened can happen.

By combining the paleoflood data with independent paleoclimatic records of mean precipitation and temperature conditions over the same time periods as the flooding, it is possible to examine the relationship between floods and climate change on long timescales (Baker, 1987; Ely, 1997; Knox, 1993, 2000; Macklin et al., 2010; Benito et al., 2015; Wilhelm, et al., 2018). Climatic variations over the past 10,000 years have played a significant role in generating temporal and spatial patterns of flooding episodes, and the growing paleoflood datasets from diverse hydrologic and climatic systems around the world indicate that region-wide flooding episodes exist on centennial to millennial timescales (Knox, 1993; Ely, et al., 1993 and 1997; Huang, et al.,

2013; Liu, et al., 2014; Benito, et al., 2015; Harden, et al., 2015; Willem, et al., 2017). The clustering of extreme floods in the UCRB also suggests a major influence by climate dynamics on the temporal distribution of flood episodes. Large flood-generating storms in the UCRB are mainly controlled by southward displacement of the Pacific airstream, including North Pacific frontal storms, Pacific tropical cyclones, warm winter storms, and the North American Monsoon (NAM) (Webb and Betancourt, 1992; Mock, 1996; McCabe, 1996; McGinnis, 2000; Hirschboeck, et al., 2000).

A number of climate proxy records from southwestern U.S. document paleoclimate conditions over the past 10,000 years (Kennett and Ingram, 1995; Thompson and Anderson, 2000; Betancourt et al., 2001; Polyak and Asmerom, 2005, Asmerom et al., 2007 and 2010; Wagner et al., 2010; Metcalfe et al., 2015 and its references). $\delta^{18}O$ records from three lakes at high elevations in the northwestern and southern Colorado Rocky Mountains (Yellow, Bison and San Luis Lakes) provide short and long-term precipitation variations (Anderson, 2011 and 2012; Yuan, et al., 2013). Long-term (since 12.3 ka BP) total precipitation variations are provided by a complete high-resolution $\delta^{18}O$ series from analysis of a speleothem in Pink Panther Cave of the Guadalupe Mountains, New Mexico (Asmerom et al., 2007). In addition, the El Niño frequency from Ecuador and the Galapagos Islands in the eastern equatorial offers important references of Holocene ENSO variability (Moy et al., 2002; Conroy et al., 2008).

Figure 3 shows the CPDF flood curves for both the UCRB (a) and for bedrock reaches of rivers and streams from throughout the lower Colorado River Basin (LCRB) and its vicinity (b). These are compared to the $\delta^{18}O$ records (c, d, e, and f) mentioned above, and to the ENSO variability index (g). All studies exhibit high $\delta^{18}O$ indicating the arid conditions with a rainfall-dominated precipitation during the early to mid-Holocene (10500-6700 a BP) (Fig. 3, light pink shading; Asmerom et al., 2007; Anderson, 2012; Yuan et al., 2013). The long-term decreasing trend of $\delta^{18}O$ values indicates a gradual decrease in the monsoon-dominated precipitation regime (Friedman et al., 1988; Yuan et al., 2013). However, the great negative excursion in a $\delta^{18}O$ stalagmite record around 8000 yrs BP indicates a winter Pacific-derived precipitation increase (Fig. 3f), which

indicates a relatively brief wet interval during prevailing dry conditions (Asmerom et al., 2007). This corresponds to the flood clustering around 8000 yrs BP observed in both the UCRB (Figure 3a) and the southwestern U.S. bedrock reaches (Figure 3b) (Harden et al., 2010). This suggests the extreme flood clustering was likely induced by abnormally increased frequent Pacific-derived storms. These storms can include winter North Pacific frontal storms, or late summer and fall storms associated with Pacific tropical cyclones over the Four Corners area in conjunction with a mid-latitude low-pressure trough.

The relatively low and decreasing trends of $\delta^{18}O$ from the three lakes records (Figures 3c, d, and e) between 6700 and ~2800 yrs BP suggest stable wet condition with a corresponding winter-dominant precipitation regime (Fig. 3 light green shadings; Anderson, 2011 and 2012; Yuan et al., 2013). This climate pattern is interpreted as a southward shift in the strengthening Pacific airstreams (e.g., the Polar Jet Stream, or PJS) (Metcalfe et al., 2015 and its references). A low-to-zero probability of extreme floods characterizes this overall wet climate period for the UCRB with the exception of relatively weak flood probability episodes at approximately 4400, 3500 and 2800 yrs BP. In contrast, this wet period coincided with two relatively long-duration flood probability episodes for the bedrock systems in the LCRB and its vicinity (Ely, et al., 1993; Ely, 1997; Harden et al., 2010). This contrast pattern in flood episodes suggests that the PJS-originated precipitation fell and was stored in the colder UCRB and was less likely to experience rapid melting to generate high-magnitude flood peaks. In contrast the overall wet climate for the entire southwestern U.S. region led to a flood prone context for its warmer southern portions.

The three weak flood episodes around 4400, 3500 and 2800 yrs BP in the UCRB and a short flood episode between 4500-3300 yrs BP in the bedrock systems of the southwest U,S. generally correspond to three pronounced negative excursions of $\delta^{18}O$ in the San Luis Lake (Figure 3c) and two in the Pink Panther Cave (Figure 3f). The period of 4000-3000 a BP, saw widespread pluvial events (a “Neopluvial”) in the greater southwest, which corresponds well with a cooling of the North Pacific and an abrupt southward displacement of the PJS (Yuan et al., 2013). This period is also consistent

with the shift in the predominantly Pacific Ocean originated NAM (Jones et al., 2015) and an increase in frequency and strength in ENSO (more frequent El Niño's) beginning around 4000 years ago (Conroy et al., 2008 and Donders et al., 2008).

After ~2800 a BP, a gradual northward shift of the PJS, indicated by the San Luis Lake $\delta^{18}O$ variability (Fig. 3c, d, and e), led to a considerable reduction in winter precipitation in southern Colorado and the Four Corners area, which includes the southern portion of the UCRB (Yuan et al., 2013). This low winter precipitation and dry condition persisted until Medieval Climate Anomaly (MCA, 1150-700 yrs BP). The northern UCRB, by contrast, experienced an increasing snowfall fraction in total precipitation until ~2300 yrs BP (Anderson, 2011 and 2012). Although the ENSO variability increased sharply between 2700-2400 yrs BP (Fig. 3g), a low probability of extreme flood episodes appeared in this period for the entire Colorado River Bains and its vicinity (Ely, et al., 1993; Ely, 1997; Harden et al., 2010). This implies that north Pacific derived precipitation was more likely to be the dominant factor of extreme floods in the southwestern U.S.

After ~2300 a BP, $\delta^{18}O$ variability in San Luis Lake Bison and Yellow lakes (Fig. 3d, e and f) suggests overall dry conditions with comparatively high summer/winter precipitation for the UCRB (Anderson, 2011 and 2012; Yuan et al., 2013). During this period, tree-ring records also provide evidence for decadal-centennial scale megadrought conditions across southwestern U.S. during MCA (Cook et al., 2004; Stahle et al., 2009; Routson et al., 2011). Negative excursions in lower overall $\delta^{18}O$ values represent an abrupt, decade-to-century increase in the fraction of winter precipitation (Anderson, 2011 and 2012). This coincides with increasing ENSO dominance (Conroy et al., 2008; Moy et al., 2002), which seems to have brought a return to slightly wetter conditions in some locations of the northern margin of the NAM region (Barron and Anderson, 2011; Metcalfe et al., 2015). This climate regime could well have triggered more rain-on-snow events during the spring snowmelt season, which would have increased the likelihood of large floods. The timing of this change coincides with the UCRB's most dominant flood probability episode (2330-700 yrs BP), which is also seen in the flood probability record for bedrock systems of the LCRB and its vicinity (Ely, et

al., 1993; Ely, 1997; Harden et al., 2010).

After 620 yrs BP the $\delta^{18}O$ values in the three lake records (Figures 3c, d, and e) indicate the prevalence of more arid conditions with slightly more winter precipitation during the Little Ice Age (LIA, ~350-200 yrs BP) in the Rocky Mountains (Anderson, 2011 and 2012; Yuan et al., 2013). This is consistent with the extreme flood episode in the bedrock systems in the LCRB and its vicinity (Harden et al., 2010) and with the prominent peaks of high-magnitude floods for river and streams in Arizona and southern Utah over the last 500-years (Ely, et al., 1993; Ely, 1997). This is also the period during which flood deposits are more likely to have been preserved given that their analyses contribute nearly a quarter of total geochronology used to construct the CPDF curve.

The UCRB flood episodes at around 8000, 3500, 2800, 2300-700, and after 600 yrs BP are consistent with flood probability records in the LCRB and its vicinity, and all of these correspond to punctuated north Pacific-derived winter precipitation during both overall wet and dry climate period. In contrast, the timing of stable dry periods (10,500-6700 yrs BP) and persistent wet periods (6700-2700 yrs BP) correspond to relatively few extreme flooding for the UCRB. Increased frequency of El Niño events seems to have played a minor role in regard to large UCRB floods, though some concurrence is seen after about 2300 yrs BP. Of course, this relation is based on the relatively small number of currently identified SWD units, indicating the need for much additional paleoflood hydrological research in the UCRB. The evidence suggests that the temporal clustering pattern of extreme paleofloods in the UCRB is a consequence of abrupt intensified North Pacific-derived storms associated with enhanced ENSO variability.

5. Discussion

We have identified extreme flood temporal patterns and their likely climatic controls for the UCRB by retrieving the Holocene extreme flood events history and comparing this with records of long-term climatic change. Although our meta-analysis is based on a relatively small dataset of extreme paleofloods, the results reflect the realities of the naturally occurring range of possibilities for flood magnitudes in the

UCRB, rather than the conventional approach of extrapolating by FFA to projected large magnitudes from samples of small-scale flood events. As a result, the natural extreme flood history and its temporal clustering pattern advances scientific understanding of extreme floods and their climatological context for the UCRB.

Our results should also be viewed as preliminary and limited to the current state of hydrologically analyzed paleoflood data. Nevertheless, the results indicate both the great potential for meta-analysis of the real extreme floods and the potential for using the immense untapped wealth of the many paleoflood sites that occur in the UCRB and in other places around the world.

Naturally well-preserved paleoflood records, historical-archival flood information, and instrumentally measured datasets all supply essential information that can be relied upon for statistical analysis and for deepening understanding of extreme floods behaviors. A periodically updated compilation of historical and paleoflood records collected by the PAGES Floods Working Group embraces the published past flood records in Europe, North America, and Asia, other places in the southern hemisphere (Wilhelm, et al., 2018).

Except for Spain, the United Kingdom (Kjeldsen et al., 2014), and China (Luo, 2006; SL44-2006), where a review of natural and historical sources is legally required, few countries legally require paleoflood and/or historical flood investigation to be undertaken prior to implementation of infrastructural measures for flood control and other water-resource projects. Hopefully the recent advances in the science of paleoflood hydrology will encourage more nations to follow these leads.

6. Conclusions

Based on extensive paleoflood investigations and geochronological analyses, we used meta-analysis to derive the history of the Holocene extreme floods in the UCRB. The flood clusters for the UCRB indicate that periods of frequent extreme flooding occurred during the age ranges of 8040-7790, 3600-3460, 2880-2740, 2330-700, and 620-0 a BP. The temporal clustering pattern of extreme paleofloods in the UCRB likely results from abrupt strengthened North Pacific-derived storms associated with enhanced El Niño variability, and this occurs regardless of the prevailing climate period

being dry or wet.

This first meta-analysis of Holocene 14C and OSL dated SWD units from across the entire UCRB demonstrates that CPDFs enable both an objective definition of flood activity periods and the identification of likely hydro-climatic controls on those flood activity periods. This approach also demonstrates the value of creating palaeohydrological databases and comparing them to hydro-climatic proxies in order to identify natural patterns and to discover possible linkages to fundamental processes such as changes in climate. Further site-based studies of the paleoflood history throughout the UCRB and other drainage basins should be encouraged so that additional data can be applied to improve our understanding of the regional response of floods to climate variability.

References:

Adams, D.K. and Comrie, A.C., 1997. The North American monsoon. Bulletin of the American Meteorological Society, 78(10): 2197-2213.

Alexander, M.A., Scott, J.D., Swales, D., Hughes, M., Mahoney, K. and Smith, C.A. (2015) Moisture pathways into the U.S. intermountain west associated with heavy winter precipitation events. Journal of Hydrometeorology, 16, 1184–1206. https://doi.org/10.1175/JHM-D-14-0139.1.

Anderson, L., 2011. Holocene record of precipitation seasonality from lake calcite delta O-18 in the central Rocky Mountains, United States. Geology 39, 211–214.

Anderson, L., 2012. Rocky Mountain hydroclimate: Holocene variability and the role of insolation, ENSO, and the North American Monsoon. Glob. Planet. Chang. 92–93, 198–208.

Asmerom, Y., Polyak, V., Burns, S., Rassmussen, J., 2007. Solar forcing of Holocene climate: newinsights froma speleothem record, southwestern United States. Geology 35, 1–4.

Asmerom, Y., Polyak, V.J., Burns, S.J., 2010. Variable winter moisture in the southwestern United States linked to rapid glacial climate shifts. Nat. Geosci. 3, 114–117.

Baker, V.R., 1982, Geology, determinism, and risk assessment, *in* Scientific basis of

water-resource management: National Academy Press, Washington, D.C., p.109-117.

Baker, V. R., 1987, Paleoflood hydrology and hydroclimatic change, The influence of the climate change and climatic variability on the hydrologic regime and water resources, IAHS Publ., 168, 123–131.

Baker, V.R., 2006. Palaeoflood hydrology in a global context. Catena 66: 141-145.

Baker V.R., 2008. Paleoflood hydrology: origin, progress, prospects. Geomorphology 101: 1–13.

Baker, V.R., 2013. Global late Quaternary fluvial paleohydrology: with special emphasis on paleofloods and megafloods. In: Shroder, J. (Editor in Chief), Wohl, E. (Ed.), Treatise on Geomorphology. Academic Press, San Diego, CA, vol. 9, Fluvial Geomorphology, pp. 511–527.

Baker, V.R., 2017. Debates—Hypothesis testing in hydrology: pursuing certainty versus pursuing uberty: Water Resources Research, DOI: 10.1002/2016WR020078.

Barron, J.A., Anderson, L., 2011. Enhanced Late Holocene ENSO/PDO expression along the margins of the eastern North Pacific. Quat. Int. 235, 3-12. http://dx.doi.org/10.1016/j.quaint.2010.02.026.

Benito, G., Macklin, M.G., Panin, A., Rossato, S., Fontana, A., Jones, A.F., Machado, M.J., Matlakhova, E., Mozzi, P., and Zielhofer, C., 2015, Recurring flood distribution patterns related to short-term Holocene climatic variability: Nature Scientific Reports, v. 5, 16398, doi: 10 .1038 /srep16398.

Betancourt, J.L., Rylander, K.A., Penalba, C., McVickar, J.L., 2001. Late Quaternary vegetation history of Rough Canyon, south-central NewMexico, USA. Palaeogeogr. Palaeoclimatol. Palaeoecol. 165, 71–95.

Bronk Ramsey, C. 2009. Bayesian analysis of radiocarbon dates. Radiocarbon, 51(1), 337-360.

Bryson, R.A. and Hare, F.K., 1974. The climates of North America. Climates of North America, World Survey of Climatology II. Elsevier, New York.

Cline, M.L. 2010. Extreme flooding in the Dolores River Basin, Colorado and Utah: Insights from paleofloods, geochronology and hydroclimatic analysis. Ph.D. Dissertation, University of Arizona, Tucson, Arizona, 221 p.

Conroy, J.L., Overpeck, J.T., Cole, J.E., Shanahan, T.M., Steinitz-Kannan, M., 2008. Holocene changes in eastern tropical Pacific climate inferred from a Galapagos lake sediment record. Quat. Sci. Rev. 27, 1166–1180.

Cook, E.R., Woodhouse, C.A., Eakin, C.M., Meko, D.M., Stahle, D.W., 2004. Long-term aridity changes in the western United States. Science 306, 1015-1018.

Dettinger, M.D., Ralph, F.M., Das, T., Neiman, P.J. and Cayan, D.R. (2011) Atmospheric rivers, floods, and the water resources of California. Water, 3, 445–478. https://doi.org/10.3390/w3020445.

Donders, T.H., Wagner-Cremer, F., Visscher, H., 2008. Integration of proxy data and model scenarios for the mid-Holocene onset of modern ENSO variability. Quat. Sci. Rev. 27, 571-579.

Dunne, T. and Leopold, L. B. 1978: Calculation of flood hazard. In Dunne, T. and Leopold, L.B., Water in environmental planning, San Francisco, WH Freeman and Co, CA: 279-391.

Ely, L.L., Enzel, Y., Baker, V.R. and Cayan, D.R., 1993. A 5000-year record of extreme floods and climate change in the southwestern United-States. Science, 262(5132): 410-412.

Ely, L. L. 1997: Response of extreme floods in the southwestern United States to climatic variations in the late Holocene. Geomorphology 19, 175-201.

Enzel, Y., Ely, L.L., House, P.K., Baker, V.R. and Webb, R.H., 1993. Paleoflood evidence for a natural upper bound to flood magnitudes in the Colorado River Basin. Water Resources Research, 29(7): 2287-2297.

Eugene Z. Stakhiv, William Werick, Robert W. Brumbaugh, 2016, Evolution of drought management policies and practices in the United States. Water Policy, 18 (S2): 122–152. doi: https://doi.org/10.2166/wp.2016.017

Friedman, I., Carrara, P., Gleason, J., 1988. Isotopic evidence of Holocene climatic change in the San Juan Mountains, Colorado. Quat. Res. 30, 350–353.

Friedman, J.M. et al., 2006. Transverse and longitudinal variation in woody riparian vegetation along a montane river. Western North American Naturalist, 66(1): 78-91.

Galbraith, R. F. 2005: Statistics for Fission Track Analysis. 240 pp. Chapman and Hall, London.

Greenbaum, N., T. M. Harden, V. R. Baker, J. Weisheit, M. L. Cline, N. Porat, R. Halevi, and J.

Dohrenwend. 2014. A 2000 year natural record of magnitudes and frequencies for the largest Upper Colorado River floods near Moab, Utah, Water Resour. Res., 50, 5249–5269, doi:10.1002/2013WR014835.

Harden, T.M., Macklin, M. G. and Baker, V. R., 2010, Holocene flood histories in south western USA: Earth Surface Processes and Landforms, v. 35, p. 707–716.

Harden, T.M., O'Connor, J.E., Driscoll, D.G., 2015. Late Holocene flood probabilities in the Black Hills, South Dakota with emphasis on the Medieval Climate Anomaly. Catena 130: 62–68.

Hirschboeck, K.K., 1987. Catastrophic flooding and atmospheric circulation anomalies, in Mayer, L. and Nash, D.B., eds., Catastrophic Flooding, Allen & Unwin, 23-56.

Hirschboeck, K.K., Ely, L.a.M. and R.A. (Editors), 2000. Hydroclimatology of meteorologic floods Inland Flood Hazards: Human, Riparian and Aquatic Communities. Cambridge University Press, p. 39-72 pp.

Huang, C.C., Pang,. J.L., Zha, X.C., et al. 2013. Extraordinary hydro-climatic events during the period AD 200–300 recorded by slackwater deposits in the upper Hanjiang River valley, China. Palaeogeogr., Palaeoclimatol., Palaeoecol., 374: 274–283.

IPCC, 2012: Managing the Risks of Extreme Events and Disasters to Advance Climate Change Adaptation. A Special Report of Working Groups I and II of the Intergovernmental Panel on Climate Change (IPCC). [Field, C.B., V. Barros, T.F. Stocker, D. Qin, D.J. Dokken, K.L. Ebi, M.D. Mastrandrea, K.J. Mach, G.K. Plattner, S.K. Allen, M. Tignor, and P.M. Midgley (eds.)]. Cambridge University Press, Cambridge, United Kingdom and New York, NY, USA, 582 pp.

Jones, A.F., Macklin, M.G., Benito, G., 2015. Meta-analysis of Holocene fluvial sedimentary archives: A methodological primer. Catena 130, 3–12.

Jones, M.D., Metcalf, S.E., Davies, S.J., Noren, A., 2015. Late Holocene reorganization and the North American Monsoon. Quat. Sci. Rev. 124, 290–295.

Keen, Richard A. "WEATHER AND CLIMATE." The Western San Juan Mountains: Their Geology, Ecology, and Human History, edited by Rob Blair et al., University Press of Colorado, 1996, pp. 113–126.

Kennett, J.P., Ingram, B.L., 1995. A 20,000-year record of ocean circulation and climate

change from the Santa Barbara Basin. Nature, 377: 510–514.

Kirk JP, Schmidlin TW. Moisture transport associated with large precipitation events in the Upper Colorado River Basin. Int J Climatol. 2018;1–16. https://doi.org/10.1002/joc.5734

Kiseiel, C.C. 1969. Time series analysis of hydrologic data. Adv. Hydrosci. 5, 1-119.

Kjeldsen, T. R., Macdonald, N., Lang, M., Mediero, L., Albuquerque, T., Bogdanowicz, E., et al. 2014. Documentary evidence of past floods in Europe and their utility in flood frequency estimation. Journal of Hydrology, 517, 963–973.

Klemeš V., 1987, Hydrological and engineering relevance of flood frequency analysis. In Singh, V. P., editor, Hydrologic Frequency Modeling: D. Reidel Publishing Company, p. 1-18.

Klemeš, V., 1989, The improbable probabilities of extreme floods and droughts, In Starosolszky, O., and O.M. Melder O.M., editors, Hydrology of Disasters: James & James, London, p. 43–51

Knox, J.C., 1993. Large increases in flood magnitude in response to modest changes in climate. Nature, 361(6411): 430-432.

Knox J C. 2000, Sensitivity of modern and Holocene floods to climate change[J]. Quaternary Science Reviews, 19(1): 439-457.

LaRue, E.C., 1925, Water power and flood control of Colorado River below Green River, Utah: U.S. Geol. Survey Water Supply Paper 556, 176 p.

Liu, T., Huang, C.C., Pang, J.L., et al., 2014. Extraordinary hydro-climatic events during 1800–1600 yr BP in the Jin–Shaan Gorges along the middle Yellow River, China. Palaeogeogr., Palaeoclimatol., Palaeoecol., 410: 143–152.

Kochel, R.C., Baker, V.R., 1982. Paleoflood hydrology. Science 215, 353–361.

Macklin, M.G., Lewin, J., 2003. River sediments, great floods and centennial-scale Holocene climate change. J. Quat. Sci., 18: 101–105.

Macklin, M.G., Benito, G., Gregory, K.J., Johnstone E., Lewin, J., Starkel, R. Soja, L., Thorndycraft, V.R.. 2006. Past hydrological events reflected in the Holocene fluvial history of Europe. Catena, 66: 145–154.

Macklin, M.G., Jones, A.F., Lewin, J., 2010. River response to rapid Holocene environmental change: evidence and explanation in British catchments. Quat. Sci. Rev. 29, 1555–1576.

Macklin M G, Toonen W H J, Woodward J C et al. 2015, A new model of river dynamics, hydroclimatic change and human settlement in the Nile Valley derived from meta-analysis of the Holocene fluvial archive. Quaternary Science Reviews, 130: 109-123.

McCabe, G.J. (1996) Effects of winter atmospheric circulation on temporal and spatial variability in annual streamflow in the western United States. Hydrology and Earth System Sciences, 41, 873–887. https://doi.org/10.1080/02626669609491556.

Metcalfe, S.E., Barron, J.A. and Davies, S.J., 2015. The Holocene history of the North American Monsoon:'known knowns' and'known unknowns' in understanding its spatial and temporal complexity. Quaternary Science Reviews, 120, pp.1-27.

Mock, C.J., 1996. Climate controls and spatial variations of precipitation in the western United States. Journal of Climate 9, 1111–1125.

Moy, C.M., Seltzer, G.O., Rodbell, D.T., Anderson, D.M., 2002. Variability of El Niño/ Southern Oscillation activity at millennial timescales during the Holocene epoch. Nature 420, 162–165.

National Research Council. 2007. Colorado River Basin Water Management: Evaluating and Adjusting to Hydroclimatic Variability. Washington, DC: The National Academies Press. doi: 10.17226/11857.

O'Connor, J. E., L. L. Ely, E. Wohl, L. E. Stevens, T. S. Melis, V. S. Kale, and V. R. Baker (1994), A 4500-year record of large floods on the Colorado River in the Grand Canyon, Arizona. J. Geol., 102, 1–9.

Polyak, V.J., Asmerom, Y., 2005. Orbital control of long-termmoisture in the southwestern USA. Geophys. Res. Lett. 32.

Ralph, F.M., Neiman, P.J., Wick, G.A., Gutman, S.I., Dettinger, M.D., Cayan, D.R. and White, A.B. (2006) Flooding on California's Russian River: role of atmospheric rivers. Geophysical Research Letters, 33, L13801. https://doi.org/10.1029/2006GL026689.

Rittenour, T. M., Goble, R. J. & Blum, M. D. 2005: Development of an OSL chronology for late Pleistocene channel belts in the lower Mississippi valley. Quaternary Science Reviews 24, 2539–2554.

Rodionov, S.N., Bond, N.A. and Overland, J.E., 2007. The Aleutian Low, storm tracks, and

winter climate variability in the Bering Sea. Deep-Sea Research Part II-Topical Studies in Oceanography, 54(23-26): 2560-2577.

Rossato, S., Fontana, A., Mozzi, P., 2015. Meta-analysis of a Holocene 14C database for the detection of paleohydrological crisis in the Venetian–Friulian Plain (NE Italy). Catena 130, 34–45.

Routson, C.C., Woodhouse, C.A., Overpeck, J.T., 2011. Second century megadrought in the Rio Grande headwaters, Colorado: how unusual was medieval drought? Geophysical Research Letters 38, http://dx.doi.org/10.1029/2011GL050015.

Sheppard, P.R., Comrie, A.C., Packin, G.D., Angersbach, K. and Hughes, M.K., 2002. The climate of the US Southwest. Climate Research, 21(3): 219-238.

Stahle, D.W., Burnette, D., Villanueva, J., Cerano, J., Fye, F.K., Griffin, R.D., Cleaveland, M.K., Stahle, D.K., Edmondson, J.R., Wolff, K.P., 2012b. Tree-ring analysis of ancient baldcypress trees and subfossil wood. Quat. Sci. Rev. 34, 1-15.

Stauch G. Multi-decadal periods of enhanced aeolian activity on the north-eastern Tibet Plateau during the last 2ka. Quaternary Science Reviews, 2016, 149: 91-101.

Seastrand, S., Serra, Y., Castro, C. and Ritchie, E., 2015. The dominant synoptic-scale modes of North American monsoon precipitation. Int. J. Climatol, 35: 2019-2032. doi:10.1002/joc.4104

Taleb, N. N., 2007, The Black Swan: The Impact of the Highly Improbable: Penguin, London.

Thompson, R.S., Anderson, K.H., 2000. Biomes of western North America at 18,000, 6000 and 0 C-14 yr BP reconstructed from pollen and packrat midden data. J. Biogeogr. 27, 555–584.

Tooth, S., Rodnight, H., Duller, G. A. T., McCarthy, T. S., Marren, P. M. & Brandt, D. 2007: Chronology and control of avulsion along a mixed bedrock–alluvial river. Geological Society of America Bulletin 119, 452–461.

U.S. Bureau of Reclamation, 2012: Colorado River basin water supply and demand study: Executive summary. U.S. Department of the Interior, Bureau of Reclamation, 28 pp., https://www.usbr.gov/watersmart//bsp/docs/finalreport/ColoradoRiver

USGS Fact Sheet 2004-3062. Climatic Fluctuations, Drought, and Flow in the Colorado River

Basin". August 2004.

Wagner, J.D.M., Cole, J.E., Beck, J.W., Patchett, P.J., Henderson, G.M., Barnett, H.R., 2010. Moisture variability in the southwestern United States linked to abrupt glacial climate change. Nat. Geosci. 3, 110–113.

Webb, RH., Betancourt, J.L., 1992. Climatic variability and flood frequency of the Santa Cruz River, Pima County, Arizona. U.S. Geol. Surv. Water-Supply Paper, 2379.

Willem H.J. Toonen, Simon A. Foulds, Mark G. Macklin, John Lewin, 2017. Events, episodes, and phases: Signal from noise in flood-sediment. Geology, doi:10.1130/G38540.1.

Wilhelm B, Ballesteros Cánovas JA, Macdonald N, et al., 2018. Interpreting historical, botanical, and geological evidence to aid preparations for future floods. WIREs Water. 2018; e1318. https://doi.org/10.1002/wat2.1318

Wohl, E. E., Fuertsch, S. J. and Baker, V. R. 1994: Sedimentary records of late holocene floods along the Fitzroy and Margaret Rivers, western Australia. Australian Journal of Earth Sciences 41, 273-280.

Yuan F, Koran MR, Valdez A. 2013. Late glacial and Holocene record of climatic change in the southern Rocky Mountains from sediments in San Luis Lake, Colorado, USA. Palaeogeogr , Palaeoclimatol , Palaeoecol. 392:146-60.

Table 1. Paleofloods used in calculating cumulative probability distribution function curves for all four reaches in the upper Colorado River Basin (UCRB). Information shown was from O'Connor, et al., (1994), Cline (2010), Greenbaum et al., (2014) and unpublished scientific reports.

River	Reach	Flood deposit #	Lab code	Dating method	Age (a BP)
Colorado Riv.	Moab	1	A13878	^{14}C	135 ± 35
	Moab	2	AA65420	^{14}C	340 ± 34
	Moab	3	A13879	^{14}C	120.5 ± 1.8
	Moab	4	A13877	^{14}C	6275 ± 160
	Moab	5	P2U5	OSL	1410 ± 110
	Moab	6	P4U4	OSL	2140 ± 220
	Moab	7	P5U1	OSL	1300 ± 90
	Moab	8	P5U2	OSL	1460 ± 80
	Moab	9	P9U5	OSL	390 ± 100
	Moab	10	P10U3	OSL	170 ± 40
	Moab	11	P10U7	OSL	410 ± 70
	Moab	12	P11U5	OSL	230 ± 60
	Moab	13	P12U5	OSL	490 ± 150
	Moab	14	P13U6	OSL	220 ± 70
	Moab	15	P14U7	OSL	460 ± 110
	Moab	16	P14U13	OSL	200 ± 60
	Cataract Canyon	17	GRV-13	OSL	370 ± 100
	Cataract Canyon	18	GRV-14	OSL	410 ± 100
	Cataract Canyon	19	USU-2309	OSL	310 ± 90
	Cataract Canyon	20	USU-2308	OSL	1160 ± 210
	Cataract Canyon	21	GRV-1	OSL	1100 ± 600
	Lees Ferry	22	GX-16055	^{14}C	1425 ± 130
	Lees Ferry	23	GX-16052	^{14}C	2150 ± 140
	Lees Ferry	24	GX-16053	^{14}C	2155 ± 75
	Lees Ferry	25	GX-16049	^{14}C	2470 ± 85
	Lees Ferry	26	GX-16050	^{14}C	2930 ± 165
	Lees Ferry	27	GX-16054	^{14}C	3530 ± 80
	Lees Ferry	28	GX-16051	^{14}C	3915 ± 85
	Lees Ferry	29	GX-16012	^{14}C	330 ± 120
	Lees Ferry	30	GX-16024	^{14}C	1470 ± 190
Green Riv.	Dead Horse Canyon	1	GRV-2	OSL	680 ± 250
	Dead Horse Canyon	2	GRV-3	OSL	470 ± 160
	Dead Horse Canyon	3	USU-2310	OSL	200 ± 80
	High Bank	4	GRV-4	OSL	320 ± 70
	High Bank	5	GRV-5	OSL	350 ± 70
	Ledge	6	GRV-6	OSL	220 ± 40
	Powell Canyon	7	GRV-7	OSL	480 ± 170

	Powell Canyon	8	GRV-8	OSL	340 ± 90
	Powell Canyon	9	USU-2306	OSL	200 ± 100
	Rockfall	10	GRV-9	OSL	400 ± 100
	Rockfall	11	GRV-10	OSL	220 ± 110
	Rockfall	12	GRV-11	OSL	550 ± 170
	Rockfall	13	GRV-12	OSL	290 ± 60
	Rockfall	14	USU-2307	OSL	190 ± 80
Dolores Riv.	Big Rock	1	AA82500	^{14}C	991 ± 37
	Big Rock	2	AA82502	^{14}C	1226 ± 38
	Big Rock	3	AA85261	^{14}C	1337 ± 36
	Big Rock	4	AA85262	^{14}C	1359 ± 36
	Big Alcove	5	AA82506	^{14}C	1231 ± 38
	Big Alcove	6	AA86680	^{14}C	1271 ± 34
	Big Alcove	7	AA86681	^{14}C	947 ± 33
	McPhee	8	AA84122	^{14}C	1526 ± 53
	McPhee	9	AA84123	^{14}C	1578 ± 45
	McPhee	10	AA86674	^{14}C	1822 ± 67
	Mucky	11	AA84126	^{14}C	7800 ± 200
	Mucky	12	AA84127	^{14}C	2089 ± 70
	Mucky	13	AA84128	^{14}C	1596 ± 43
	Mucky	14	AA85263	^{14}C	3322 ± 62
	Mucky	15	AA85264	^{14}C	2212 ± 97
	Mucky	16	AA85267	^{14}C	1342 ± 50
	Mucky	17	AA86675	^{14}C	1750 ± 38
	Mucky	18	AA86676	^{14}C	1735 ± 38
	Mucky	19	AA86677	^{14}C	1626 ± 38
	Mucky	20	AA86678	^{14}C	1821 ± 39
	Mucky	21	AA84130	^{14}C	2680 ± 64
	Tafoni	22	AA85258	^{14}C	893 ± 51
	Tafoni	23	AA85259	^{14}C	1995 ± 94
	Juniper	24	AA86019	^{14}C	8033 ± 55
	Juniper	25	AA86021	^{14}C	7153 ± 48
	Tributary	26	AA86024	^{14}C	7060 ± 190
	Tafoni	27	USU-330	OSL	2940 ± 320
	Big Alcove	28	USU-331	OSL	1440 ± 180
	Big Alcove	29	USU-332	OSL	990 ± 80
	Big Rock	30	USU-626	OSL	1100 ± 130
	Tafoni	31	USU-627	OSL	1110 ± 170
	Juniper	32	USU-628	OSL	7840 ± 660
	Tributary	33	USU-630	OSL	8210 ± 790

Figure 1. Map showing the location of sample sites included the 14C and OSL dated paleoflood slack-water deposits (SWDs) dataset in the upper Colorado River basin (UCRB). Locations of $\delta^{18}O$ records of Yellow, Bison and San Luis Lakes are also labeled.

Figure 2. Annual maximum peak discharges in the Colorado River at the USGS gauging station near Lees Ferry, Arizona 1884-2015.

Figure 3. Comparison of the cumulative probability distribution function (CPDF) from (a) the Upper Colorado River Basin (UCRB), (b) the bedrock reaches in the southwest US (Harden et al., 2010), and climate records from (c) $\delta^{18}O$ of San Luis Lake (Yuan et al., 2013); (d and e) $\delta^{18}O$ of Yellow and Bison Lake (Anderson, 2011, 2012); (f) δ18O of a speleothem from Pink Panther Cave (Asmerom et al., 2007) and (g) ENSO frequency reconstructions from El Junco Lake (dashed line, Conroy et al., 2008) and Laguna Palcacocha (black line, Moy et al., 2002). Light pink shadings (10500-6700 a BP and after 2800 a BP) are overall dry periods; green shading (6700-2800 a BP) is relatively stable wet period, and blue shadings (8040-7790, 3600-3460, 2880-2740, 2330-700, and 620-0 a BP) are five flood episodes.

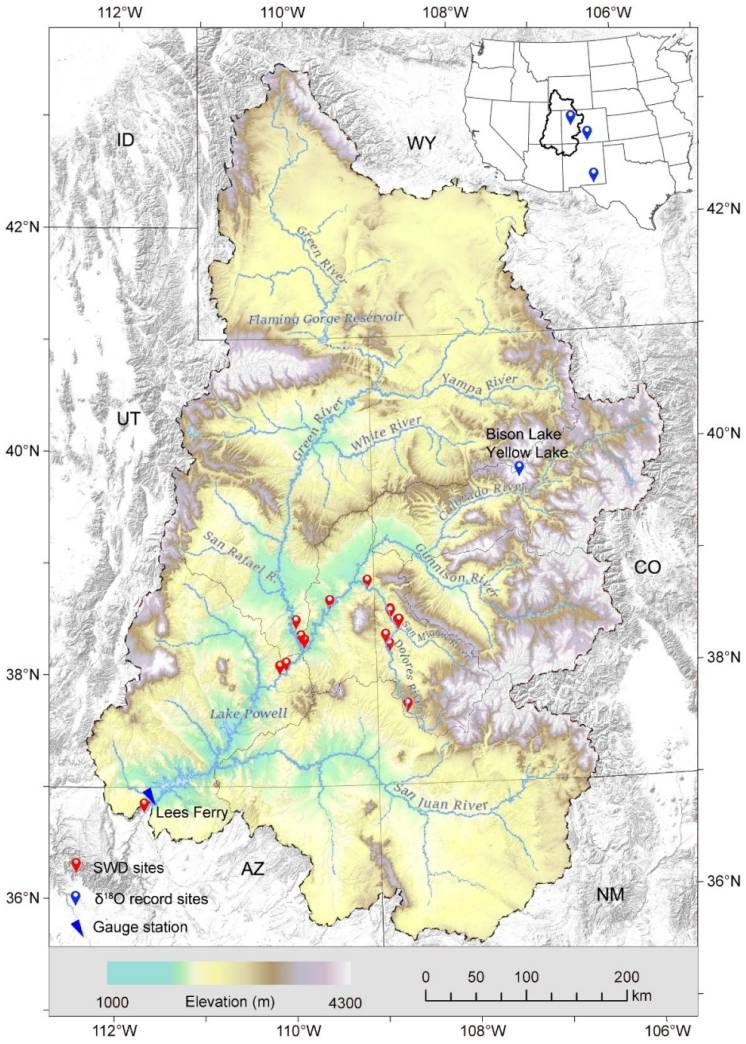

135x189mm (220 x 220 DPI)

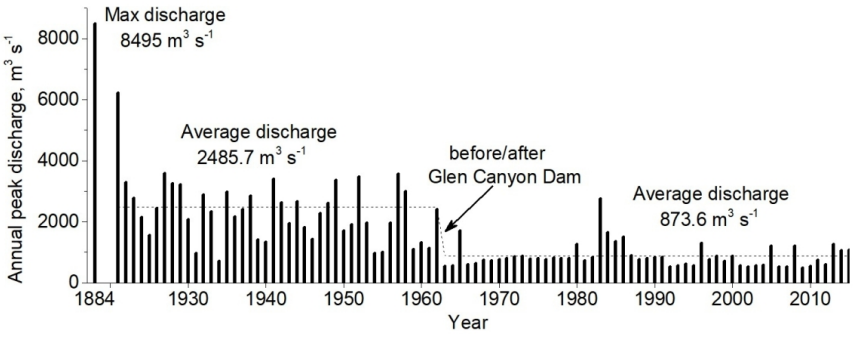

129x50mm (300 x 300 DPI)

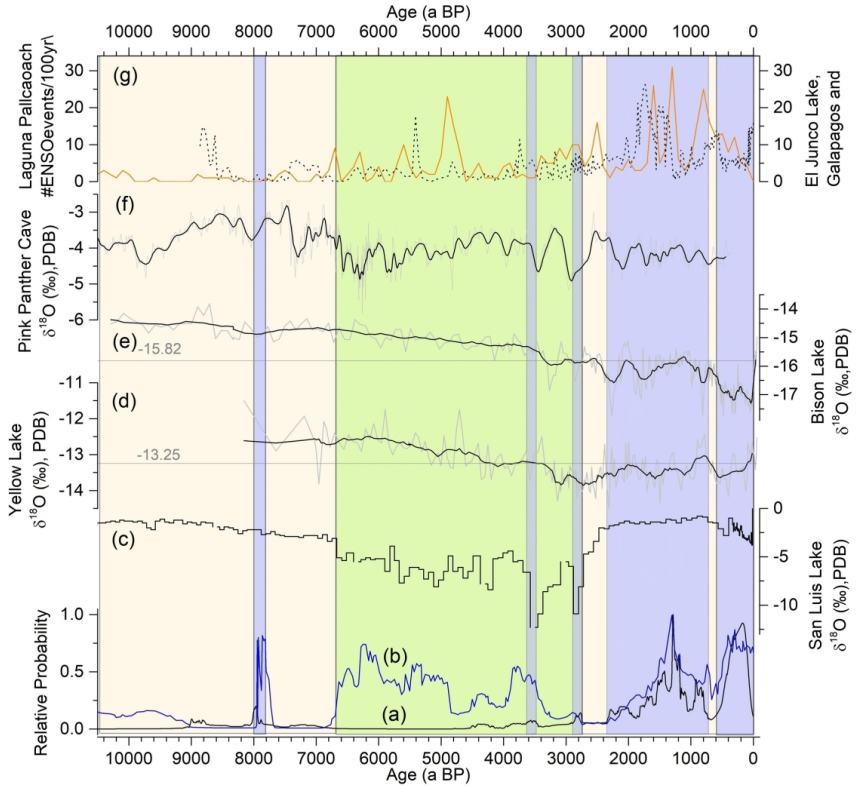

194x176mm (300 x 300 DPI)

Appendix C – Final Program Performance Report: Paleoflood Hydrology of the Colorado River System

FINAL PROGRAM PERFORMANCE REPORT, 12/31/2018

U.S. Bureau of Reclamation Agreement No. **R16AC00021**

Project Title: **Paleoflood Hydrology of the Colorado River System**

Final Period: October 1, 2018 – December 30, 2018

Recipient/Project Manager: Dr. Victor R. Baker, The University of Arizona

This report covers the final 3-month period of the project timeline. The nominal project period officially terminated on December 31, 2018, after a 3-month, no-cost extension. Discussions were on-going at that time about a continuation of the project, but details were not finalized as of this writing, partly related to agency budget considerations related to federal budgetary uncertainties. Though this report is technically the "Final Project Report," in reality our project has been continuing without funding in anticipation of renewal. As a result, this report will include summaries of work that has been accomplished, is ongoing, and is planned for the future.

1. Green River and Cataract Canyon Paleoflood Study

Work on this aspect of the project was completed, and a journal article on the results has been written, as follows:

Liu, T., Greenbaum, N., Baker, V. R., Ji, L., Rittenour, T., Porat, N., Onken, J., and Weisheit, J., in review, Paleoflood hydrology of the lower Green River, upper Colorado River Basin, USA.

Through a comprehensive paleoflood hydrological investigation we documented natural evidence for 70 high-magnitude paleofloods at six sites on the Lower Green River, Utah. Hydraulic analysis, using the Sedimentation and River Hydraulic-2D model (SRH-2D), showed that the responsible peak paleoflood discharges ranged between 500 and 7500 m^3/s. At least 14

of these paleoflood discharge peaks exceed a level twice that of the maximum systematic record of gauged flows: 1929 m^3/s. Geochronological analyses, employing optically stimulated luminescence (OSL) and radiocarbon dating techniques, demonstrated that these 14 largest paleoflood peaks occurred during the past 700 years. Integration of the paleoflood data into flood frequency analyses (FFA) revealed considerably higher values for the upper tails of the flood distribution than did a FFA based solely on the systematic gauged record, indicating that extreme floods are larger and more frequent than implied by the relatively short gauged record. Through examination of three approaches to extreme flood estimation – conventional FFA, probable maximum flood estimation (PMF), and paleoflood hydrology (PFH) – we showed the significance of the natural evidence for advancing scientific understanding of extreme floods that naturally occur in the Colorado River system. We argue that this kind of scientific understanding is absolutely essential for achieving a credible evaluation of extreme flood risk in a watershed of immense importance to economic prosperity of the southwestern U.S.

Data from 2 paleoflood sites in Cataract Canyon of the Colorado Rive are being incorporated into a regional study of Colorado River paleoflood hydrology.

2. Delores/San Miguel Studies

This aspect of the study has been completed, and a journal article on the results has been written, as follows:

Liu, T., Ji, L., Baker, V.R., Harden, T.M., Cline, M.L., in review, Holocene paleoflood events and their climatological and physiographic context, upper Colorado River Basin, USA.

Given its singular importance for water resources in the southwestern U.S., the Upper Colorado River Basin (UCRB) is remarkable for the paucity of its conventional hydrological record of extreme flooding. This study used paleoflood hydrology to examine a small portion the underutilized, but very extensive natural record of Holocene extreme floods in the UCRB. We performed a meta-analysis of 77 extreme paleofloods from seven slackwater deposit (SWD) sites in the UCRB (Table 1) to show linkages between Holocene climate patterns and rare, extreme floods (Figure 1). The analysis demonstrated several clusters of extreme flood activity: 8040-7790, 3600-3460, 2880-2740, 2330-700, and 620-0 years BP. The extreme paleofloods were found to occur during both dry and wet periods in the paleoclimate record. When compared with independent paleoclimatic records across the Rocky Mountains and the southwestern US, the observed temporal clustering pattern of UCRB extreme paleofloods was found to be associated with periods of abruptly intensified North Pacific-derived storms connected with enhanced El Niño variability.

Table 1. Paleofloods used in calculating cumulative probability distribution function curves for all four reaches in the upper Colorado River Basin (UCRB). Source: O'Connor, et al., (1994), Cline (2010), Greenbaum et al., (2014), and unpublished data from this study and other scientific reports.

River	Reach	Flood deposit #	Lab code	Dating method	Age (a BP)
Colorado Riv.	Moab	1	A13878	^{14}C	135 ± 35
	Moab	2	AA65420	^{14}C	340 ± 34
	Moab	3	A13879	^{14}C	120.5 ± 1.8
	Moab	4	A13877	^{14}C	6275 ± 160
	Moab	5	P2U5	OSL	1410 ± 110
	Moab	6	P4U4	OSL	2140 ± 220
	Moab	7	P5U1	OSL	1300 ± 90
	Moab	8	P5U2	OSL	1460 ± 80
	Moab	9	P9U5	OSL	390 ± 100
	Moab	10	P10U3	OSL	170 ± 40
	Moab	11	P10U7	OSL	410 ± 70
	Moab	12	P11U5	OSL	230 ± 60
	Moab	13	P12U5	OSL	490 ± 150
	Moab	14	P13U6	OSL	220 ± 70
	Moab	15	P14U7	OSL	460 ± 110
	Moab	16	P14U13	OSL	200 ± 60
	Cataract Canyon	17	GRV-13	OSL	370 ± 100
	Cataract Canyon	18	GRV-14	OSL	410 ± 100
	Cataract Canyon	19	USU-2309	OSL	310 ± 90
	Cataract Canyon	20	USU-2308	OSL	1160 ± 210
	Cataract Canyon	21	GRV-1	OSL	1100 ± 600
	Lees Ferry	22	GX-16055	^{14}C	1425 ± 130
	Lees Ferry	23	GX-16052	^{14}C	2150 ± 140
	Lees Ferry	24	GX-16053	^{14}C	2155 ± 75
	Lees Ferry	25	GX-16049	^{14}C	2470 ± 85
	Lees Ferry	26	GX-16050	^{14}C	2930 ± 165

	Lees Ferry	27	GX-16054	^{14}C	3530 ± 80
	Lees Ferry	28	GX-16051	^{14}C	3915 ± 85
	Lees Ferry	29	GX-16012	^{14}C	330 ± 120
	Lees Ferry	30	GX-16024	^{14}C	1470 ± 190
Green Riv.	Dead Horse Canyon	1	GRV-2	OSL	680 ± 250
	Dead Horse Canyon	2	GRV-3	OSL	470 ± 160
	Dead Horse Canyon	3	USU-2310	OSL	200 ± 80
	High Bank	4	GRV-4	OSL	320 ± 70
	High Bank	5	GRV-5	OSL	350 ± 70
	Ledge	6	GRV-6	OSL	220 ± 40
	Powell Canyon	7	GRV-7	OSL	480 ± 170
	Powell Canyon	8	GRV-8	OSL	340 ± 90
	Powell Canyon	9	USU-2306	OSL	200 ± 100
	Rockfall	10	GRV-9	OSL	400 ± 100
	Rockfall	11	GRV-10	OSL	220 ± 110
	Rockfall	12	GRV-11	OSL	550 ± 170
	Rockfall	13	GRV-12	OSL	290 ± 60
	Rockfall	14	USU-2307	OSL	190 ± 80
Dolores Riv.	Big Rock	1	AA82500	^{14}C	991 ± 37
	Big Rock	2	AA82502	^{14}C	1226 ± 38
	Big Rock	3	AA85261	^{14}C	1337 ± 36
	Big Rock	4	AA85262	^{14}C	1359 ± 36
	Big Alcove	5	AA82506	^{14}C	1231 ± 38
	Big Alcove	6	AA86680	^{14}C	1271 ± 34
	Big Alcove	7	AA86681	^{14}C	947 ± 33
	McPhee	8	AA84122	^{14}C	1526 ± 53
	McPhee	9	AA84123	^{14}C	1578 ± 45
	McPhee	10	AA86674	^{14}C	1822 ± 67
	Mucky	11	AA84126	^{14}C	7800 ± 200

Mucky	12	AA84127	^{14}C	2089 ± 70
Mucky	13	AA84128	^{14}C	1596 ± 43
Mucky	14	AA85263	^{14}C	3322 ± 62
Mucky	15	AA85264	^{14}C	2212 ± 97
Mucky	16	AA85267	^{14}C	1342 ± 50
Mucky	17	AA86675	^{14}C	1750 ± 38
Mucky	18	AA86676	^{14}C	1735 ± 38
Mucky	19	AA86677	^{14}C	1626 ± 38
Mucky	20	AA86678	^{14}C	1821 ± 39
Mucky	21	AA84130	^{14}C	2680 ± 64
Tafoni	22	AA85258	^{14}C	893 ± 51
Tafoni	23	AA85259	^{14}C	1995 ± 94
Juniper	24	AA86019	^{14}C	8033 ± 55
Juniper	25	AA86021	^{14}C	7153 ± 48
Tributary	26	AA86024	^{14}C	7060 ± 190
Tafoni	27	USU-330	OSL	2940 ± 320
Big Alcove	28	USU-331	OSL	1440 ± 180
Big Alcove	29	USU-332	OSL	990 ± 80
Big Rock	30	USU-626	OSL	1100 ± 130
Tafoni	31	USU-627	OSL	1110 ± 170
Juniper	32	USU-628	OSL	7840 ± 660
Tributary	33	USU-630	OSL	8210 ± 790

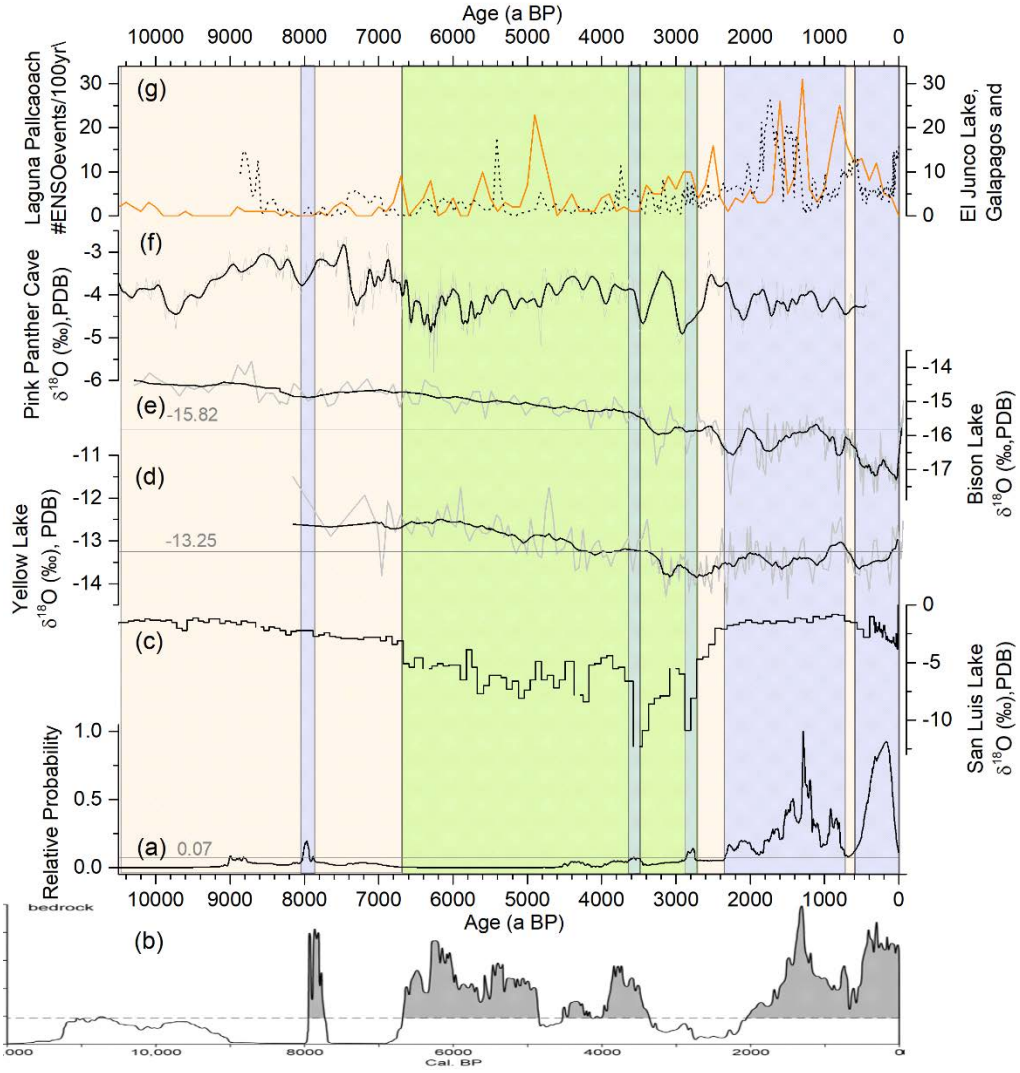

Figure 1. Comparison of the cumulative probability distribution function (CPDF) from (a) the Dolores River Basin (DRB), (b) the bedrock reaches in the southwest US (Harden et al., 2010), and climate records from (c) $\delta^{18}O$ of San Luis Lake (Yuan et al., 2013); (d and e) $\delta^{18}O$ of Yellow and Bison Lake (Anderson, 2011, 2012); (f) δ18O of a speleothem from Pink Panther Cave (Asmerom et al., 2007) and (g) ENSO frequency reconstructions from El Junco Lake (dashed line, Conroy et al., 2008) and Laguna Palcacocha (black line, Moy et al., 2002).

3. Marble Canyon

The Marble Canyon study site (Colorado River Mile 2.1), originally described by O'Connor et al. (1994), was re-visited as part of the April 2018 Grand Canyon reconnaissance. That study also identified a nearby site, Cathedral Wash (Mile 2.8), where crevice slack-water deposits were found at 22 m above the current river water level (compared to a 14 m maximum paleoflood high-water stage at the Mile 2.1 site).

As a result of this discovery, it was concluded that the earlier work at Colorado River Mile 2.1 would be best extended in a continuation of the original project that also incorporated the evidence at Mile 2.8, the mouth of Cathedral Wash. The Cathedral Wash site can be reached without the need for a river trip, so, with the projected new funding, we plan to incorporate its analysis into a study that improve upon the earlier O'Connor et al. (1994) results.

4. Grand Canyon paleoflood Sites

The in-depth reconnaissance of the Grand Canyon was accomplished in April 2018. The research trip departed Lees Ferry on the morning of Thursday, April 19, and finished at Diamond Creek on the morning of Saturday, April 28. The trip participants were Victor R. Baker, PI; Dr. Tessa Harden, U.S. Geological Survey; Tao Liu, Dept. of Hydrology and Atmospheric Sciences, Univ. of Arizona; Joanna Redwine, U.S. Bureau of Reclamation; and John Weisheit, Living Rivers, Moab, UT.

By comparison to a previously studied site, Axehandle Alcove at Mile 2.1L in Marble Canyon (O'Connor et al., 1994), this survey allowed us to estimate the probable magnitudes of past extreme floods (last few thousand years) at multiple "slackwater deposit" (SWD) sites in Marble and Grand Canyons. This was accomplished by measuring the elevations of the highest emplacement of ancient flood sediments (SWDs) relative to the current river level, which averaged about 12,000 ft^3/s during the study period. At the Axehandle site the highest flood evidence ("paleostage indicator" – PSI) occurs at 14 m above the current river level, corresponding to a peak paleoflood discharge of 14,000 m^3/s (nearly 500,000 ft^3/s) (O'Connor et al., 1994). This flow is 1.65 times that of the largest historical flood for the Colorado River at Lees Ferry, which occurred in 1884.

The reconnaissance study discovered multiple sites that preserve evidence of flows that exceeded what is preserved at the Axehandle Alcove site. At Cathedral Wash (Mile 2.8L) crevice SWDs were found at 22 m above the current river water level. At Mile 42.5L and Mile 120.3L mounded SWDs were measured to a height of 20 m above the river water level. The peak discharges that produced these deposits were very likely to have been considerably in excess of that preserved at Axehandle Alcove. Our preliminary estimate is that the flows were about 20,000 m^3/s (about 700,000 ft^3/s). This equals or exceeds the Probably Maximum Flood (PMF) that was calculated for the construction of the Glen Canyon Dam.

At one site, Mile 49.7R, located downstream from the mouth of Saddle Canyon, we measured a SWD to an elevation of about 35 m above the current river level. This extraordinary flood level may be the result of special hydraulic conditions that prevailed during extreme the flooding of the site, but its extreme character certainly indicates a need for further study.

Conclusions from this reconnaissance study are as follows:

(1) Numerous SWD and PSI sites (we documented more than 40) exist in Marble and Grand Canyons.

(2) The high elevations of some sites (20+ m above current river level) indicate that extremely large paleofloods occurred during the last several thousand years.

(3) Some of the extreme paleofloods may have exceeded the PMF that has been used to evaluate the risk to Glen Canyon Dam (20,000 m^3/s).

(4) The extreme character of the paleofloods in Marble and Grand Canyon is broadly consistent with results from studies done on the Upper Colorado River near Moab Utah (Greenbaum et al., 2014) and on the Green River near its junction with the Colorado (see section 1 above).

(5) The study results indicate the potential need for a reevaluation of extreme flood risk on the Colorado River, with potential implications for dam safety, the security of cultural resources in Grand Canyon National Park, risk to infrastructure, etc.

(6) An in-depth analysis of the newly discovered SWD-PSI sites is clearly warranted.

We hope to be able to follow-on from these discoveries during a funded extension of the current project, and/or with the support of new project funding during the upcoming fiscal year. In the meantime, we will work on completing the review of manuscripts and submit them for journal submission. We will also work on the planning needed for a detailed survey of the Grand Canyon sites that were identified by the April reconnaissance expedition.

Reference Cited

Anderson, L., 2011. Holocene record of precipitation seasonality from lake calcite delta O 18 in the central Rocky Mountains, United States. Geology 39, 211–214.

Anderson, L., 2012. Rocky Mountain hydroclimate: Holocene variability and the role of insolation, ENSO, and the North American Monsoon. Glob. Planet. Chang. 92–93, 198–208.

Asmerom, Y., Polyak, V.J., Burns, S.J., 2010. Variable winter moisture in the southwestern United States linked to rapid glacial climate shifts. Nat. Geosci. 3, 114–117.

Cline, M.L. 2010. Extreme flooding in the Dolores River Basin, Colorado and Utah: Insights from paleofloods, geochronology and hydroclimatic analysis. Ph.D. Dissertation, University of Arizona, Tucson, Arizona, 221.

Conroy, J.L., Overpeck, J.T., Cole, J.E., Shanahan, T.M., Steinitz-Kannan, M., 2008. Holocene changes in eastern tropical Pacific climate inferred from a Galapagos lake sediment record. Quat. Sci. Rev. 27, 1166–1180.

Greenbaum, N., Harden, T.M., Baker, V.R., Weisheit, J., Cline, M.L., Porat, N., Halevi, R.,and Dohernwend, J., 2014, A 2000-year natural record of magnitudes and frequencies for the largest upper Colorado River floods near Moab, Utah: Water Resources Research, v. 50, p. 5249-5269.

Harden, T.M., O'Connor, J.E., Driscoll, D.G., 2015. Late Holocene flood probabilities in the

Black Hills, South Dakota with emphasis on the Medieval Climate Anomaly. Catena 130: 62 68.

Moy, C.M., Seltzer, G.O., Rodbell, D.T., Anderson, D.M., 2002. Variability of El Niño/ Southern Oscillation activity at millennial timescales during the Holocene epoch. Nature 420, 162 165.

O'Connor, J.E., Ely, L.L., Wohl, E.E., Stevens, L.E., Melis, T.S., Kale, V.S., and Baker, V.R., 1994, A 4500-year record of large floods on the Colorado River in the Grand Canyon, Arizona: Journal of Geology, v. 102, p. 1-9.

Yuan, F., Koran, M.R., Valdez, A., 2013, Late glacial and Holocene record of climatic change in the southern Rocky Mountains from sediments in San Luis Lake, Colorado, USA. Palaeogeogr, Palaeoclimatol , Palaeoecol. 392:146-60.